รายงานการวิจัยฉบับสมบูรณ์

ผลกระทบของการปนเปื้อนเชื้อเพลิงไบโอดีเซลและเขม่าต่อการสึกหรอของเครื่องยนต์โดยเครื่องทดสอบการสึกหรอแบบโฟร์บอลและการวัดขนาดอนุภาคด้วยเลเซอร์

IMPACT OF BIODIESEL CONTAMINATION AND SOOT ON ENGINE WEAR USING FOUR-BALL, LASER PARTICLE DISTRIBUTION

ผศ.ดร. ปรีชา การินทร์

งานวิจัยนี้ได้รับทุนสนับสนุนงานวิจัย
จากงบประมาณเงินรายได้ประจำปีงบประมาณ พ.ศ. 2560
วิทยาลัยนานาชาติ
สถาบันเทคโนโลยีพระจอมเกล้าเจ้าคุณทหารลาดกระบัง

ชื่อโครงการ	ผลกระทบของการปนเปื้อนเชื้อเพลิงไบโอดีเซลและเขม่าต่อการสึกหรอของเครื่องยนต์โดยเครื่องทดสอบการสึกหรอแบบโฟร์บอลและการวัดขนาดอนุภาคด้วยเลเซอร์ Impact of Biodiesel Contamination and Soot on Engine Wear using Four-ball, Laser Particle Distribution
แหล่งเงิน	งบประมาณรายได้ วิทยาลัยนานาชาติ
ประจำปีงบประมาณ	2560 จำนวนเงินที่ได้รับการสนับสนุน 100,000 บาท
ระยะเวลาทำการวิจัย	1 ปี ตั้งแต่ 1 ตุลาคม 2559 ถึง 31 กันยายน 2560
หัวหน้าโครงการ	ผศ.ดร. ปรีชา การินทร์
หน่วยงานต้นสังกัด	วิทยาลัยนานาชาติ
	preechar.ka@kmitl.ac.th

RESEARCH REPORT

IMPACT OF BIODIESEL CONTAMINATION AND SOOT ON ENGINE WEAR USING FOUR-BALL, LASER PARTICLE DISTRIBUTION

ASST. PROF. DR. PREECHAR KARIN

FISCAL YEAR 2017

INTERNATIONAL COLLEGE

KING MONGKUT'S INSTITUTE OF TECHNOLOGY LADKRABANG

ABSTRACT

This research aimed to investigate physical and chemical properties of the diesel engine used oil by collecting the oil from the small diesel engine. The oil properties were tested according to ASTM standard test methods. The effect of biodiesel contamination on metal wear was studied. The difference blends of biodiesel were mixed with SAE0W30 engine oil. The metal wear behavior was studied by means of a Four-Ball tribology test with wear measured. Wear roughness in micro- scale was also investigated by high resolution Optical microscopy (OM) , 3D rendering optical technique and SEM image processing method. Moreover, the impact of soot contamination on engine oil degradation and metal wear was also reported. Soot particle contamination in engine oil was simulated using pure carbon black. Micro-structure of soot particles were studied by scanning electron microscopy (SEM), Transmission electron microscopy (TEM) and Laser diffraction spectroscopy (LDS). The results showed that the ball wear scar diameter (WSD) increased when the primary particle size of carbon black was increased. In conclusion, it might be expected that the soot particle which was larger than the oil film thickness can increase the metal wear. In this research, soot wear mechanisms might be expected as three-body abrasive wear. The role of lubricating oil is to generate an oil film between two surfaces and trap soot particles. If the soot particle size is larger the oil film thickness, then soot might occurr as three body abrasion. Therefore, viscosity improver additives would be a key to preventing soot abrasive wear. Soot particle distributions in liquids were observed by Laser Diffraction Spectroscopy. It was found that there were highly agglomerated in water, a smaller group of agglomeration in palm oil and well distribution in formulated lubricant. The impact of soot nanoparticle affecting on metal wear was investigated by Four-ball wear tester. It was found that the ball WSD increased proportionally to the soot primary particle size. It is expected that the soot particle which is larger than the oil film thickness can increase the metal wear.

TABLE OF CONTENTS

TABLE OF CONTENTS

(Continuous)

CHAPTER 1

INTRODUCTION

1.1 Background

Diesel engine is a compression ignition engine which converts chemical energy within the fuel into mechanical energy. Diesel fuel is injected under high pressure into the combustion chamber where the combustion process occurs. Soot is remain of incomplete combustion which consists mostly of carbon, hydrocarbon and metallic ash. The primary and agglomerated soot particles observed by Transmission Electron Microscopy (TEM) are in the range of 20 - 80 nm and 100 - 300 nm, respectively [1]. Soot can be entered into the engine oil through the piston ring clearance during the combustion process [2].

Khamsrisuk et al. [3] performed the used oil analysis by collecting the engine oil from the small diesel engine vehicles. The results showed that the percentage of wear metal, soot and fuel contamination increased as the engine mileage increase. The average of soot contamination was about 0.69 percent by weight. Guatam et al. [4] investigated the effect of soot contamination on engine oil viscosity by increasing the percentage of soot contamination. The results showed that the engine oil viscosity increased with the increase of soot contamination. The engine testing for evaluated soot tribological properties is challenging, because of the uncontrolled test parameter and the difficulty of wear measurement [5]. The specimen bench test which is easy to control test parameter and good repeatable results are used. Carbon black is a synthesis soot which has similar particle size and physical properties to engine soot. It can be used as soot representative. Ryason et al. [6] performed wear tests on a ball-on-flat-disk wear tester using carbon black, alumina and silica. The results showed that the balls were worn similarly in three different kinds of the samples. Karin et al. [7] performed wear tests on Four-Ball Wear Tester. He found that the Wear Scar Diameter (WSD) of the ball in the oil containing carbon black was higher than that of the oil alone. Hu et al. [8] also performed Four-Ball Wear Tester using base oil and formulated lubricant. The results showed that the WSD was high when carbon black levels increased. But, the WSD of the formulated lubricant was lower than that of the pure base oil. They suggested that the wear mechanism of soot-contaminated lubricant might be abrasion.

Biodiesel is an alternative fuel that plays an importance role in replacement using petroleum diesel. It is an oxygenated fuel that promotes more completely combustion. The soot diameter size and quantity from biodiesel engine emission is lower than that of diesel [9]. However, soot induced wear mechanisms are still not fully understood. This research aimed to investigate the effects of soot Nanoparticles on metal wear characteristics using Four-Ball Wear Tester, Laser Diffraction Spectroscopy, and Electron Microscopy.

1.2 Objective

1.2.1 To investigate physical and chemical properties of the diesel engine used oil including the amount of fuel and soot contamination, and also investigate shape and size distribution of the particle in the used oil.

1.2.2 To investigate the effect of the difference blend of biodiesel contamination on the metal wear including wear scar diameter, surface roughness and micro-surface analysis. And also investigate the tested oil's particle size distribution.

1.2.3 To investigate the effect of soot Nanoparticle on the metal wear including wear scar diameter, surface roughness and micro-surface analysis. And also investigate the tested oil's particle size distribution.

1.3 Scope of work

1.3.1 The used oils were collected from the 1.4 L small diesel engine vehicles which used a commercial diesel (B3-7) as a fuel and used SAE0W30 as an engine oil. The engine oil's mileage and oil aged were in the range 3,000 - 20,000 and 0-10,000 km, respectively.

1.3.2 The commercial diesel (B3-7) and palm biodiesel blends (B20, B50 and B100) were mixed with a new SAE0W30 engine oil at concentration of 2% by weight for simulating biodiesel contaminated engine oil.

1.3.3 The commercial carbon black (N220, N330, N550 and N660) were mixed with a new SAE0W30 engine oil at concentration of 1% by weight per volume for simulating soot difference Nanoparticle size contaminated engine oil.

1.3.4 The investigation of both biodiesel and soot contamination on metal wear were investigated using Four-ball wear tester.

1.4 Structure of the research

The research methodologies in this this are divided as follows.

Chapter 1 discuss the research background, objective, and scope.

Chapter 2 discuss the relevant theory and literature including fundamental of tribology, used oil analysis, fuel and soot contamination on metal wear.

Chapter 3 discuss the research materials and methods.

Chapter 4 discuss the results of used oil analysis, used oil's particles shape and size distribution, the results of biodiesel and soot contamination on metal wear by using Four-ball wear tester, optical microscopy, scanning electron microscopy and laser diffraction spectroscopy.

Chapter 5 is experimental results and suggestions.

1.5 Expected benefits

This research is helped to know the physical and chemical properties of the diesel engine used oil including the amounts of contaminants and properties of wear particles after certain period of running the engine. It also helped to know the impact of biodiesel and soot contamination on metal wear that can help to reduce wear and prolong the engine parts.

CHAPTER 2

LITERATURE REVIEW

2.1 Tribological Contacts

A tribological contact is defined as two solid bodies in contact under relative motion. It can be either unlubricated or lubricated. The tribological contact is characterized by its operating conditions (e.g. velocity, load and type of motions), material parameters (e.g. surface material, surface roughness and hardness), and environmental conditions (e.g. temperature and humidity) and, in the lubricated case, lubricant properties (e.g. viscosity) (see Figure 2.1). The tribological contact can be observed at different scales, that is at macroscopic scale (or macro scale) or at microscopic scale (or micro scale) (see Figure 2.2). The macro scale will give global information of the contact, while the micro scale will give local information within the contact. For example, a contact that appears smooth at macro scale may appear very rough and uneven at micro scale. The real contact area between the surfaces is the sum of a large number of small areas where surface peaks from the two surfaces get into contact. As a consequence, the apparent contact area at the macro scale is much larger than the real contact area between the two surfaces in contact.

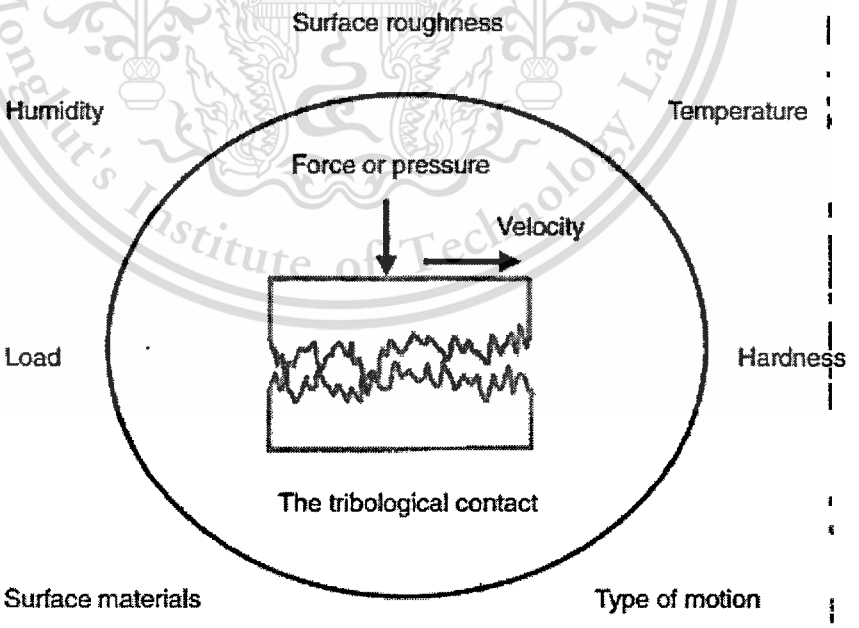

Figure 2.1 Tribological contacts are affected by different conditions [10]

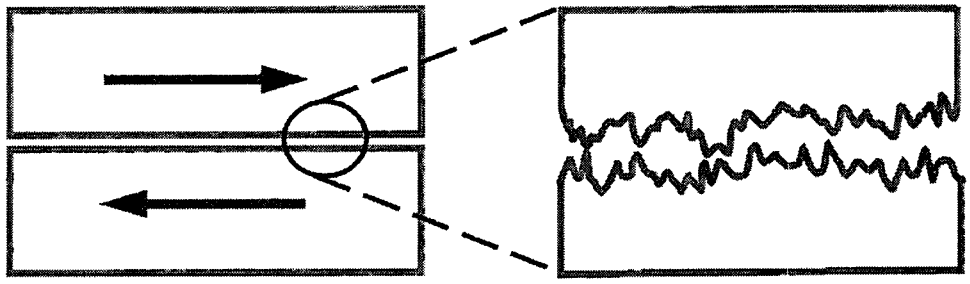

Figure 2.2. The tribological contact can be observed at macro scale (left) or at micro scale (right). [10]

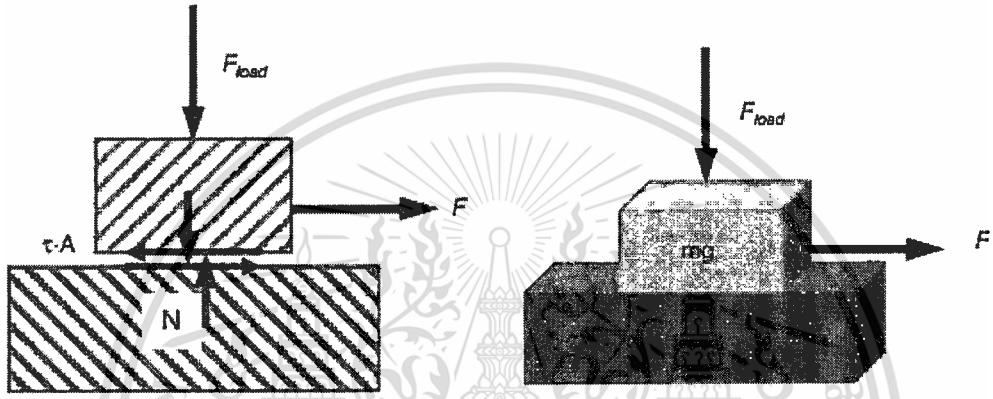

Figure 2.3 Friction visualized as pulling a small box across a flat surface [10]

2.2 Friction

Friction is the force resisting the relative motion between two surfaces in contact. It is commonly divided into *dry friction* and *viscous friction*. It may be *static* that is the solid bodies have no relative motion, or *dynamic*, when the solid bodies are moving relative to each other. Dry friction occurs between two dry solid bodies. Viscous friction occurs when the two solid bodies are more or less separated by a fluid, for example a lubricant.

2.2.1 The Coefficient of Friction

The coefficient of friction μ is defined as the ratio of the friction force F and the normal force N between the bodies, as shown in Figure 2.3 and expressed by

$$\mu = \frac{F}{N} \tag{2.1}$$

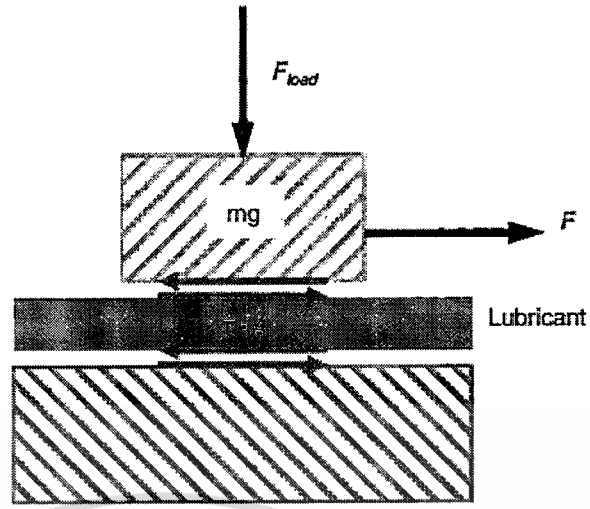

Figure 2.4 Coefficient of friction versus film parameter in lubricated sliding contacts [10]

Where the normal force is actually the sum of the load of the mass *mg* and any externally applied load, F_{load}

$$N = mg + F_{load} \quad (2.2)$$

The normal force always acts perpendicular to the contact area. When sliding the mass the friction force is the force required to maintain the sliding and it always acts tangential (i.e. parallel) to the contact area.

For a contact where the surfaces are fully separated by a lubricant the friction force is commonly expressed by

$$F = \tau A \quad (2.3)$$

Where τ is the shear stress in the lubricant and A is the contact area. The shear stress is determined by the lubricant properties, the velocity of the motion and the distance between the bodies. The forces in the lubricated contact act on both the solid bodies and the fluid, as shown in Figure 2.4.

2.2.2 Lubrication Regimes

A general description of the friction behavior in a lubricated contact can be seen in Figure 2.5, where the dependence of the coefficient of friction μ versus the film parameter λ is shown. The film parameter λ is calculated as

$$\Lambda = \frac{h}{\sqrt{{R_{qA}}^2 + {R_{qb}}^2}} \tag{2.4}$$

Where h is the lubricant film thickness and R_{qA} and R_{qb} represent the surface roughness of the two surfaces A and B in contact. The contact is classified as boundary, mixed or full flm lubricated depending on the degree of mechanical contact between the solid surfaces. The curve in Figure 2.5 originates from the Stribeck curve. The contact is classified as boundary, mixed or full film as shown in Figure 2.6.

Boundary lubrication implies heavy contacting between the asperities with a film parameter below 1. The load is carried by the solid surfaces in. The lubricant is mainly acting as a carrier of additives. The presence of additives is necessary to ensure the performance and build-up of a boundary film. This regime is characterized by high load and low speed. A slowly rotating shaft and a bushing mainly work in the boundary lubrication regime even if they are lubricated.

In mixed film lubrication the surfaces are less separated than in the full film regime. The surfaces are close enough for asperity contact to occur occasionally. The mixed film lubrication regime is a combination of full film lubrication and boundary lubrication with film parameter between 1 and 3. Thus, the load is carried partly by a pressure in the fluid film and partly by the asperities in contact, as shown in Figure 2.6. The lubricant will support the contact with necessary additives to reduce wear.

In full film lubrication the solid bodies are lubricated by a thick enough lubricant film to ensure full separation of the surfaces. In this regime the coefficient of friction is very low. A Λ -value higher than 3 indicates full film lubrication.

The lubricant film thickness h is determined by the lubricant the operating conditions, the contact geometry and the solid surface's material properties. In practice, typical lubricant film thicknesses are about 1–100 microns.

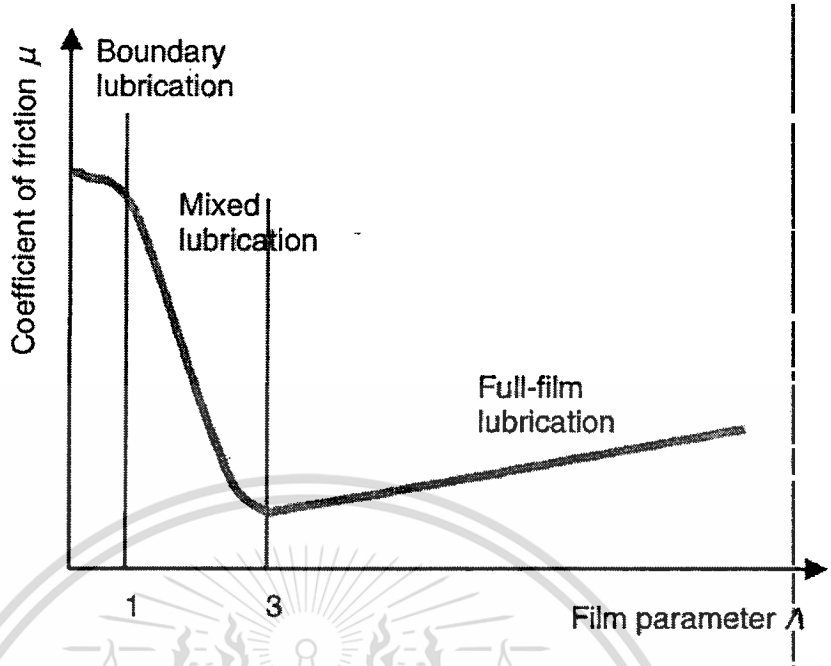

Figure 2.5 Coefficient of friction versus film parameter in lubricated sliding contacts [10]

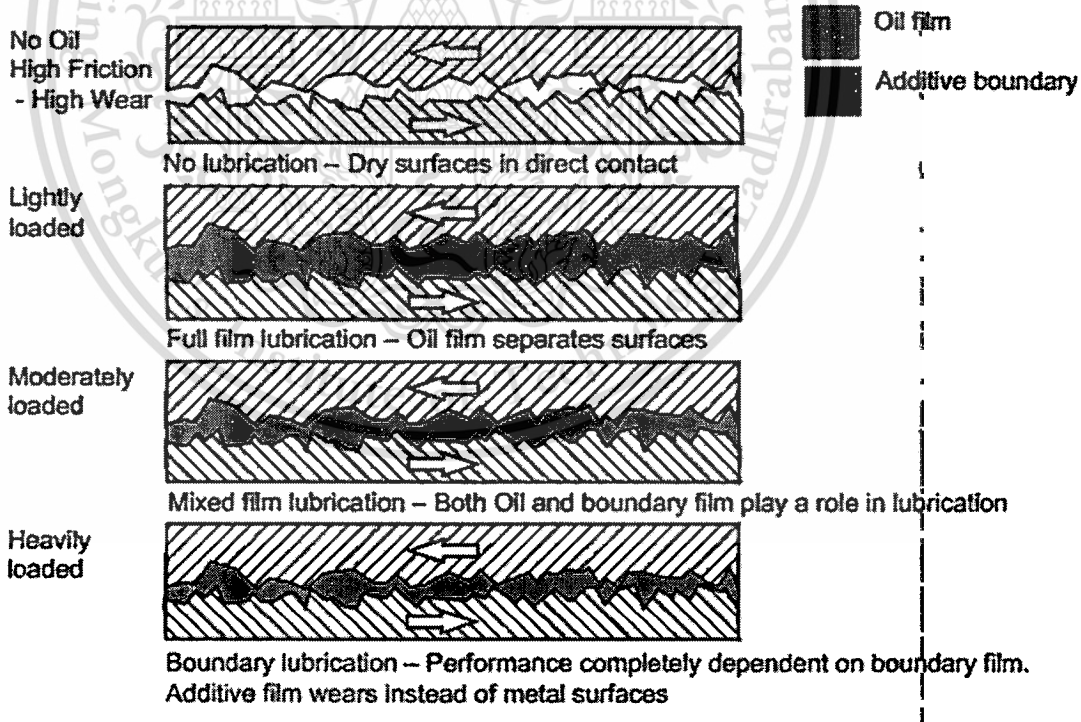

Figure 2.6 Engine lubrication regimes [11]

2.2.2.1 Film Thickness Estimation between Two Sphere Contacts

In this topic, the fundamental mechanisms of film generation in elastohydrodynamic contacts, together with the methods for calculating the minimum film thickness between spherical balls.

The shape of the contact area depends on the shape (curvature) of the contacting bodies. For example, point contacts occur between two balls, line contacts occur between two parallel cylinders and elliptical contacts, which are most frequently found in many practical engineering applications, occur when two cylinders are crossed, or a moving ball is in contact with the inner ring of a bearing, or two gear teeth are in contact. The curvature of the bodies can be convex, flat or concave. It is defined by convention that convex surfaces possess a 'positive curvature' and concave surfaces have a 'negative curvature'. The following general rule can be applied to distinguish between these surfaces: if the center of curvature lies within the solid then the curvature is positive, if it lies outside the solid then the curvature is negative. This distinction is critical in defining the parameter characterizing the contact geometry which is known as the reduced radius of curvature.

The configuration of two elastic bodies with convex surfaces in contact was originally considered by Hertz in 1881 and is shown in **Figure 2.7**

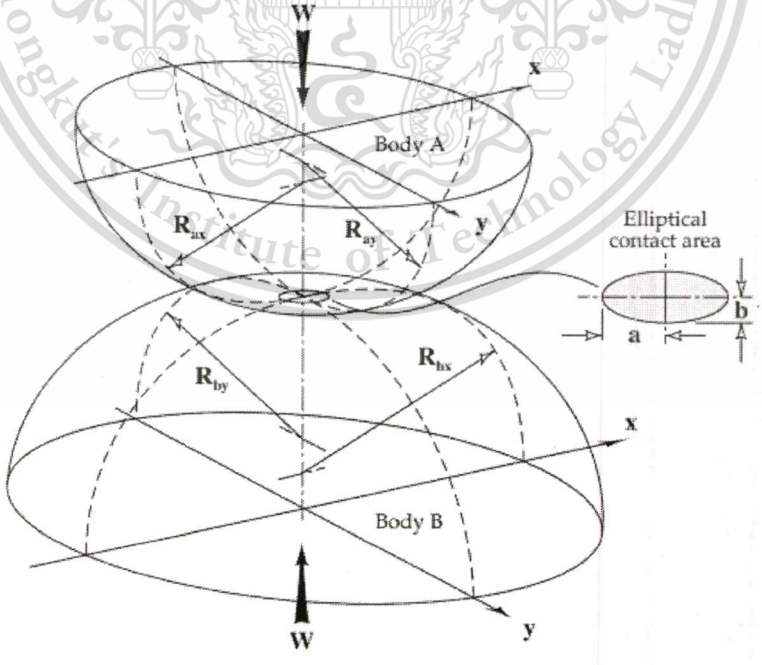

Figure 2.7 Geometry of two elastic bodies with convex surfaces [12]

$$\frac{1}{R'} = \frac{1}{R_x} + \frac{1}{R_y} = \frac{1}{R_{ax}} + \frac{1}{R_{ay}} + \frac{1}{R_{bx}} + \frac{1}{R_{by}} \tag{2.5}$$

Where:

$$\frac{1}{R_x} = \frac{1}{R_{ax}} + \frac{1}{R_{ay}}$$

$$\frac{1}{R_y} = \frac{1}{R_{bx}} + \frac{1}{R_{by}}$$

R_x is the reduced radius of curvature in the x direction [m].

R_y is the reduced radius of curvature in the y direction [m].

R_{ax} is the reduced radius of curvature of body A in the x direction [m].

R_{ay} is the reduced radius of curvature of body A in the y direction [m].

R_{bx} is the reduced radius of curvature of body B in the x direction [m].

R_{by} is the reduced radius of curvature of body B in the y direction [m].

The reduced Young's modulus is defined as:

$$\frac{1}{E'} = \frac{1}{2}\left[\frac{1-\vartheta_A{}^2}{E_A} + \frac{1-\vartheta_B{}^2}{E_B}\right] \tag{2.6}$$

Where:

ϑ_A and ϑ_B are the Poisson's rations of the contacting bodies A and B.

E_A and E_B are the Young's moduli of the contacting bodies A and B.

It can be noted that for the spheres:

$R_{ax} = R_{ay} = R_A$ and $R_{bx} = R_{by} = R_B$

Where:

R_A and R_b are the radii of the spheres A and B, respectively.

Substituting into equation (2.6) gives:

$$\frac{1}{R'} = \frac{1}{R_x} + \frac{1}{R_y} = \frac{1}{R_A} + \frac{1}{R_B} + \frac{1}{R_A} + \frac{1}{R_B} = 2\left(\frac{1}{R_A} + \frac{1}{R_B}\right) \tag{2.7}$$

Where:

$$\frac{1}{R_x} = \frac{1}{R_y} = \frac{1}{R_A} + \frac{1}{R_B}$$

2.2.2.2 Elastohydrodynamic Film Thickness Formulae

The exact analysis of elastohydrodynamic lubrication by Hamrock and Dowson [7,16] provided the most important information about EHL. The results of this analysis are the formulae for the calculation of the minimum film thickness in elastohydrodynamic contacts. The formulae derived by Hamrock and Dowson apply to any contact, such as point, linear or elliptical, and are now routinely used in EHL film thickness calculations. They can be used with confidence for many material combinations including steel on steel even up to maximum pressures of 3-4 [GPa] [11]. The numerically derived formulae for the central and minimum film thicknesses, as shown in Figure 7.16, are in the following form [7]

$$\frac{h_{mean}}{R} = 2.69\left(\frac{U\eta_0}{ER}\right)^{0.67}(\alpha E)^{0.53}\left(\frac{W}{ER^2}\right)^{-0.067}(1 - 0.61e^{-0.73k}) \quad (2.8)$$

$$\frac{h_{min}}{R} = 3.63\left(\frac{U\eta_0}{ER}\right)^{0.68}(\alpha E)^{0.49}\left(\frac{W}{ER^2}\right)^{-0.073}(1 - e^{-0.68k}) \quad (2.9)$$

Where:

h_{mean} is mean oil film thickness [m].

h_{min} is minimum oil film thickness [m].

η_0 is viscosity at atmospheric pressure of the lubricant [Pa.s].

R is Radius of curvature [m].

U is Entering surface velocity [ms^{-1}].

E is Young's modulus [Pa].

α is Pressure-viscosity coefficient [$\frac{m^2\ Pa}{N}$].

W is contract load [N].

K is Elasticity parameter.

2.3 Wear

Wear is loss of material from a solid surface. Wear can appear in many ways depending on the material of the interacting contact surfaces, the environment and the operating conditions. At least five principal wear processes can be distinguished: abrasive wear, adhesive wear, surface fatigue and fretting and erosive wear. These are briefly described below.

2.3.1 Abrasive Wear

Abrasive wear is the most common form of wear. According to statistics, about half of the total loss of wear damage in production is caused by abrasive wear thus study of abrasive wear is very important. In general, abrasive wear mechanism is the plowing action of the abrasive particle so it is a micro-cutting process. Clearly, the relative hardness of the material to the abrasive particles, load and sliding velocity play important parts in abrasive wear. There are three types of abrasive wear:

1. An abrasive particle moves along a solid surface to produce surface wear which is called two-body abrasive wear. If an abrasive particle moves in the direction parallel to a solid surface, the contact stress on the surface is low such that scratches or minor furrows appear on the surface. If the abrasive particle moves in the direction vertical to the solid surface, the wear caused is referred to as impact wear. In such a situation, the particle collides on the surface in high stress such that a deep groove will be grinded on the surface and the large particular material is shed from the surface. Impact wear capacity is related to impact energy.
2. In a friction pair, where a hard surface roughness peak acts as an abrasive particle on the soft surface, this is also known as two-body abrasive wear and is usually a low-stress abrasive wear.
3. When the outside abrasive particles move between the two surfaces, similar to grinding, this is known as three-body abrasive wear. Usually, the three-body abrasive wear has high contact stress on the metal surface, often exceeding the crush strength of the abrasive particle. The compressive stress makes the friction surface of the ductile metal form the plastic deformation or fatigue, thus making the surface of the brittle metal form brittle fracture or spalling.

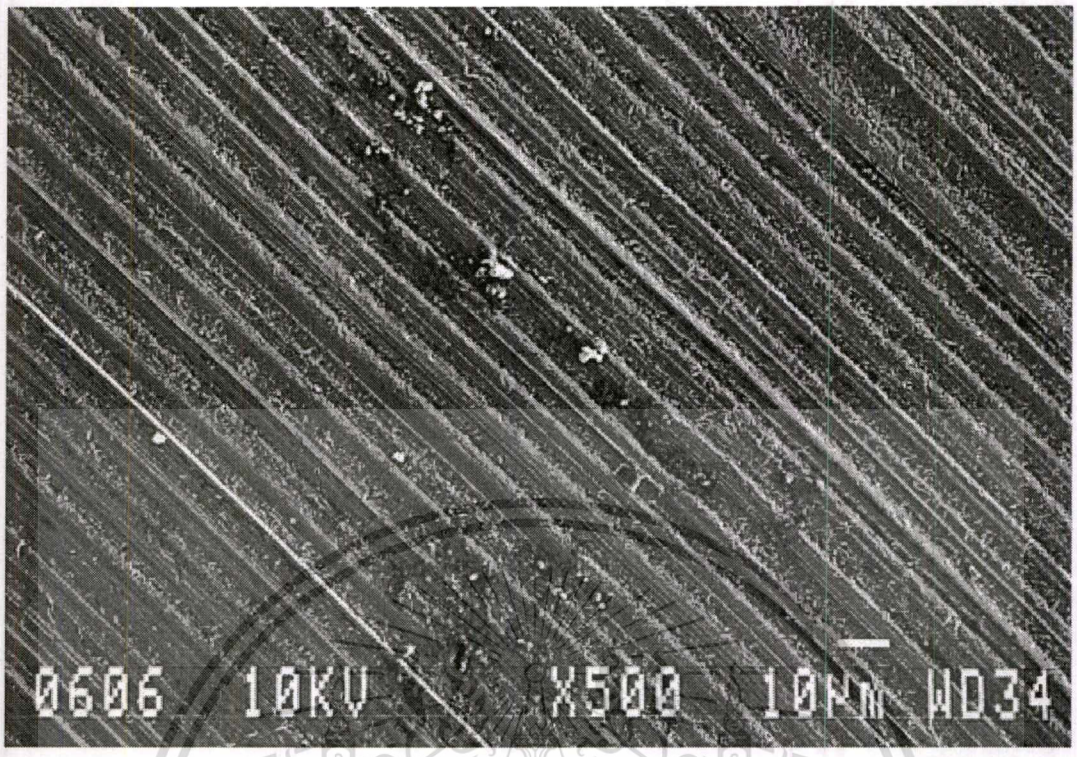

(a) SEM image of the worn surface of a quenched and tempered tool steel produced by microscale abrasion at a normal. [10]

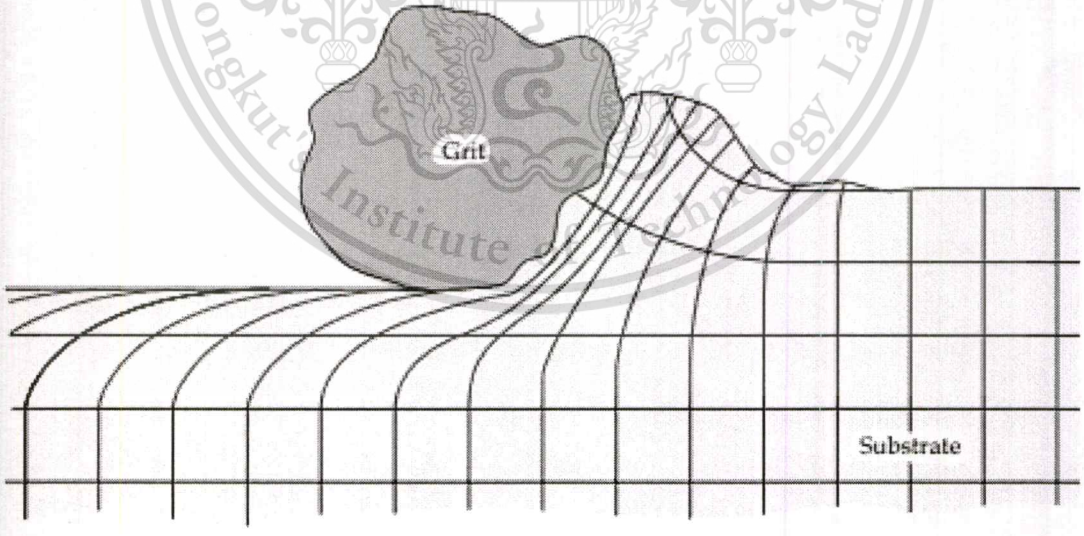

Subsurface deformation during passage of a grit. []

Figure 2.8 Subsurface deformation during passage of a grit

.

Delamination Wear Theory

It is generally believed that the mechanisms of the abrasive wear and the corrosion wear are relatively understood. However, although the adhesive wear, fretting and fatigue wear have many common features, there is no theory to explain these three kinds of wear yet. The delamination wear theory was proposed by Suh in 1973 [8]. This theory is based on the analysis and experiments of the elastic-plastic mechanics and summarizes the extensive research results. It can well explain a lot of wear phenomena. It has been proven that the delamination wear theory promotes the in-depth study on the common nature of wear.

Analysis with a scanning electron microscope showed that the shape of wear debris is of a long and thin layer structure, which is produced from the surface crack. The delamination wear theory is based on dislocation theory, the fracture and plastic deformation near the surface explain the formation of the wear debris.

The basic arguments are: during the relative sliding friction, the roughness of the soft surface is easily deformed. Therefore, under the cyclic load, the soft asperity is first fractured to be smoothed. In this way, the contact state is no longer between the asperities, but the hard roughness to the relatively smooth soft surface. When a hard asperity slides on the soft surface, the soft surface is subjected to the cyclic load and plastic shear deformation in the surface layer continually accumulates to bring about cyclic dislocation beneath the surface. Because of the action of the image force, dislocation beneath the surface of tens of microns thick disappears. So, the dislocation density close to the surface is less than that inside the body, that is, the maximum shear deformation occurs at a certain depth. With the continuous accumulation of the shear deformation, cracks or holes finally form. When a crack has formed, according to stress analysis, it can only extend parallel to the surface because the normal stress prevents it from developing in the depth direction. When the crack extends to the critical length, it will be peeled off the surface to form the debris.

The delamination wear theory can well describe many wear phenomena. For example, the surface layer deformation, the formation and expansion of the crack, the formation of the Babbitt layer as well as the influences of the lubricant, the sliding speed and the composite load on wear.

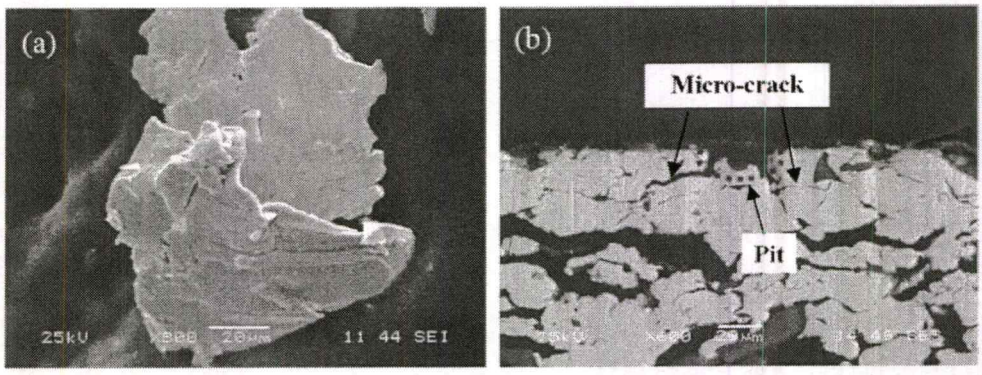

(a) Morphology of the thin flake debris (b) Cross section of the copper-based [10]

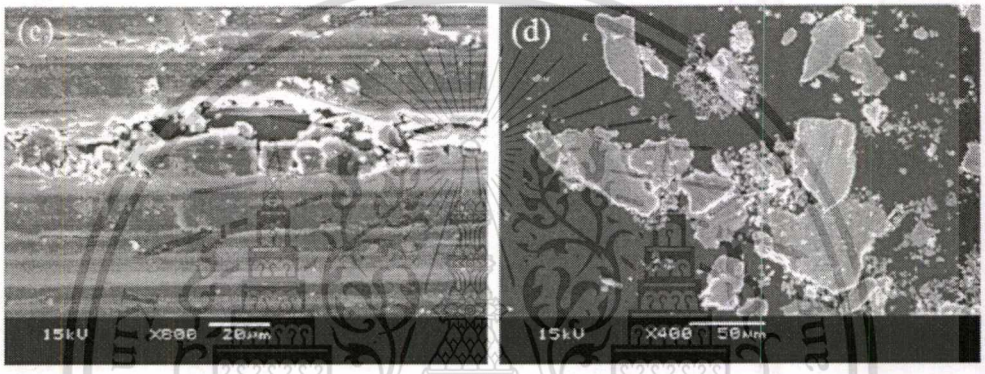

(c) cracks and crater in AZ31B (d) Sheet-like laminates wear debris [10]

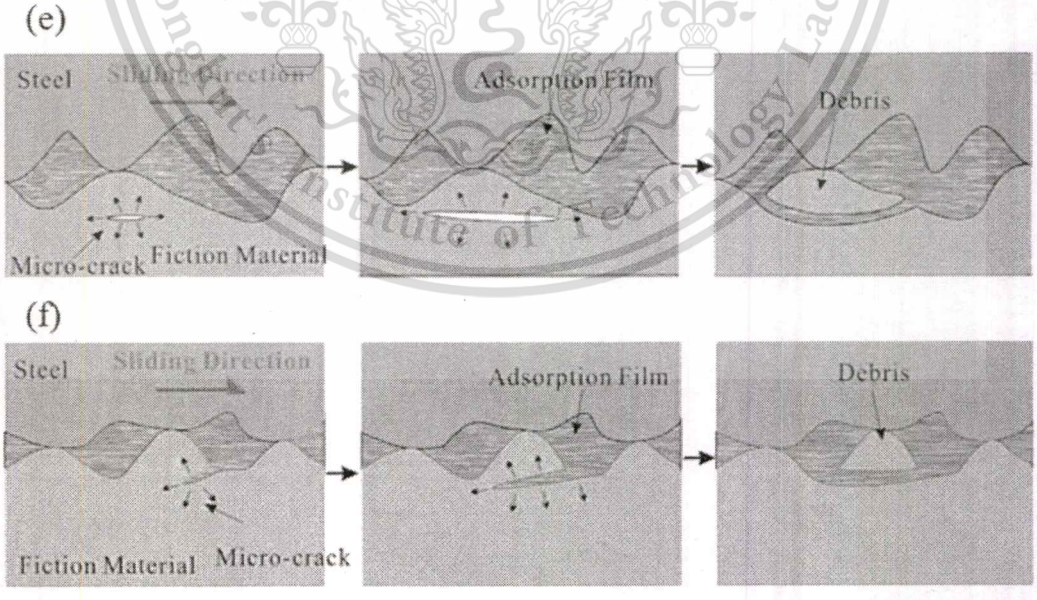

Delamination wear resulting from (a) fatigue and (b) oil-wedge []

Figure 2.8 Delamination Wear Theory

Surface fatigue occurs when cyclic loading weakens the material and can be the predominant wear mechanism in rolling contacts involving some sliding. This may result in subsurface cracks that may propagate and lead to material losses. Surface fatigue is sometimes also called pitting when small pieces of material break away from the surface, forming pits.

Fretting wear, or fretting, occurs when there is a very small oscillatory relative motion between two surfaces in contact. Often the intention is that the surfaces should be fixed, but due to, for example, vibrations some motion still occurs. The term fretting is often used to denote damage mechanisms such as fretting fatigue, fretting wear and fretting corrosion.

Erosive wear occurs in situations where hard particles impact a solid surface and remove material. The impacting particles can be stones, ore pieces, or small particles carried in a water or air jet

Often more than one wear mechanism is active at the same time. For example, small, abrasive particles may be generated due to adhesive wear or surface fatigue, which may also lead to abrasive wear. In addition, tribochemical wear can occur, which involves chemical reactions between the solid surfaces and surrounding lubricant or environment. The chemical reactions, such as corrosion, can weaken the surface layer, which will enhance the effect of other wear mechanisms.

2.4 Description of Combustion Engines

The engine operation will be described from the four-stroke engine perspective (see **Figure 2.9**). During intake, air is sucked into the combustion chamber. Fuel is injected during the compression stroke. Different fuels are used for different engines. Fuels generally consist of carbon and hydrogen, CxHy. They may include gasoline (having 5–12 carbons), diesel or biodiesel (having 10–15 carbons), ethanol or gaseous fuels (e.g. natural gas, biogas.). Fuel and air react during the compression stroke (having

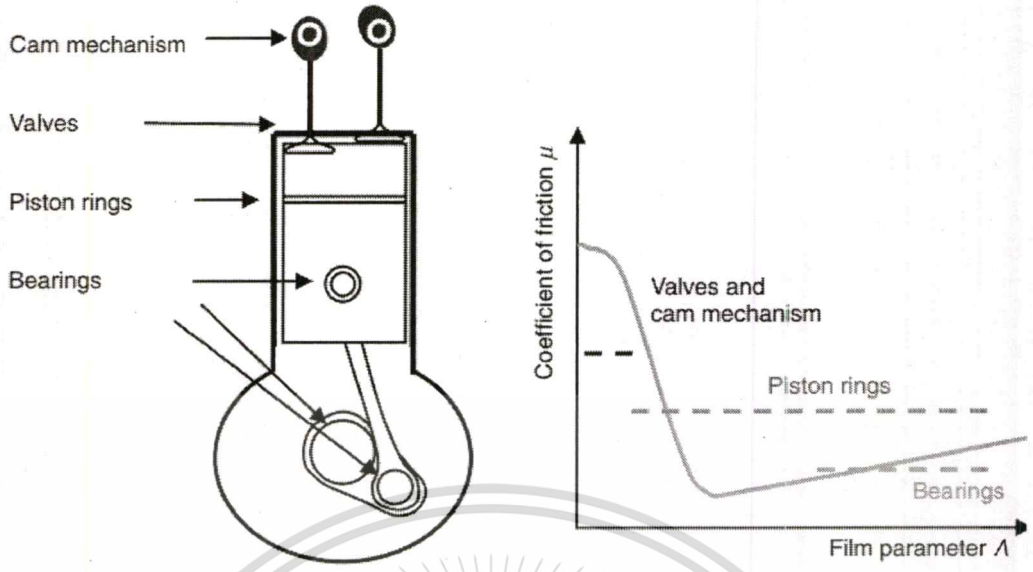

Figure 2.9 The lubricated parts in an engine (left) and the corresponding lubricating conditions indicated in the diagram (right) [10]

5–12 carbons), diesel or biodiesel (having 10–15 carbons), ethanol or gaseous uels (e.g. natural gas, biogas.). Fuel and air react during the compression stroke. The combustion energy released pushes the piston downwards, yielding power, heat and friction during the expansion stroke.

The final stroke releases the exhaust components. The current emission legislation (i.e. Euro V) has limits on the allowable exhaust components (e.g. CO, hydrocarbons, NOx and particulate matters, i.e. soot). Emissions may be reduced by after-treatment of the exhaust gas or optimizing the combustion. The whole engine uses one single lubricant, which should lubricate, for instance, the piston ring-cylinder, the bearings and the valve train, as well as cool the pistons. The piston ring cylinder operates in the boundary regime at the turning points and reaches full-film lubrication in between the turning points. The rotating engine bearings are full-film lubricated. The valve train with the cam and follower interface is in the boundary and the mixed lubrication regimes.

2.4.1 Soot generation

Soot is a microscopic carbonaceous particle that is a product of incomplete combustion of hydrocarbons (in this case, gasoline or diesel fuel). It consists of carbon, ash, and unsaturated (unburned) hydrocarbons. The unsaturated hydrocarbons are

essentially acetylene and polycyclic aromatic hydrocarbons. These components have particularly high levels of acidity and volatility. Measurements have shown that it typically contains 90 per cent carbon, 4 per cent oxygen, and 3 per cent hydrogen with the remainder consisting of nitrogen, sulphur, and traces of metal. Individual or primary soot particles from diesel combustion have been measured to be approximately 40 nm. Because of soot's colloidal properties, the particles agglomerate up to a maximum of approximately 500 nm, with a mean soot agglomerate size of 200 nm.

Soot particles tend to be more prevalent in diesel engines than in gasoline engines owing to the differences in the combustion mechanisms. Diesel engines are operated at higher air-to-fuel ratios, which tend to produce greater levels of engine soot. The majority of modern diesel engines operate using direct fuel injection and swirl within the combustion chamber to assist fuel–air mixing. Combustion initiates close to the injection point and occurs very rapidly as a diffusion flame. At this point, the air and fuel mix well, but the mixture is very fuel rich, causing very high levels of soot to be produced. After diffusion burning, the combustion process progresses through the rest of the combustion chamber by pyrolysis burning, which slowly burns the majority of the remaining fuel. This slow burning produces more particulates (soot) and unburned hydrocarbons at the end of the combustion process. Throughout the combustion process, soot particles are produced and destroyed. They are created by the process explained above and destroyed by oxidation. Oxidation is a mechanism that occurs when soot or soot precursors come into contact with various oxidizing species.

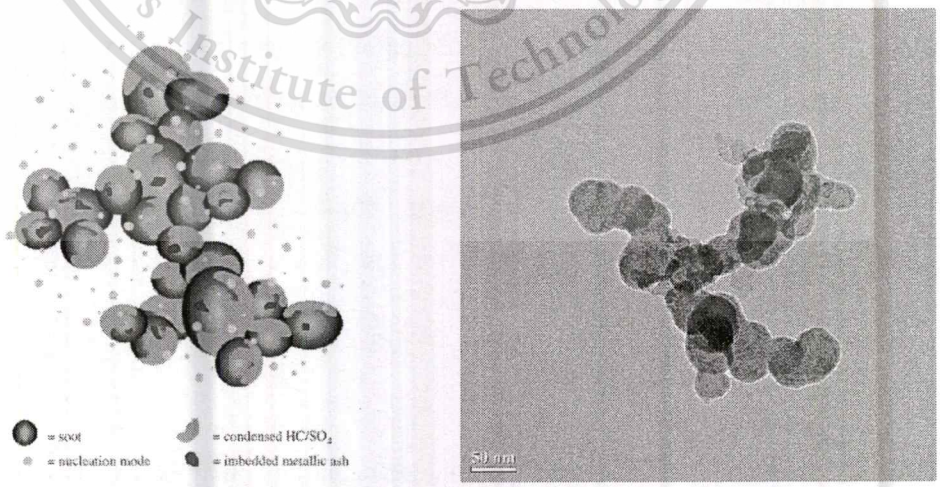

Figure 2.10 Artist's conception of diesel particulate matter (left) and diesel soot from TEM micrograph (right) [13]

When this happens, the hydrocarbons that are trapped inside the soot are burned out and the particle size reduces. During the diffusion burning stage of the combustion process, the soot particles produced in the initial phase of the combustion process come into contact with a much higher volume of air compared with fuel, and a large proportion of the soot particles are oxidized.

Further oxidation is required to reduce the amount of soot finally exhausted. When the exhaust valve opens, the combustion products are emitted to the exhaust system, which contains more oxidizing species. Oxidizing catalytic converters are used to reduce further the amount of soot emitted from the tailpipe. The majority of the soot formed is oxidized prior to exhaust. This is possibly why most soot particles are absorbed by the lubricant and relatively little is exhausted.

The concentration of the soot particles produced increases with an increasing air-to-fuel ratio. When the air-to-fuel ratio nears stoichiometric (14.5 for diesel fuel) [4], the rate of soot production increases dramatically. This is because near the stoichiometric ratio there is not enough time and oxygen in the cycle to burn all the fuel completely; also, there will be a low proportion of oxidizing species to oxidize the soot. Generally, at values of 20 per cent fuel lean of stoichiometric and higher, which are now being used, excessive amounts of soot are produced from the combustion process. Excess air is required to increase diesel cycle efficiency and to reduce hydrocarbon emissions.

Soot particles are generally assumed to be extremely hard individually and much softer when agglomerated. The harnesses of a variety of soots produced during a standard Cummins M-11 engine test were measured by Li et al. They were determined by carbon Plasmon energy methods, obtained from the electron energy loss spectra, which were measured using a high-resolution transmission electron microscope. It can be seen that soot taken from an engine operating with EGR is slightly harder than soot from an engine without EGR. This increase in hardness is possibly due to the secondary heating and oxidation process that the particles experience.

2.4.2 Soot Simulants

To investigate soot wear, there are essentially three options to choose from regarding the test particles. These are as follows:

- Used engine oil
- Extracted engine soot mixed with fresh engine oil
- Carbon black mixed with fresh engine oil.

Used engine oil is the most realistic option, but adds complications as the oil will contain other contaminants and wear debris, all of which will affect wear results. An extra complication of testing with used oils is that they are naturally degraded, but this is extremely dependent on use. Test oils would each need to be produced in an identical manner in an attempt to degrade the lubricant consistently by the same amount each time, as used engine oils will be mixed together to produce the required soot content for testing purposes. However, even this will not allow full control over the final amount of soot produced, which will vary from batch to batch. Laboratory techniques exist for ageing engine oils outside of an engine (without producing soot), studied by Mascolo et al. This is quite an unpredictable process, however, and would add further complications to the process. The process of producing used engine oils is expensive and time consuming.

The second method of extracting engine soot alone from a used lubricant allows for the assessment of the effect of soot alone on wear without any other contaminants or lubricant degradation issues. Using this method, the extracted soot is simply mixed in with the desired test lubricant. This method is more time consuming and expensive than the first method and reasonably practical for experimental purposes. The final method of using carbon black has for many years been the standard method for assessing the wear level due to soot contamination. This method is quick and inexpensive. The major drawbacks of this method are that carbon black, although very

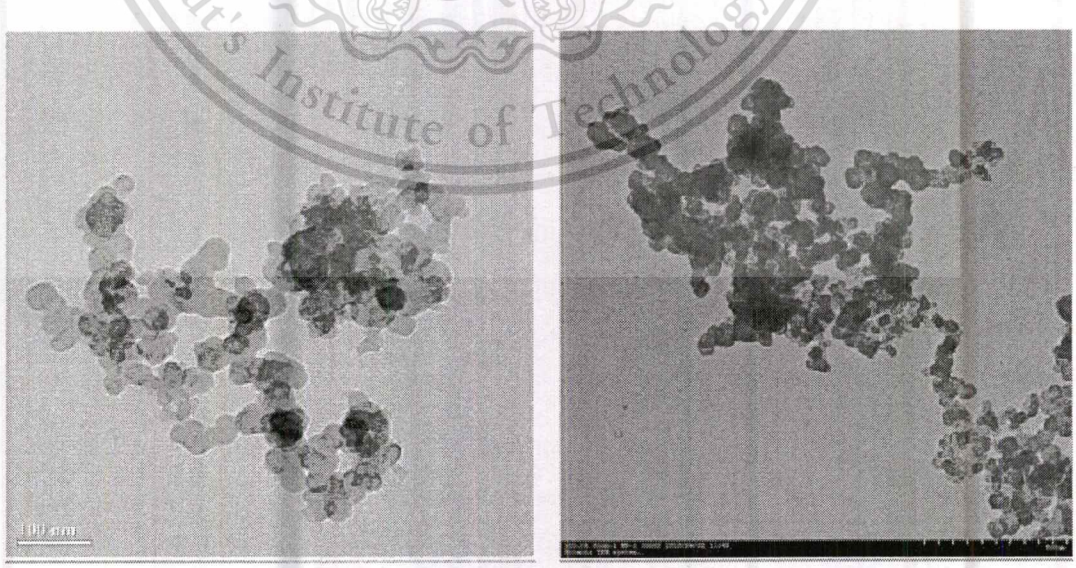

Figure 2.11 Morphological differences of diesel soot (left) and carbon black (right) [14]

similar to engine soot, is not engine soot, and produces results that industry has argued may be relative to tests with soot from used engine oil, but not directly comparable.

Carbon black particles do have the capability of mimicking the behavior of soot from engine oils, investigated by Clague et al. Findings showed that, whenlooking at primary soot particles (30–50 nm) using electron microscopy techniques, there is very little difference between engine soot and carbon black. There was a great deal of similarity in particle size and structure, confirming that the two are essentially the same on a nanometer scale. When investigating agglomerated soot and carbon black particles (up to 500 nm), carbon black was again found to be similar to engine soot, although a slight difference was discovered. The carbon black particles disperse in a similar fashion, but create a larger agglomerate diameter than extracted engine soot, greater by approximately 50 nm. Chemical analysis of soot and carbon black particles showed that contents. Oxygen and hydrogen were shown to concentrate on the surface of the carbon black, creating a relatively polar surface, meaning it will tend to have a greater tendency to interact with other polar species, for example, other carbon black particles. Prior to extraction from its lubricant, the engine soot displays a higher polar surface than carbon black, but, once the soot has been extracted from the lubricant, it becomes less polar than carbon black. This explains why carbon black particles created a larger-diameter agglomerate than extracted engine soot. Carbon black particles display higher carbon contents and lower ash and volatile.

2.4.3 Soot transport and entrainment in component contacts

It has been shown that, of the soot produced within the engine, only 29 per cent reaches the atmosphere through the exhaust pipe, with the remainder being deposited on the cylinder walls and piston crown. Of the soot that is retained in the engine (mainly in the lubricant), 3 per cent is attributable to blow-by gases; the remainder results from piston rings scraping away soot deposits in the cylinder,which then end up in the sump. It is then transported around the engine where it can be entrained into component contacts. Within the valve train, there are many component interfaces, all of differing geometries and motions, as shown in **Figure 2.6**. Sliding, rolling–sliding, and reciprocating contacts exist, some of which are conformal and some non-conformal. Because of the varying motion and loads at each interface, different regimes of lubrication will be apparent. This is further complicated by the mechanisms for lubrication application, which range from contacts where positive lubrication is used,

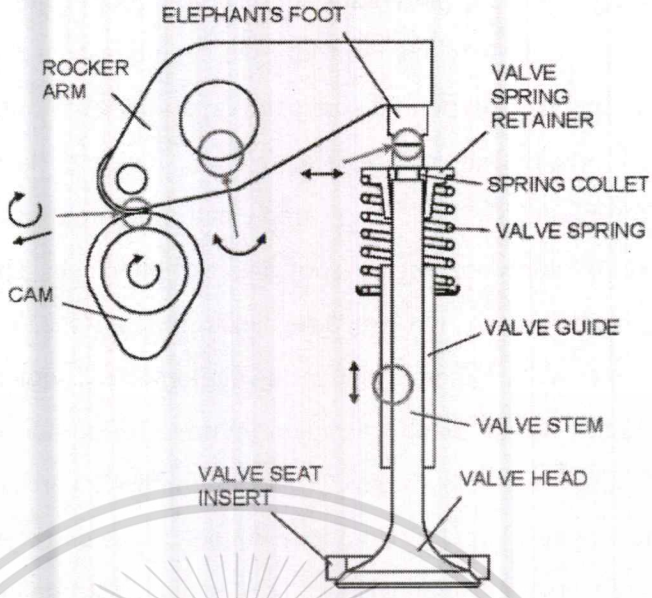

Figure 2.12 Sample valve train component contacts [5]

to those where lubricant reaches the contact indirectly by splash lubrication. In some cases, contacts receive little lubrication because of their location, and starvation problems can exist; the presence of soot will further exacerbate this.

2.5 Oil and wear analysis

Oil analysis (OA) is an extensive subject whose focus can be subdivided into (a) fluid Composition and thermo physical properties (e.g., room temperature viscosity, volatility, thermal conductivity, temperature-viscosity coefficient), (b) external contamination level, and (c) tribosystem-generated wear debris. It can help to indicate how much wear is occurring, from where the debris is originating, and even what form of wear is taking place.

Trending is an important element of oil analysis. By studying periodic oil samples, it is possible to track the progression of wear (including running-in) within a tribosystem in which the individual components may be difficult or impossible to inspect without disassembly. For example, oil analysis from an internal combustion engine may reveal whether wear is occurring in the main bearings, on the piston skirts, or piston rings. It may indicate whether the wear is abrasive in nature (cutting chip like debris) or more adhesive (metallic flakes). Therefore, OA can indicate both the locations and types of wear in a tribosystem.

2.5.1 Viscosity

The viscosity values most frequently reported for a lubricant are at 40 °C and 100 °C at atmospheric pressure and low-shear rates. Viscosity is a measure of a fluid's resistance to flow. The basic unit for absolute or dynamic viscosity is the Pascal-second (10 Poise). The common unit of absolute viscosity is centipoise, cP (1 mPa·s). The most common method of viscosity measurement is described in the ASTM D445 standard. Viscometers are devices that are used to measure viscosity. Most depend on the force of gravity to drive the fluid through a capillary. The viscosity value thus obtained is referred to as kinematic viscosity. The unit of kinematic viscosity is Stoke (St) or cent-Stokes (CST=0.01 St). One centistoke equals $1mm^2/s$. Absolute viscosity in centipoise (cP) is equal to kinematic viscosity in centistokes multiplied by the density of the fluid in kg/m^3 Viscosity index (VI), which is a measure of a lubricant's viscosity-temperature relationship, is based on 40 °C and 100 °C viscosity values (ASTM D2270).

2.5.2 Density and Specific Gravity

Density of a substance is defined by mass per unit volume and in liquids, such as lubricants, is expressed as gram/ milliliter (g/mL). Relative density, also known as specific gravity, is a measure of the density of a material relative to another material. Specific gravity of the liquids is equal to the density of the liquid divided by the density of water, and in gases, it is the density of the gas divided by the density of air. Specific gravity has no units. For liquids, density, hence specific gravity, is typically measured at 60°F or 15.6°C. Density of a material depends upon both pressure and temperature. Density change with temperature is called coefficient of thermal expansion and for liquids the more appropriate term is volumetric thermal expansion coefficient. This coefficient in liquids affects volume and is more sensitive to the boiling point of the hydrocarbon material or the component than to its density. Specific gravity is often used to identify specific lubricants, for example to distinguish between primarily paraffinic, naphthenic, and aromatic-based stocks.

2.5.3 Wear debris analysis

Ferrography is a very useful and comprehensive analysis for trending and reporting. At a minimum, the use can obtain an analytical means of monitoring the wear condition; and, at the same time, accrue the necessary sample points required to

establish a wear particle concentration baseline and retain the presence of non-magnetic particles for visual inspection and evaluation.

The advantage of Ferrography over other preventive maintenance systems is its capacity to detect a broader range of types and sizes (0.1-500 microns) of wear particles. A micron is 10-6 meters. Ferrographic analysis encompasses wear (metallic and non-metallic), contaminant (crystals, water, and organic and inorganic compounds), and lubricant (friction polymers) monitoring.

Typical wear problems identified by Ferrography; gear teeth wear through excessive load or speed, misalignments, fractures, rolling contact failure, water in the oil or poor lubricant condition, oil additive depletion, outside contaminants such as sand or dust, cam shaft and cylinder wall failure, oil filter failure. There are many others.

Industrial application of Ferrography entails the non-interruptive machine condition monitoring of heavily used lubricated mechanical systems. Hence, an operational baseline can easily be established by sampling every 50-500 hours of operation (approximately every one to three months, depending on system criticality), and used for quantitative trending analysis. Any anomalies in the wear particle concentration, especially in the generation rate of large particles (>20 microns), is symptomatic of the onset of failure. For consistent results and accurate trending, lubricant samples are taken from the same places in the system each time. The method of sample extraction assures that the lubricant samples contain a Representative selection of wear particles. The samples are then ferrographically Analyzed both quantitatively and qualitatively.

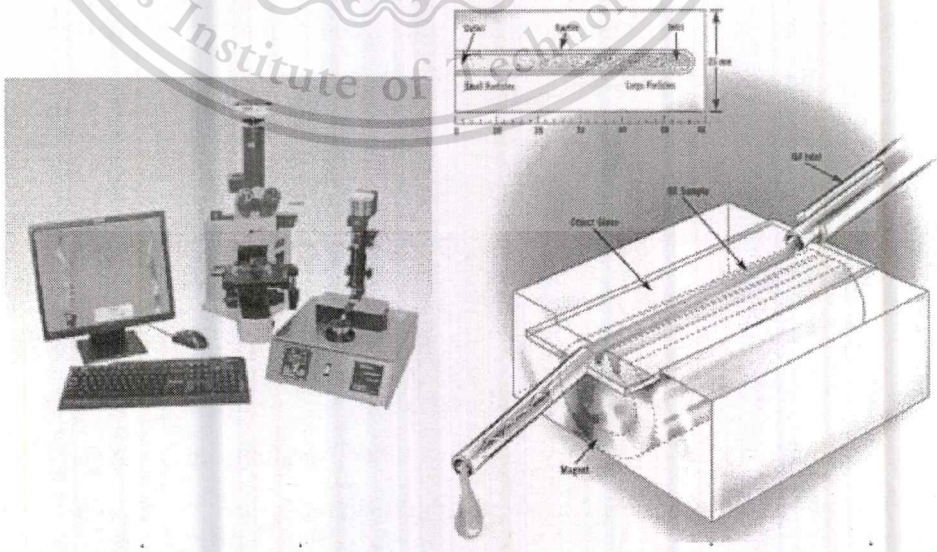

Figure 2.9.1 Bichromatic microscope and Ferrogram analysis method [15, 16]

The ferromagnetic particles are sorted by gravity according to relative size, with larger particles appearing at the leading entry of the ferrogram. Non-magnetic particles (including contaminants and friction polymers) are distributed throughout the ferrogram. This process indicates the presence of contaminants, the condition of the lubricant, and the material composition of the abnormal wear particles being generated, from which the source of the wear may be deduced.

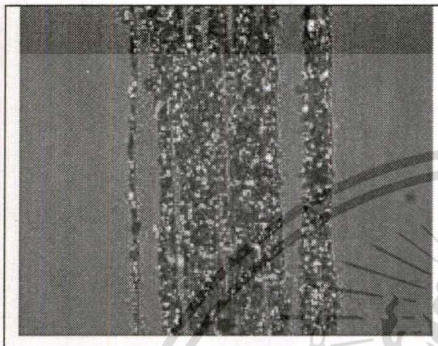	**Normal rubbing wear** Individual particles are generally 5 Microns and below. The quantity of these particles determines the wear Rate. There should be little or no visible texture to the surface, and the thickness should be 1 μm or less.
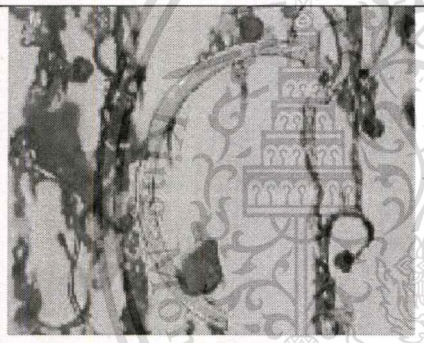	**Curled cutting wear particles** Such as this are usually generated as a Result of misalignment or abrasive particle embedded in a Babbitt bearing cutting wear particles may resemble wire, drill turnings, whittling chips, or gouged-out curls.
	**Red oxide** These particles resemble severe sliding wear particles, except that they are usually gray. They are formed in conditions of inadequate lubrication.
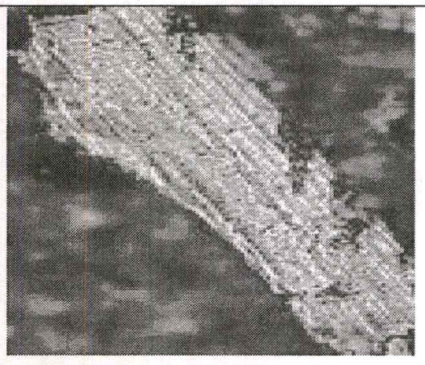	**Severe sliding wear** These particles are identified by parallel striations on the surface. Sliding wear particles sometimes show evidence of temper colors, which may change the appearance of the particle after heat treatment.

Figure 2.9.2 Wear particle and wear mechanisms [17]

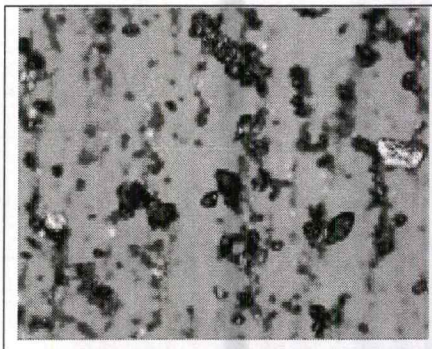	**Black oxides** Black oxides are dark gray to black, and they resemble pebbles. More iron is being consumed in the oxidation process, as a result of inadequate lubrication.
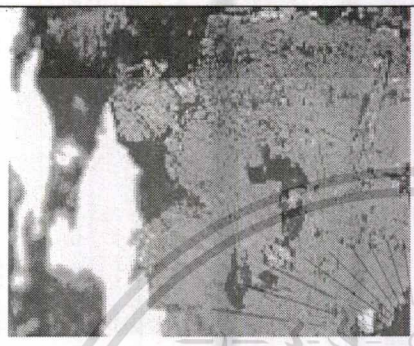	**Chunks** Chunks are generally greater than 5 μm in major dimension, with the length-to-thickness ratio being less than 5:1. There is generally some surface texture, and the particles do not appear flat. Instead, they are rough and shaped like chunks, but they are thinner.
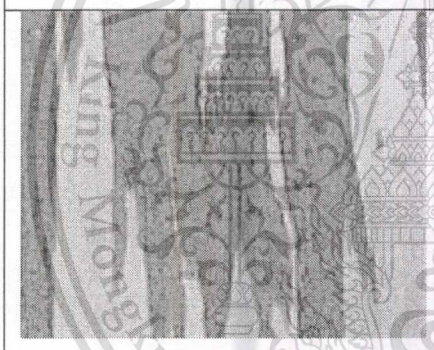	**Corrosive wear** When acids and other corrosive agents attack the surfaces of the machine and its wear particles, submicron-sized free metal particles, oxides, and other metal compounds are yielded. The size of this deposit can warn of chemical attack on the equipment
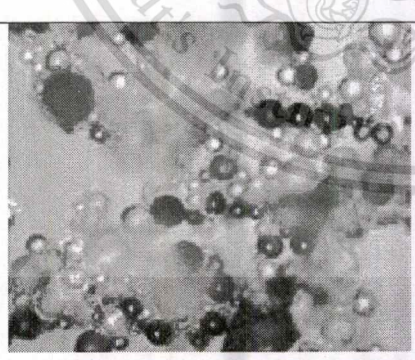	**Dirt and dust** Dirt and Dust are contaminants particles which are transported into the engine oil during combustion process.

Figure 2.9.2 Wear particle and wear mechanisms (continues) [17]

2.5.3.1 Scanning electron microscope

The scanning electron microscope (SEM) uses a focused beam of high-energy electrons to generate a variety of signals at the surface of solid specimens. The signals that derive from electron-sample interactions reveal information about the sample including external morphology (texture), chemical composition, and crystalline structure and orientation of materials making up the sample. In most applications, data are collected over a selected area of the surface of the sample, and a 2-dimensional image is generated that displays spatial variations in these properties. Areas ranging from approximately 1 cm to 5 microns in width can be imaged in a scanning mode using conventional SEM techniques (magnification ranging from 20X to approximately 30,000X, spatial resolution of 50 to 100 nm). Electrons are produced at the top of the column, accelerated down and passed through a combination of lenses and apertures to produce a focused beam of electrons which hits the surface of the sample. The sample is mounted on a stage in the chamber area and, unless the microscope is designed to operate at low vacuums, both the column and the chamber are evacuated by a combination of pumps. The level of the vacuum will depend on the design of the microscope. The position of the electron beam on the sample is controlled by scan coils situated above the objective lens. These coils allow the beam to be scanned over the surface of the sample. This beam scanning, as the name of the microscope

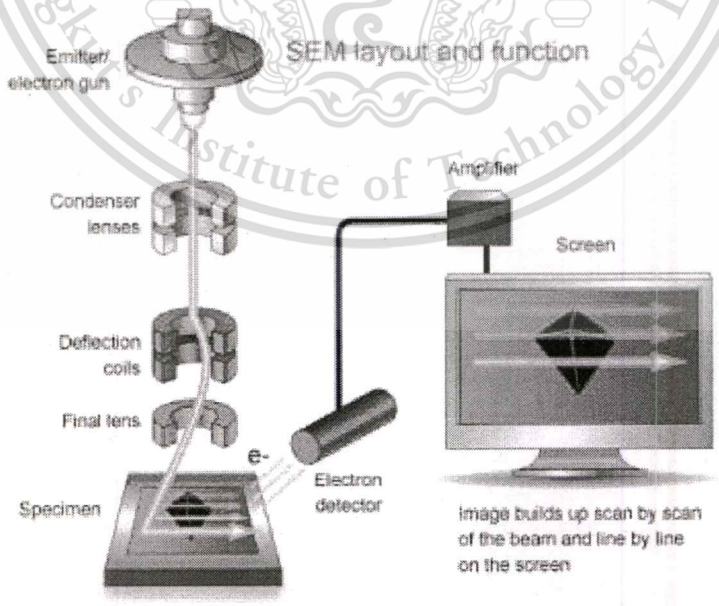

Figure 2.9.1 Schematics of scanning electron microscopy operation [18]

suggests, enables information about a defined area on the sample to be collected. As a result of the electron-sample interaction, a number of signals are produced. These signals are then detected by appropriate detectors.

2.5.3.2 Transmission electron microscope

The transmission electron microscope (TEM) is a very powerful tool for material science. A figure 2.14 shown schematic of transmission electron microscopy operation by a high energy beam of electrons is shone through a very thin sample, and the interactions between the electrons and the atoms can be used to observe features such as the crystal structure and features in the structure like dislocations and grain boundaries. Chemical analysis can also be performed. TEM can be used to study the growth of layers, their composition and defects in semiconductors. High resolution can be used to analyze the quality, shape, size and density of quantum wells, wires and dots. The TEM operates on the same basic principles as the light microscope but uses electrons instead of light. Because the wavelength of electrons is much smaller than that of light, the optimal resolution attainable for TEM images is many orders of magnitude better than that from a light microscope. Thus, TEMs can reveal the finest details of internal structure - in some cases as small as individual atoms.

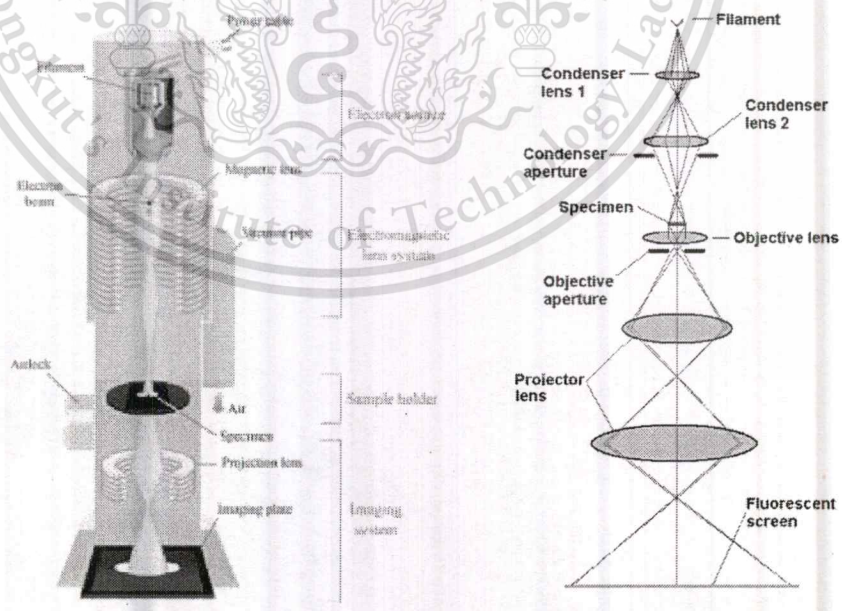

Figure 2.9.1 Schematics of transmission electron microscopy operation [19]

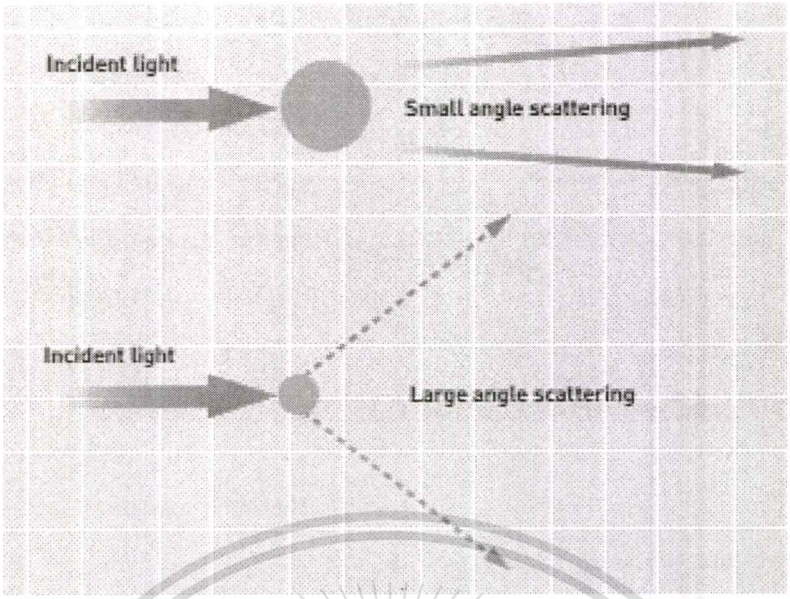

Figure 2.9.1 light scatted pattern of the small and large particle [20]

2.5.3.3 Laser Diffraction spectroscopy

Laser Diffraction spectroscopy is widely used for ranging a particle size distribution from hundreds of nanonetrs yp tomilimaters in size. It hits a laser beam passes through a particle and measure the intensity of the scattered light. Diffracted and refracted light is useful for this purpose; absorbed and reflected light works against this purpose and must be taken into account during measurement and size calculation. Large particles scatter light at small angles relative to the laser beam and small particles scatter light at large angles as shown in Figure 2.9.1. The angular scattering intensity data is then analyzed to calculate the size of the particles that created the scattering pattern using the Mie theory of light scattering. The particle size is reported as a volume equivalent sphere diameter. In this study used MALVERN Mastersizer 3000. The machine is capable for measuring particles between 0.01 and 20000 microns.

2.5.4 Oxidation Stability

Most lubricant applications are in the presence of air or oxygen; hence a lubricant to have good oxidation stability is highly desirable. All hydrocarbon materials undergo oxidative degradation. Unlike thermal stability which is inherent to the base stock, oxidation stability can be greatly improved by the use of the oxidation inhibitors. The consequences of oxidation are a lubricant's viscosity increase and the formation of acids and deposits, such as varnish and sludge. A wide variety of tests are available to

assess a lubricant's oxidation stability. These include tests that are described in the ASTM Standards D2272 and D1313. These tests are suitable for measuring a lubricant's stable life and the effectiveness of the oxidation inhibitors. To monitor the oxidation process, a micro-oxidation test, such as the Penn State micro-oxidation test, has been developed along with the analytical procedures based on gel permeation Chromatography (GPC) and atomic absorption spectroscopy (AAS).

2.5.5 Nitration

Nitration: The combustion chambers of engines provide one of the few environments where there is sufficient heat and pressure to break the atmospheric nitrogen molecule down to two atoms that can react with oxygen to form nitrous oxides (NOx). This becomes a major problem for some engines, especially EGR engines. When nitrogen oxide products enter the lube oil through EGR and normal blow-by, they react with moisture present in the lube and become very acidic and rapidly accelerate the oxidation rate of the oil. The GCF Filter controls the effects of nitration in the same ways it controls oxidation. By delivering cleaner oil to offer as a seal between the ring and liner, blow-by of NOx is kept to a minimum. Also, the GCF Filter keeps the oil chemically dry and prevents the mixing of NOx and moisture, which controls NOx acid formation and accelerated oxidation of the oil.

2.5.6 Total base number

The total base number, or TBN, of the detergent reflects its ability to neutralize acids. In the case of the basic suffocate and phosphate detergents, only the over based portion of the detergent, i.e., the carbonate and the hydroxide, possess this capability. The neutral metal sulfates and phosphates, or the soaps, lack this ability. However, in the case of the basic carboxylates, salicylates, and phonates, the soaps also possess the acid neutralizing ability. This is because unlike the sulfates and phosphates that are strong acid—strong base salts, metal carboxylates, metal salicylates, and metal phonates are strong base-weak acid salts. This makes them Lewis bases, hence the acid neutralizing ability. The total acid number (TAN) of oil is synonymous with neutralization number. The TAN of oil is the weight in milligrams of potassium hydroxide required to neutralize one gram of oil and is a measure of all the materials in oil that will react with potassium hydroxide under specified test conditions.

2.5.7 Elemental and Structural Analysis

Petroleum, or crude oil, contains a wide variety of elements, some of which are present at percent levels and others at parts per million levels. However, refining processes used to manufacture fuels and mineral base oils remove most elements other than carbon, hydrogen, oxygen, nitrogen, and perhaps sulfur. Additives used to formulate lubricants contain elements that are used either to facilitate their solubility in base fluids or impart special properties. Common elements include nitrogen, sulfur, phosphorus, alkaline earth metals, zinc, copper, and molybdenum. A list of elements That are generally used in lubricants is provided in **Table 2.1**, along with their role X-Ray Fluorescence Spectrometer (WDXRF) is a powerful analytical instrumental method used in a wide variety of industries to determine the elemental composition of various materials.

Table 2.1 Chemical elements present in lubricants and their role [10]

Element	Compounds	Performance
Boron (B)	Borax and esters	Anti-wear agents, oxidation inhibitors, deodorant cutting oils
Barium (Ba)	Sulfonates, phenates, phenates, dialkyl phosphates, phosphonates and thiophosphonates	Detergents inhibitors, corrosion inhibitors, detergent and rust inhibitors
Calcium (Ca)	Sulfonates, phenates, carboxylates, and salicylates	Detergents, detergent inhibitors, dispersants
Magnesium (Mg)	Sulfonates and phenates	Detergents inhibitors
Molybdenum (Mo)	Molybdenum disulfide and alkyl phosphate	Extreme-pressure additives
Phosphorus (P)	Metal dialkyl dithophosphates	Oxidation inhibitors, anti-wear agents, rust inhibitors
Zinc (Zn)	Dialkyl dithiophosphates, dithiocarbamates and pheolates	Oxidation inhibitors, corrosion inhibitors, detergents, extreme – pressure additive and anti-wear agents, rust inhibitors

2.6 Tribology Tests

Torbacke *et al.* [14] wrote an introduction to tribological test methods that there are many reasons for carrying out tribology test or tribotest. One reason is to study wear and friction mechanism appearing in specific tribological application. Other reasons are ranking of materials and lubricants for existing equipment or selection of materials and lubricants for new application. Tribotesting may also be performed for general characterization of wear and friction. Tribotests can be classified into tests that simulate the function of real components or tribological systems and tests that simulate the critical tribological load. The former class includes field tests, bench tests and component tests. The latter class comprises different model tests. All testing aims at increasing the tribological understanding at the fundamental or system level in order to enable development of design, construction and function of tribological systems. The complexity of testing may differ as well as the time and cost for testing.

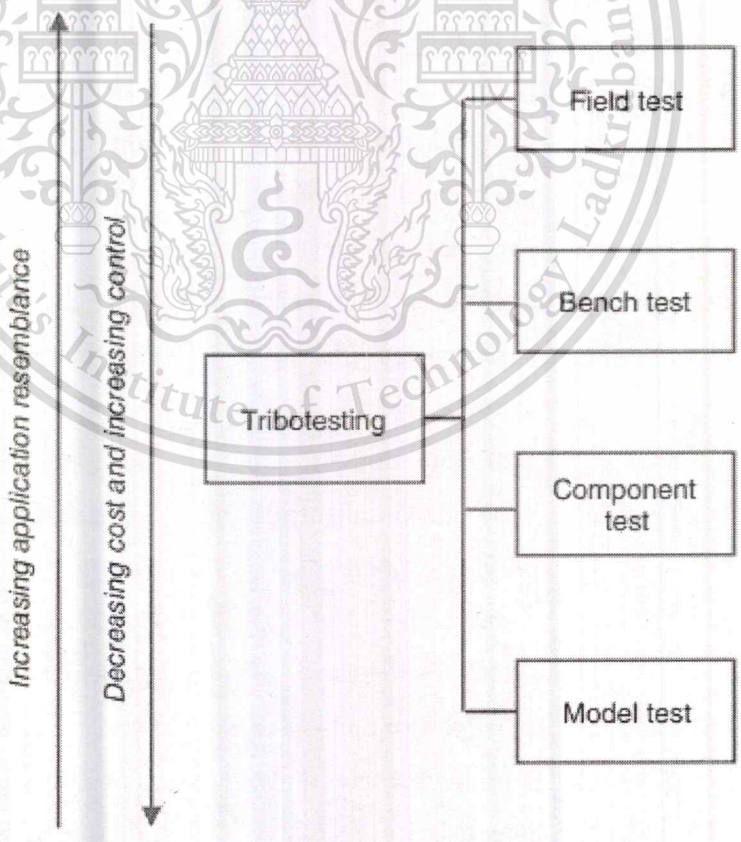

Figure 2.9 Different types of tribological tests [10]

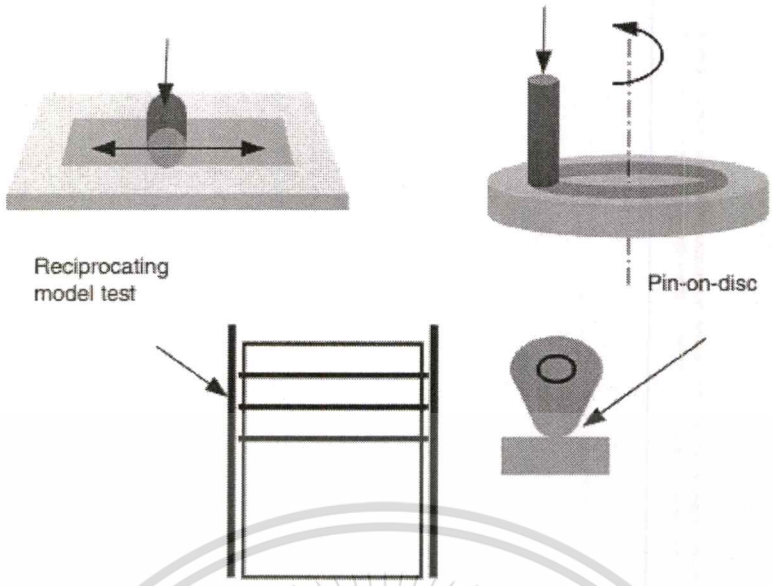

Figure 2.10 Tribology selection for typical combustion engine [12]

With testing involving contaminants, it is essential that a good representation of the contact motion, loading, and geometry is achieved if bench testing is to be used. Entrainment of the contaminants will be directly affected by these and is key to determining which wear process may occur. This means that the best approach would probably be to use actual components. Engine tests are always problematical. It is difficult to control many of the test parameters and to provide good wear measurements. However, standard engine test cycles designed to promote soot production have been defined, as will be outlined in a later section, that allow soot wear studies to be carried out.

The model test selected should provide the closest possible resemblance to the application in mind. The first step is to evaluate the contact geometry that is the form or shape of the contacting bodies and whether the contact is formed. The contact geometry directly affects the local conditions in the contact and is considered to be the primary variable for selecting model test and for scaling up and scaling down of tests. Finally, the test duration must be set long enough for the test to be correctly evaluated.

The combustion engine is lubricated with one lubricant operating in the boundary to the full-film regime. Two parts of a combustion engine have been selected to show the use of model testing, seeing on Figure 2-2. The piston–

cylinder liner and the cam–follower represent two different types of lubricated contacts in an engine. Due to the combustion in the engine, the piston–cylinder is exposed to very high temperatures. The cam–follower is exposed to very lower temperatures.

The piston–cylinder liner shows a start–stop phenomenon at the turning points of the piston, that is reciprocating motion. The lubrication regime changes from boundary to mixed lubrication for each stroke. Therefore, the reciprocating tribotest is chosen. The environment can be controlled and monitored by adding a hood to the tribotest. This will make it possible to run tests at temperatures relevant for the application.

2.7 Prior state of research

Previous studies have attempted to understand the soot induced wear mechanism and have suggested various phenomenological models. Although these models have contrasting explanation among themselves but have provided the better understanding of the subject matter.

Rounds performed tests on a four-ball wear testing machine with soot contaminated oil samples. The oil samples were obtained from a number of sources by normal oil drain process. Tests were performed on a four-ball wear testing machine using the collected samples to evaluate the oil properties in presence of soot. According to Rounds, soot did not act as an abrasive, but soot preferentially adsorbed the anti-wear additive. This was the plausible reason he provided for the wear taking place in a diesel engine. He concluded that ZDP was the most effective anti-wear additive in the presence of diesel soot.

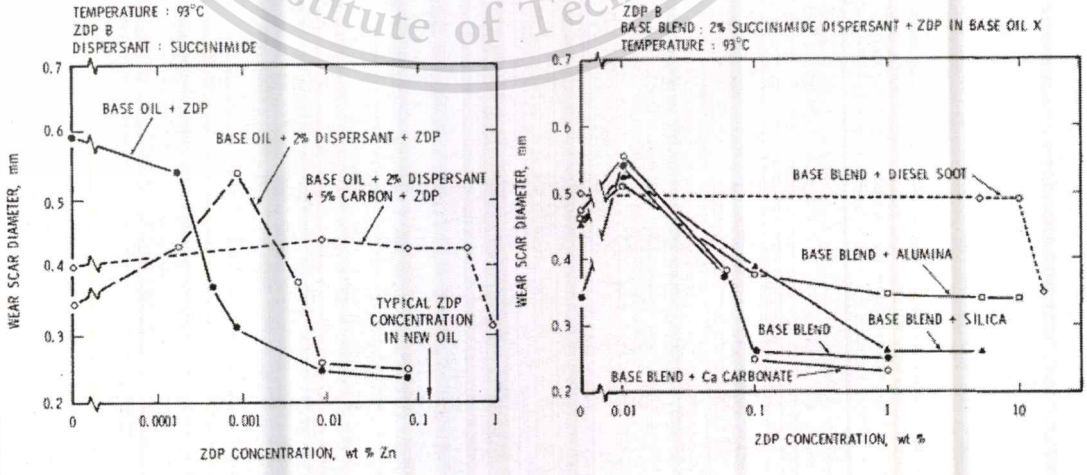

Figure 2.11 Effect of Carbon black on wear and Effect of potential abrasion on wear [21]

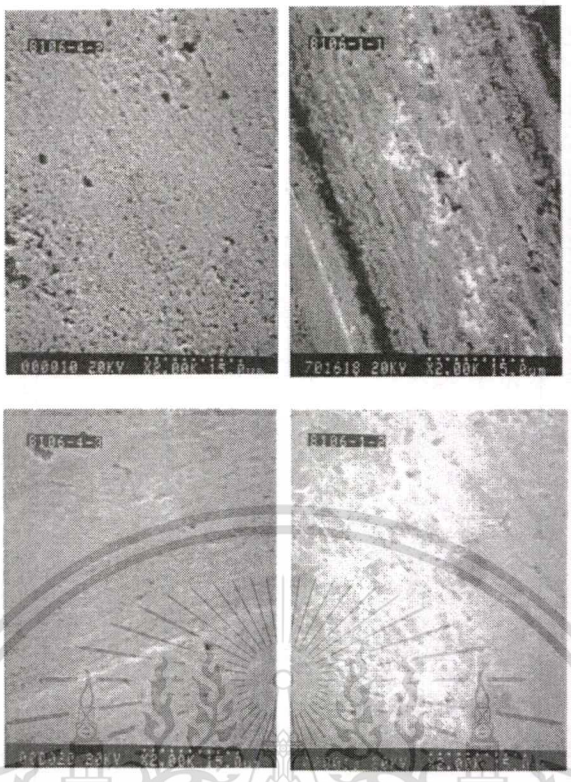

Figure 2.12 SEM micrographs of the ball surface in the oil (a) alone and oil containing (b) Cab-O-Si, (c) Alon C and (d) Carbon black [22]

He also performed hardness tests on soot and alumina, which is a known abrasive. Rounds disagreed with the concept that soot removed the surface coating by abrasive phenomenon, since the hardness of soot is lower than the hardness of alumina. He also suggested that engine load and EGR have a large effect on the soot pro-wear characteristics. Many authors have disputed the adsorption theory proposed by Rounds.

Ryason et al. performed wear tests on a ball-on flat- disk tribometer using carbon black and steel balls made of AISI 52100 steel. Wear tests were performed on carbon black, alumina and silica. Investigations were carried out on the wear scars from the tests using scanning electron microscope (SEM) and electron probe microanalysis. The SEM pictures showed that the scars on the surfaces of the balls worn in the presence of oils containing carbon black, alumina and silica were similar, and differ from that of the ball worn in the presence of oil alone. Ryason concluded that the wear that occurred was polishing in nature. He also suggested that although the wear was abrasive in nature, the cutting of the material did not take place. The soot particles ploughed through the surface, forming a groove with a smooth curved cross-section, depressed at the center and raised at the edges.

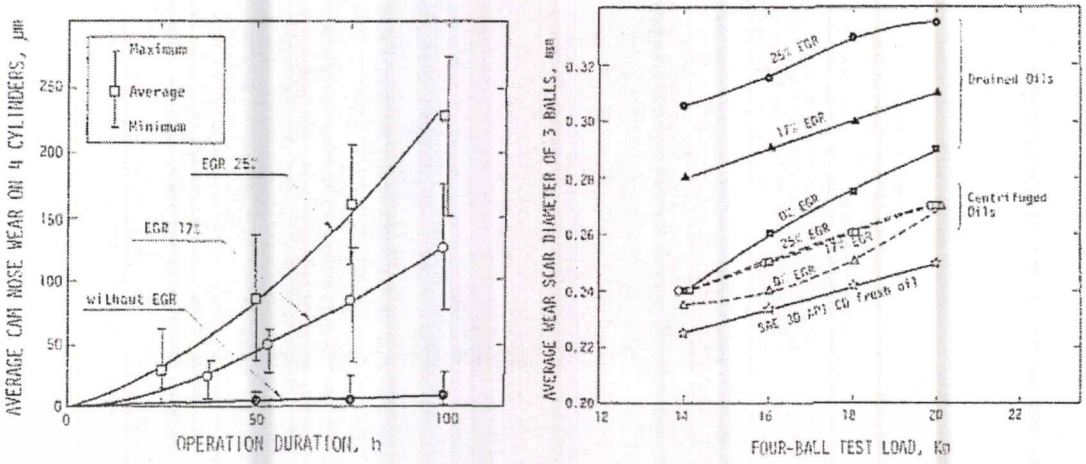

Figure 2.13 Engine cam wear and Four-balls wear test [23]

Nagai et al. performed tests on valve train and studied the wear in the presence of soot. They concluded that the wear of cam noses and rocker arm tips was found to increase significantly with the increase in EGR rate. The drain oil analysis at the end of each EGR test run indicated evidence of elements such as zinc and phosphorous. This contradicted the adsorption theory proposed by Rounds initially. Tests were also performed on four-ball wear testing machine and it was concluded that, soot strips off the anti-wear film formed on the lubricated metal surface and the subsequent metallic contact accelerated the wear process. They also concluded that soot
Might change to a very hard particle under the high-pressure conditions and might be abrasive to the metal.

Needelman and Madhavan studied the effect of lubricating oil components, and nature of contamination on engine wear. They proposed the chain-reaction of wear and conducted a survey of engine oil contamination and the necessary improvements that had to be accomplished to reduce this contamination. They concluded that contamination of the lube oil causes wear of engine components and also suggested that, a special relationship is present between the size of the contaminant particles and the thickness of dynamic oil films. The contaminant particles larger than the oil film cause wear of engine components by making simultaneous contact with both the surfaces.

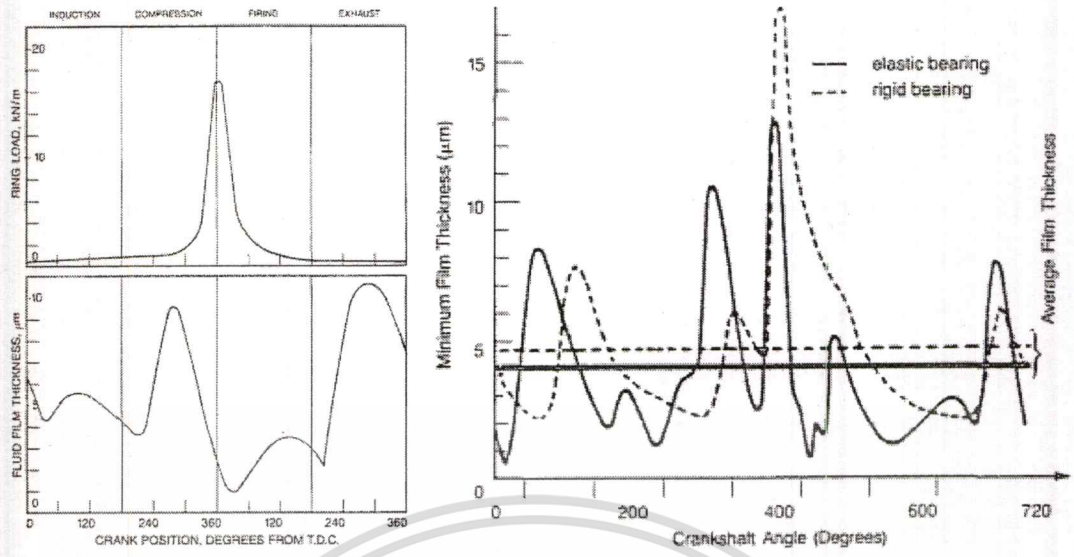

Figure 2.14 Predicted ring loads and film thicknesses (left) and film thickness for elastic and rigid bearing (right) [24]

Gautam et al. investigated the effects of soot contaminated engine oil on three-body wear. Phosphorous level, dispersant level and sulfonate substrate level were the three oil additives they tested and concluded that there is an interaction between oil additives and soot in reducing the oil's anti-wear properties. They also concluded that wear increases with higher soot concentration and decreases with higher phosphorous concentration. They also performed tests on the ball-on-flat-disk setup with soot and alumina and compared their wear ratios. It was concluded that abrasion could be the major mechanism involved in the diesel engine wear.

Gautam et al. also investigated the effects of base stock, dispersant level, and ZDP level on three-body wear. The study considered soot at two levels and hence could not determine the non-linear effect of soot on three-body wear. Results indicated that the oil's anti-wear properties were reduced as a result of soot. The statistical analysis led to the conclusion that base stock and dispersant levels were significant on oil's wear Performance, while the effect of ZDP was negligible within the range of concentrations tested. Ball-on-flat-disk tests showed that the wear scar diameter as a result of soot was similar to that due to alumina indicating that the wear due to soot is abrasive in nature. EDAX (energy dispersive X-ray analysis) tests performed on soot samples showed that there was no adsorption of anti-wear agents by soot.

CHAPTER 3

RESEARCH METHODOLOGY

3.1 The Study of the physical and chemical properties of diesel engine used oil

In this study, the used engine oils were collected from the small diesel engine vehicles. The details of the diesel engine specification were shown in **Table 3.1.** The engine was used a formulated engine SAE0W30 engine oil. The engine oil conditions including kinematic viscosity, oxidation, nitration and total base number were measured according to ASTM standard test methods. Engine oil additive elements were measured by x-ray fluorescence. In order to investigate the physical and chemical properties of diesel engine used oil in the real situations. The used engine oils were collected from the small diesel engine vehicles with different oil changed interval. The engine oil's mileage and oil aged were in the range 3,000-20,000 and 0-10,000 km, respectively as shown in **Table 3.2** After that, the contaminants including fuel, soot and metal wear particles were measured according to ASTM standard.

1. Physical and chemical properties
   - Kinematic viscosity @ 40°C (ASTM D-445)
   - Kinematic viscosity @ 100°C (ASTM D-445)
   - Oxidation (ASTM E-2412M)
   - Nitration (ASTM E-2412M)
   - Total base number (ASTM D-4739)
2. Contaminants
   - Soot contamination (ASTM E-2412M)
   - Fuel contamination (ASTM E-2412M)
   - Metal elements (ASTM D-6595)
3. Wear particle analysis
   - Wear mechanisms (Ferrography)
   - Particle size distribution (Laser diffraction spectroscopy)

This study is trying to inspect the amount of fuel and soot contamination in used oil and expecting to see the relationship between the amount of the contaminants level

Table 3.1 Engine specification

Engine parameter	Specification
Displacement volume	1,500 cc
Bore x Stroke	76.0 x 82.6 (mm)
Compression ratio	14.8
Maximum Power	105/4000 (hp/rpm)
Maximum Torque	280/1,500-2,500 (Nm/rpm)
Lubricant	SAE 0W-30

Table 3.2 Used oil's mileage and oil age

Used oil samples	Mileage (km)	Lubricating oil age (km)
1	1,980	1,980
2	3,975	3,975
3	6,275	6,275
4	8,468	8,468
5	9,993	9,993
6	11,237	11,237
7	19,046	9,362
8	19,500	9,800
9	19,613	9,448
10	19,779	9,811

and oil condition changing. The assumption is that soot particle is consisting of carbon, unburned hydrocarbon, and other combustion products such as sulfur, oxygen, nitrogen. Then when the contaminants contaminate into lubricating oil, it may react with oil by chemical reaction and then oil's properties change (oxidation, nitration, TBN). It may also react with oil by physical reaction and then viscosity change. Furthermore, from all publication literature review, they suggested that fuel and soot contamination is the main factor which induces more wear in automobile engine.

3.2 The study of commercial carbon blacks morphology

Transmission Electron Microscope (TEM) was used to investigate the physical properties and nanostructure parameters of different types of commercial carbon black. The main target is to define the average carbon black's primary particles size and primary particle's size distribution. The TEM machine **(JEOL JEM-2010)** which used in this study is shown in **Figure 3.1** The following carbon black were used. They were commercial carbon black N220, N330, N550 and N660. The CB sample was prepared by following method. The CB powder was isolated by using ultracentrifugation with heptane as the diluent and it was adhered to TEM grid. Then, the CB which was adhered on the grid was observed in Nano - scale by using TEM. After that, the TEM micrographs of CB was used to determine the primary particle size distribution by using measurement program (Image J). The area of primary particle were measured by using an elliptical shape selection and convert that area to diameter as shown in **Figure 3.2** The results showed a comparison of primary particle size distribution of each tpyes of comercial carbonblack.

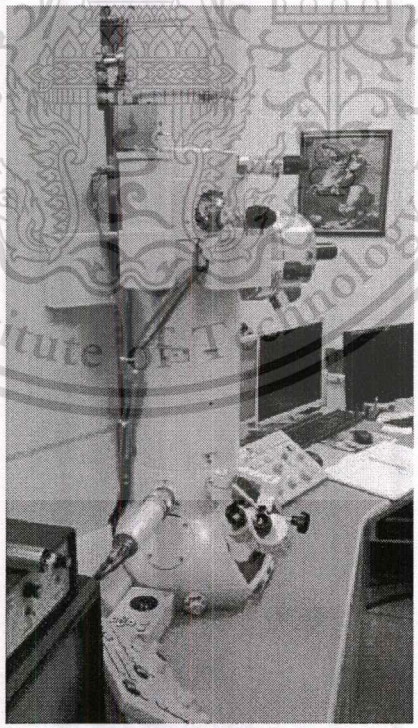

Figure 3.1 Transmission electron microscope (JEOL JEM-2010)

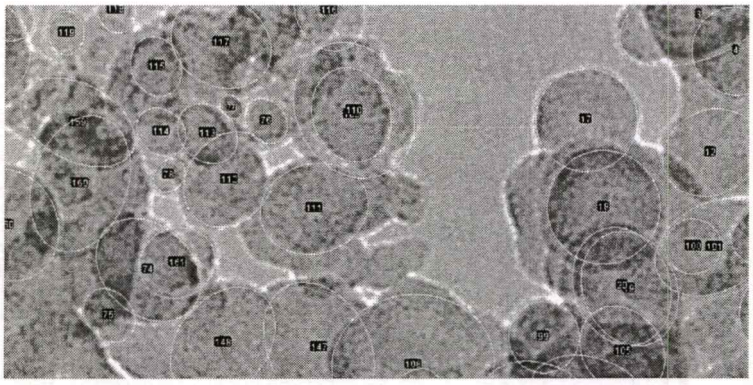

Figure 3.2 The measurement of carbon black primary particle

3.3 The study of carbon blacks size distribution in formulated engine oil

The main purpose of this test is to analyze the statistical association of different types of carbon black distribution in formulated engine oil by means of Laser particle size detector.

In this case study, there are 2 major conditions for testing.

1) Behavior of different types of carbon black dispersing in formulated engine oil.

2) Oil additives in formulated oil are investigated by X-ray fluorescence tool (XRF).

The angular scattering intensity data is then analyzed to calculate the size of the particles responsible for creating the scattering pattern, using the Mie theory of light scattering. The particle size is reported as a volume equivalent sphere diameter.

The second test, there are a trying to study the ability of additive in modern oil so more samples are tested with laser diffraction technique and checked additive by XRF. X-ray fluorescence (XRF) is a powerful analytical instrumental method used in a wide variety of industries to determine the elemental composition of various materials. In oil analysis especially, XRF techniques have gained wide acceptance. Among other applications, XRF is used to determine Sulphur in petroleum products and residual catalysts, monitor additives in lubricating oils, analyze regular wear metal in lubricants and analyze wear debris. The oil samples were mixed with a suitable solvent and introduced into the plasma of the pectrometer. The plasma is generated by a powerful radio frequency discharge and very high temperatures. When the different elements are subjected to such high temperatures, they will emit light of different frequencies.

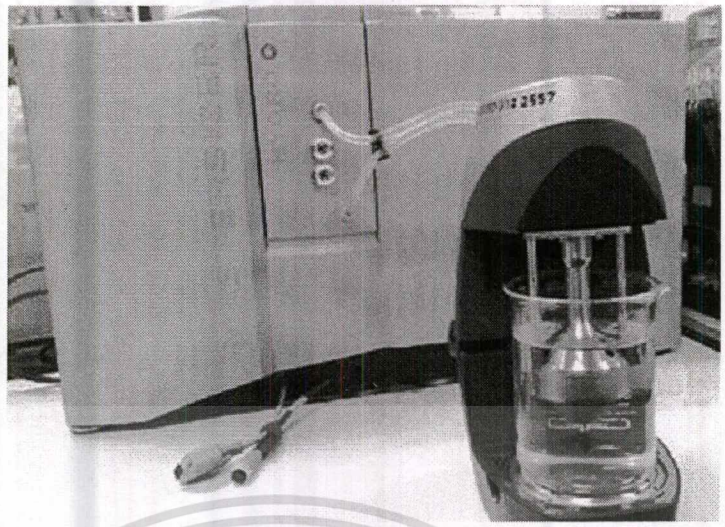

Figure 3.3 MALVERN Laser Diffraction Spectroscopy

3.4 The Impact of Biodiesel and Soot Contamination on Metal Wear

The four-ball wear tester is well-known a tribology test bench. This test method can be used to determine the relative wear preventive properties of lubricating fluid in sliding contact under the prescribed test conditions. No attempt has been made to correlate this test with balls in rolling contact [43]. In this wear test, the test methods and conditions followed the standard ASTM D4172 as shown in **Table 3.3.** The machine consists of four 12.7 mm. steel balls which covered with lubricating oil as shown in **Figure 3.4**. The three lower balls were held in a steel cup with fixed position and the top ball was pressed with 300 N of force. The operating temperature was regulated at 75 °C and the top ball was rotating at 1,200 rpm for 60 min. Circular wear scars will appear on the three lower balls, while a circular wear track will appear on the upper ball.

In this wear tests, there are 2 major conditions for testing.

-The impact of biodiesel contamination on metal wear, the different types of palm biodiesel blend were mixed with the engine oil at 2% by volume. The types of biodiesel were B7, B20, B50 and B100. The details of engine oil mixed with biodiesel were shown in **Table 3.4.**

- The impact soot Nano particle sizes on metal wear. The different types of carbon blacks (CB) were mixed with the engine oil at 1% by weight per volume. The types of commercial Carbon black N**220**, N**330**, N**550** and N**660**. The details of oil samples and CB average particle size were shown in **Table 3.5.**

Table 3.3 ASTM D-4172 conditions tests

Test conditions		Ball material	
Parameter	**Specification**	**Parameter**	**Specification**
Rotational speed	1200 rpm	Ball material grade	25 EP
Load	392 N	Surface roughness	0.005 microns
Duration per load	60 min	Ball hardness	64 – 66 (HRC)
Temperature	75°C	(Rock well)	

Table 3.4 Engine oil mixed with biodiesel

Samples	%SAE 0W30 (Vol.)	Biodiesel	% Fuel (Vol.)
NE	100 %	-	-
EB7	98 %	B7	2 %
EB20	98 %	B20	2 %
EB50	98 %	B50	2 %
EB100	98 %	B100	2 %

Table 3.5 Engine oils mixed with carbon black

Samples	Carbon Black	Average Primary Particle size according to standard (nm)	% CB (wt. / vol.)
NE	-	-	-
EC2	N220	21	1 %
EC3	N330	31	1 %
EC5	N550	53	1 %
EC6	N660	63	1 %

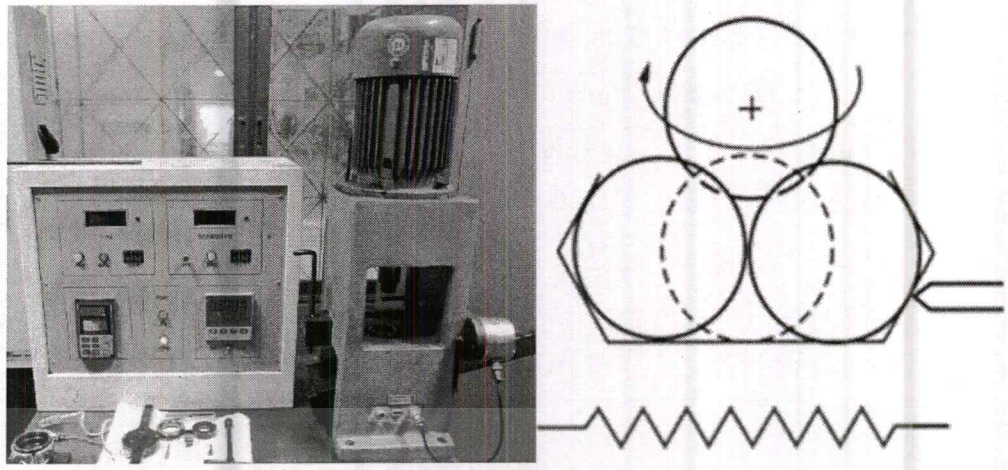

Figure 3.4 Schematic of Four-ball wear tester followed ASTM - D4172

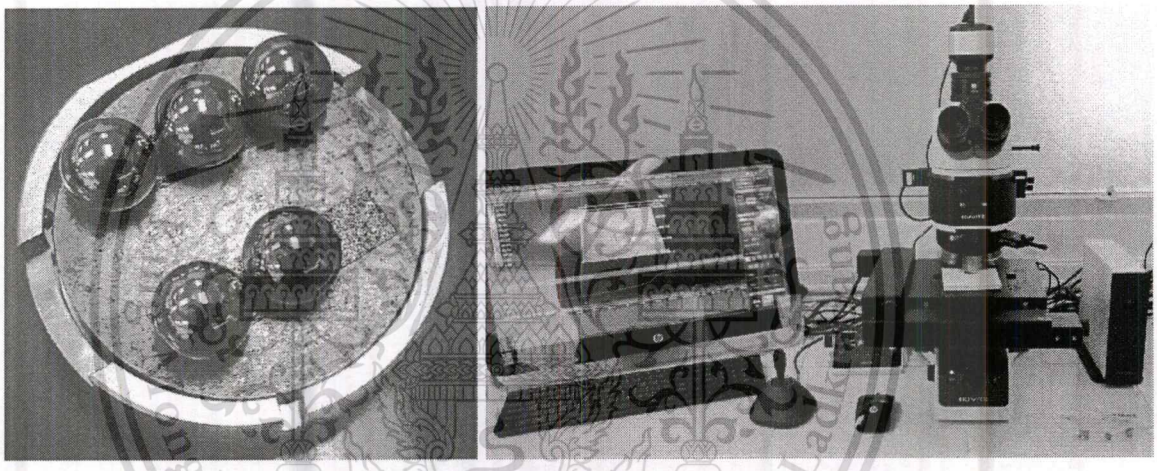

Figure 3.5 Four-ball tested balls and optical microscopy

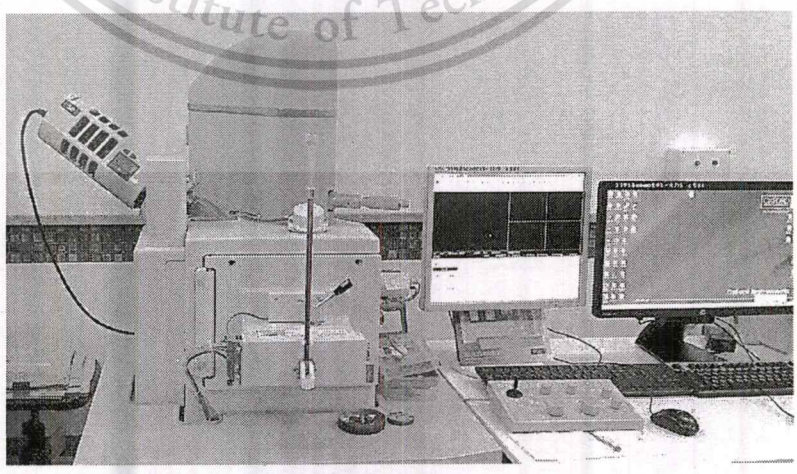

Figure 3.6 Schematics of Scanning Electron Microscope and Energy Dispersive X-Ray

CHAPTER 4

RESULTS AND DISCUSSION

A formulated engine oil which had the same grade as SAE0W30 was used in this research. The engine oil condition including viscosity, oxidation, nitration and total base number (TBN) were measured according to ASTM standard test methods. Oil additives were measured by x-ray fluorescence. Additives used to formulate lubricants contain elements that are used to impart special properties. Common elements include nitrogen, sulfur, phosphorus, alkaline earth metals, zinc, copper, and molybdenum. The oil conditions and additives are shown in **Table 1.** According to Table 4-1 [42], the sources of each element can be classified as following:

Sulphur (S) is a natural constituent of base oil, so it appears in almost all oil samples. It is also found in many additives, including anti-wear, antioxidant, extreme pressure, corrosion inhibitor and metal deactivator additives.

Calcium (Ca) is often found in conjunction with magnesium and forms the detergent and corrosion inhibitor part of the additive package.

Zinc (Zn) is found in chemicals used to make anti-wear, anti-oxidant, detergent and corrosion inhibitor additives.

Phosphorus (P) is a non-metal and is found in many additives. These include: anti-wear, anti-oxidant, extreme pressure, corrosion inhibitor, friction modifiers, metal deactivator, and biocide chemicals.

Magnesium (Mg) is used in the formulation of detergents and corrosion inhibitors.

Molybdenum (Mo) is seen as an additive in engine oils as part of the antioxidant package.

Table 4.1 Properties of SAE0W30 engine oil

Oil conditions			Oil additives		
Kinematic Viscosity @ 40 °C	cSt	44.5	S	%	214.0
Kinematic Viscosity @ 100 °C	cSt	9.6	Ca	%	166.0
Oxidation	Abs	18.1	Zn	ppm	847.0
Nitration	Abs	6.1	P	ppm	779.0
TBN	mg KOH/g	5.6	Mo	ppm	454.0

4.1 Soot and metal wear contamination in used engine oil

The used engine oils were collected from the small diesel engine vehicles with different oil changed interval. The engine oil's mileage and oil aged were in the range 3,000-20,000 and 0-10,000 km, respectively. After that, the engine oil conditions and contaminants were measured. They are including kinematic viscosity, fuel, soot and metal wear contamination. The used oil's kinematic viscosity at 40 and 100 °C were measured as shown in **Figure 4.1.a** and **b**. The viscosity at 40 °C fall in the range of 45 – 37 Cst and the average value was 36.63 Cst. The viscosity at 100 °C also fall in the range of 10 – 8 cSt and the average value was 8 cSt. The results shows that the viscosity decrease with the increasing of the engine mileage and oil aged. Two major factors are mainly responsible for lubricant oil viscosity changes, (i) formation of resinous products because of oil oxidation, evaporation of lighter fractions, depletion of anti-wear additives and contamination by insoluble compounds tend to increase viscosity and (ii) moisture addition, fuel dilution and shearing of viscosity index improvers tend to reduce the oil viscosity.

Fuel and soot contamination in used oils were measured as shown in **Figure 4.1.c**. and **d,** respectively. The fuel contamination were in the range of 1.57 – 2.5 percent by weight. And the soot contamination were in the range of 0.6 – 1 percent by weight. The oil analysis showed that the fuel and soot contamination increased as the mileage and oil age increase. Fuel and soot are remain of the incomplete combustion process that can be transported to the engine oil during combustion process. The average fuel contamination in the small diesel engine vehicles was about 2 % by weight and the average soot was about 0.69 % by weight.

Total wear metal contamination in used oils were also measured as shown in **Figure 4.1.e.** The wear contamination were in the range of 9 – 280 ppm. The oil analysis showed that the wear contamination increased as the mileage and oil age increase. The element of wear metal are shown in Figure 4.1.f. The common metallic wear elements found in used lubricating oil were iron (Fe), copper (Cu), aluminum (Al) and lead (Pb) as shown in **Figure 4.1.g.**

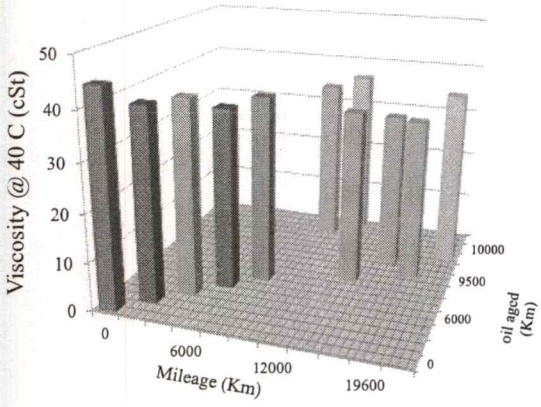

(a) Kinematic viscosity @ 40 °C (cSt.)

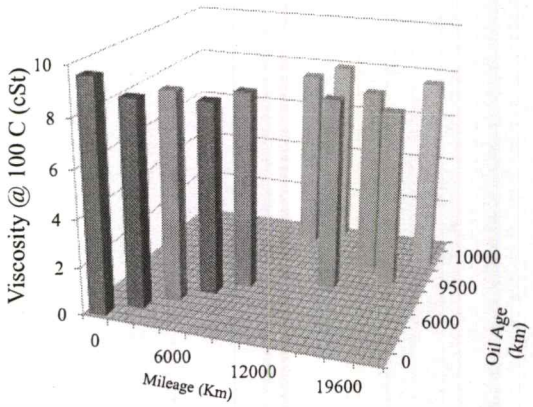

(b) Kinematic viscosity @ 100 °C (cSt.)

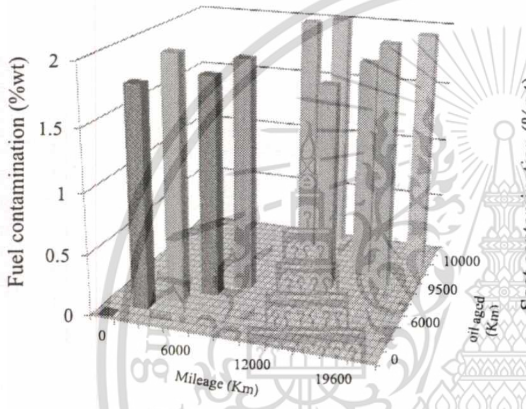

(c) Fuel contamination (%wt.)

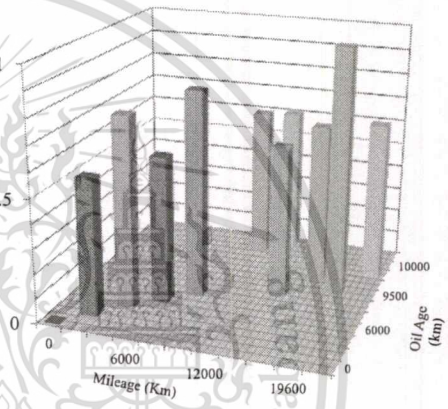

(d) Soot contamination (%wt)

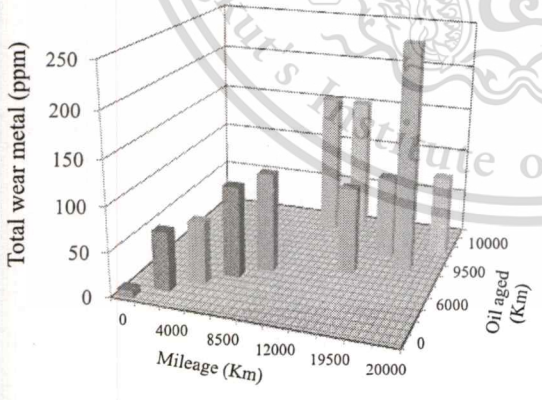

(e) Total wear metal contamination (%wt.)

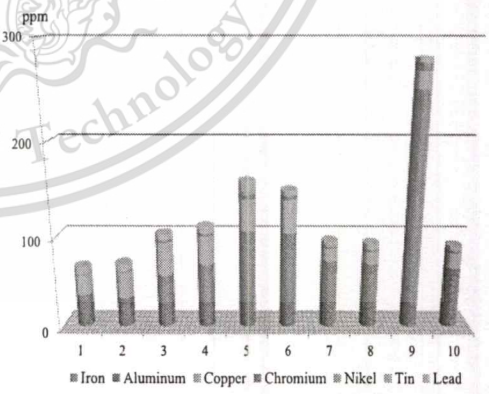

(f) Total wear metal elements (ppm)

Figure 4.1 kinematic viscosity, fuel, soot, and wear metal contamination in the used oil of the small diesel engine and wear metal elements [25]

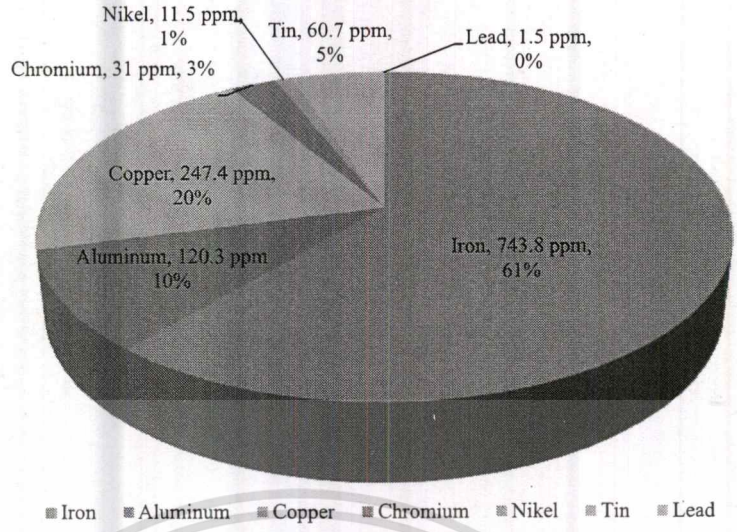

(g) Pie chart total wear metal elements (ppm)

Figure 4.1 kinematic viscosity, fuel, soot, and wear metal contamination in the used oil of the small diesel engine and wear metal elements (continuous) [25]

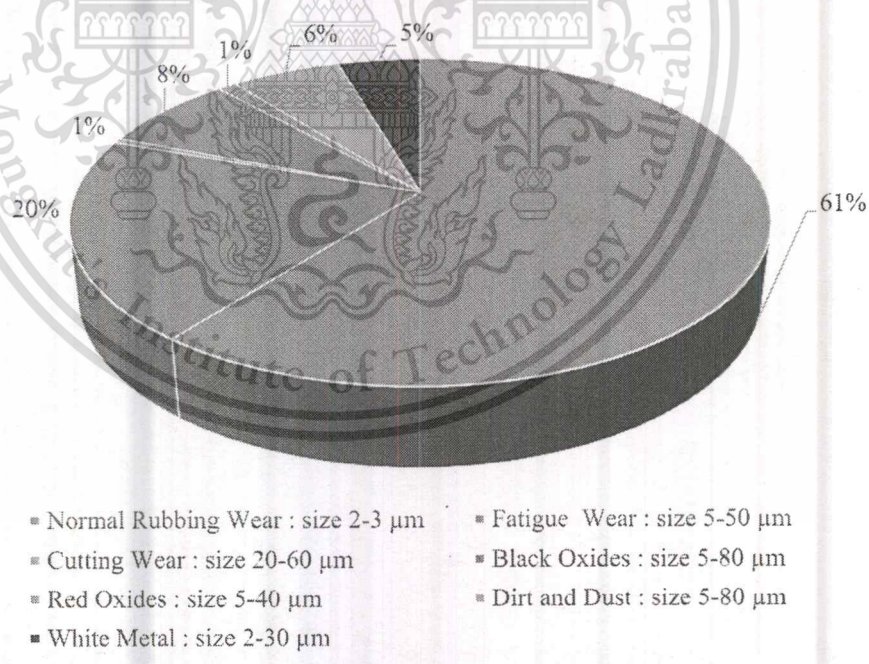

Figure 4.2 Average wear mechanisms in used oil from commercial diesel fuelled engine after 2,000-10,000 km of oil aged (10 samples). [26]

Ferrography is a technique for analyzing the particles present in fluids that indicate mechanical wear. Ferrography provides Microscopic Examination and Analysis of Debris (particles) found in lubricating oils. These particles consist of metallic and non-metallic matter. The metallic particle is a wear condition that separates different size and shapes of metallic dust from components like all type of bearings, gears or coupling (if lubricated in path). Non-metallic particle consists of dirt, sand or corroded metallic particle. **Figure 4.2.1** show average wear mechanisms in used oil from commercial diesel fuelled engine (10 samples). The example of Ferrogram and filtergram images of wear parcels are shown in **Figure 4.2.2**. Wear is loss of material from a solid surface. Wear can appear in many ways depending on the material of the interacting contact surfaces, the environment and the operating conditions. The wear mechanisms which are classified with ferrography analysis can be described below.

Normal rubbing wear is a common wear mechanisms which occurs under sliding conditions where asperities are plastically deformed. The size of normal rubbing wear particles are in the range of 2-3 microns.

Fatigue bearing wear occurs when cyclic loading weakens the material and can be the predominant wear mechanism in rolling contacts involving some sliding. The size of fatigue bearing wear particles are in the range of 5-20 microns.

Cutting wear or Abrasive wear may occur when a rough hard surface mates a softer material where the asperities of the hard material scratch the softer surface. This process is called two-body abrasive wear. The size of cutting wear particles are in the range of 20-60 microns.

Black oxides occurs under sliding conditions where asperities are plastically deformed by high local temperature. The size of black oxides wear are in the range of 5-80 microns.

Dirt and dust are contaminant which are contaminated in to the engine oil during combustion process. . When that particles are present between the mating surfaces one or both surfaces can be worn by scratching. This situation is called three-body abrasive wear. The size of dirt and dust are in the range of 5-80 microns.

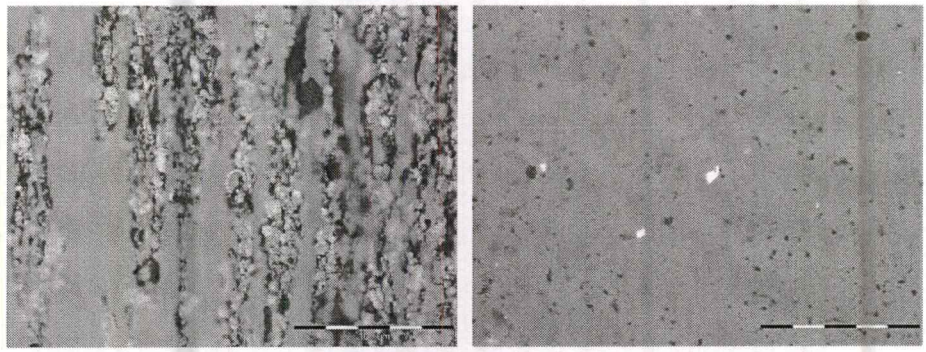

(a) 1,980 km of oil aged

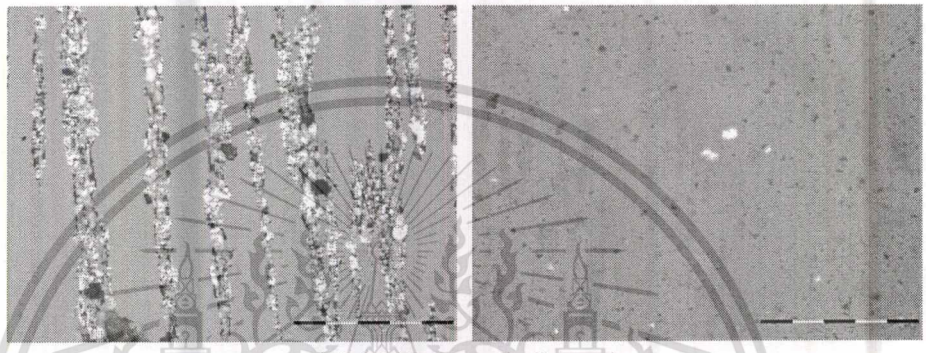

(b) 3,975 km of oil aged

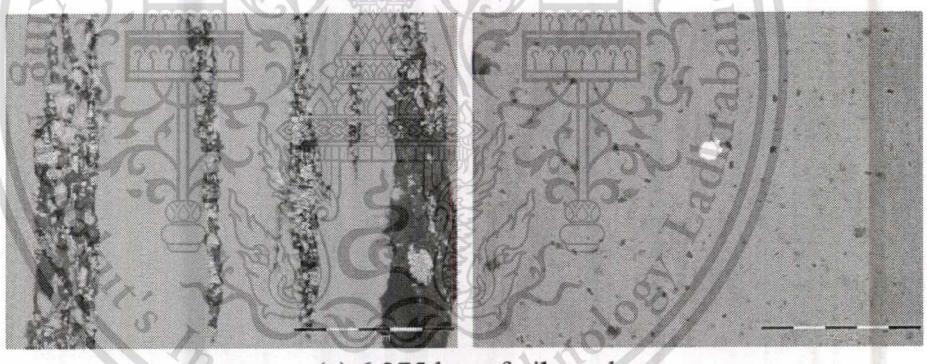

(c) 6,275 km of oil aged

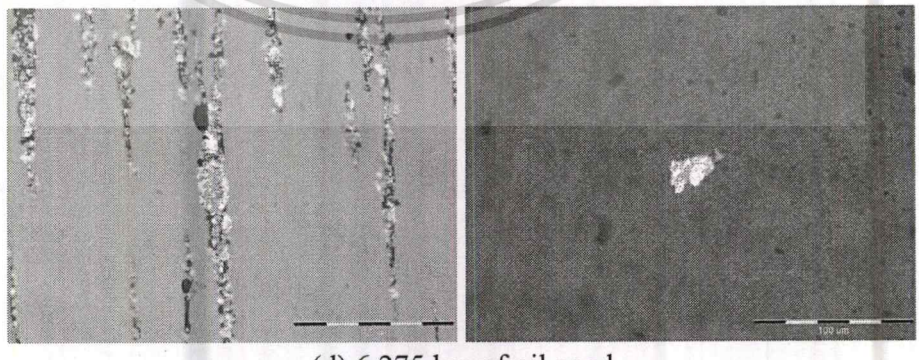

(d) 6,275 km of oil aged

Figure 4.3 Ferrogram and filtergram showing wear particles in used oil from commercial diesel fuelled engine after 2,000-6,300 km of oil aged [26]

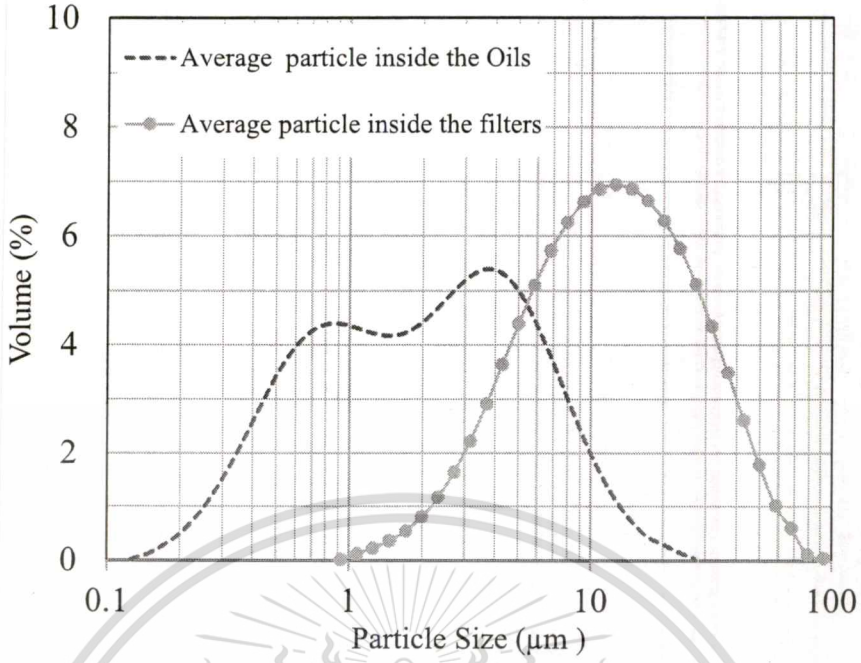

Figure 4.4 Used oil and used filter particles size distribution using laser diffraction spectroscopy. [26]

After that, laser diffraction spectroscopy was used to measure particle size distribution inside the used oil and used filter. **Figure 4** shows particle size distributions of used lubricating oils and used oil filters. They were both collected from the small diesel engine vehicles at the oil end interval. The particle sizes of the used oil were in the range of 0.1-30 microns. It was bimodal distribution. The first and the second fraction were in the range of 0-1.4 and 1.4 – 30 microns, respectively. Moreover, the particle sizes of the used filter were in the range of 1 – 100 microns.

4.2 The effect of biodiesel contamination on metal wear

The pure engine oil and engine oil with difference types of biodiesel contamination were brought to test four-ball wear tester under controlled condition, 60 minutes duration, apply load 392 N, speed 1200 rpm, and temperature at 75°C. The wear scar diameters (WSD) and surface roughness of the lower balls were measured by using an optical microscope and 3D rendering analysis, they were the average value of the three lower balls. In addition, the micro surface analyses were investigated by using Scanning Electron Microscopy (SEM). **Figure 4.5** shows wear surfaces under 3D optical microscope and scanning electron microscope of each sample the engine oil without fuel and engine oil containing 2% wt. of Biodiesel (b) B7, (c) B20, (d) B50 and

Table 4.2 WSD and Roughness of each sample

Samples	Wear Scar Diameter (Micron)	Roughness (Micron)
Lubricating oil without biodiesel	533	1.32
Lubricating oil with B7	588	1.18
Lubricating oil with B20	569	1.17
Lubricating oil with B50	604	1.21
Lubricating oil with B100	615	1.68

(e) B100. The average wear scar diameter and surface roughness were shown in **Table 4.2**. The results showed that WSD increased when the concentration of biodiesel was increased but the surface roughness were not significantly changed. It might be expected that Fuel contamination may decreases the viscosity of the engine oil that resulting in reducing oil film thickness, Moreover, it might decreases the strength of anti-wear additives that make higher wear on metal surface.

After Four-ball tests, the Four-ball tested oils were measured the particle size distribution by using laser particle size analyzer. Fig. 8 shows (a) Particle size distribution and (b) Cumulative Volume of Four-ball tested oils. The particles sizes were in the range of 0- 125 μm. The size distributions occur as bimodal distribution. The first and the second fraction were in the range of 0-15 μm and 15-125 μm, respectively. The results showed that the EB7 and EB20 consist mostly of the small particles. However, the NE, EB50 and EB100 consist mostly of the large particles. At 20 % cumulative volume of NE, EB7, EB20, EB50 and EB100, the particle sizes were in the range of 0- 3.2, 0-1.9, 0-1.6, 0-13.7 and 0-4.0 μm, respectively. At 40% cumulative volume, the particle sizes of each sample were in the range of 0-15.9, 0-3.2, 0-2.7, 0- 25.3 and 0-23.3 μm, respectively. At 80% cumulative volume, the particle sizes of each sample were in the range of 0-54.4, 0-39, 0-40.7, 0-50.2 and 0-54.4 μm, respectively.

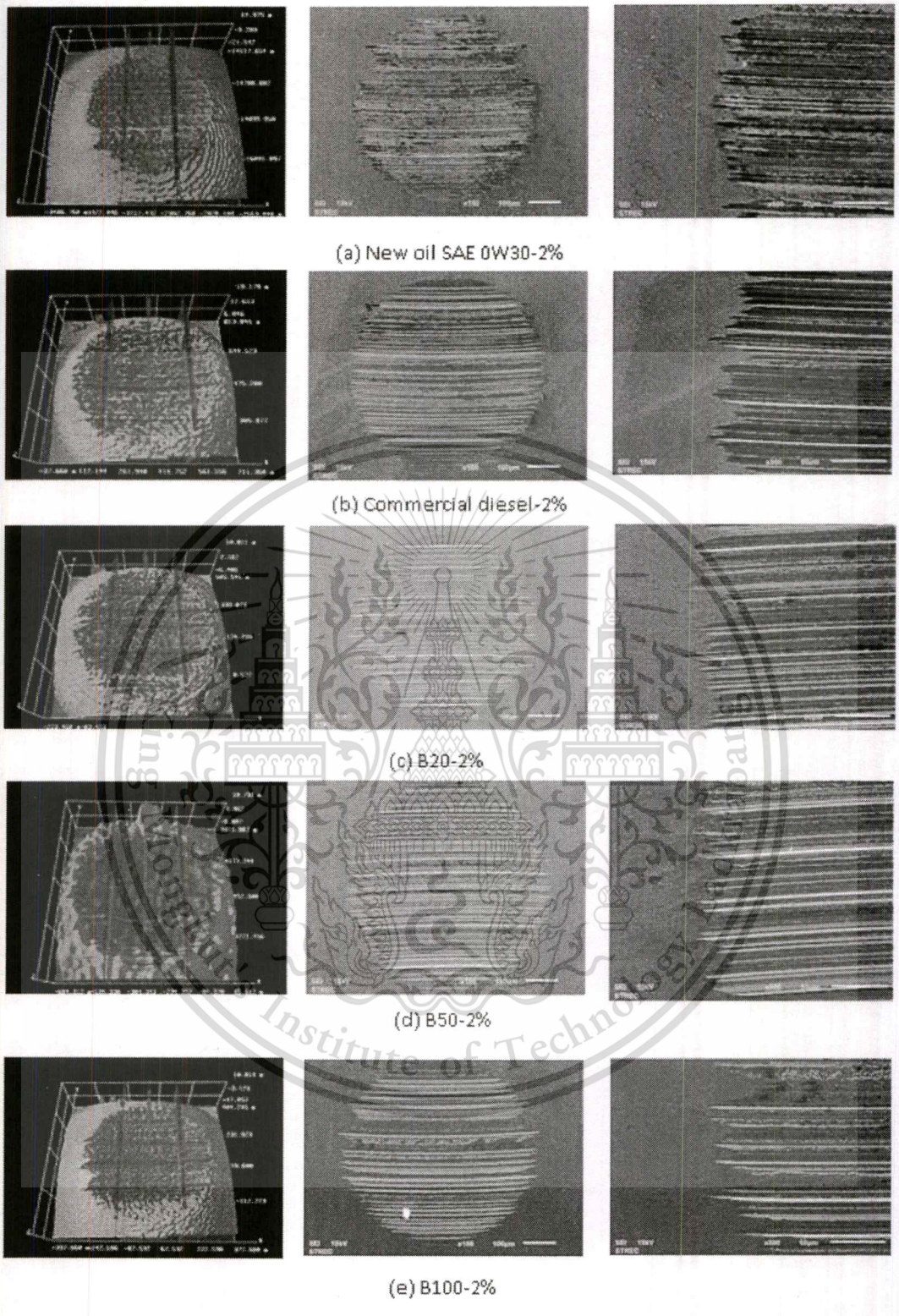

Figure 4.5 Wear surfaces and SEM micrographs of the ball from (a) engine oil without fuel and engine oil with 2% by weight of (b) commercial diesel, (c) B20, (d) B50, and (e) B100.

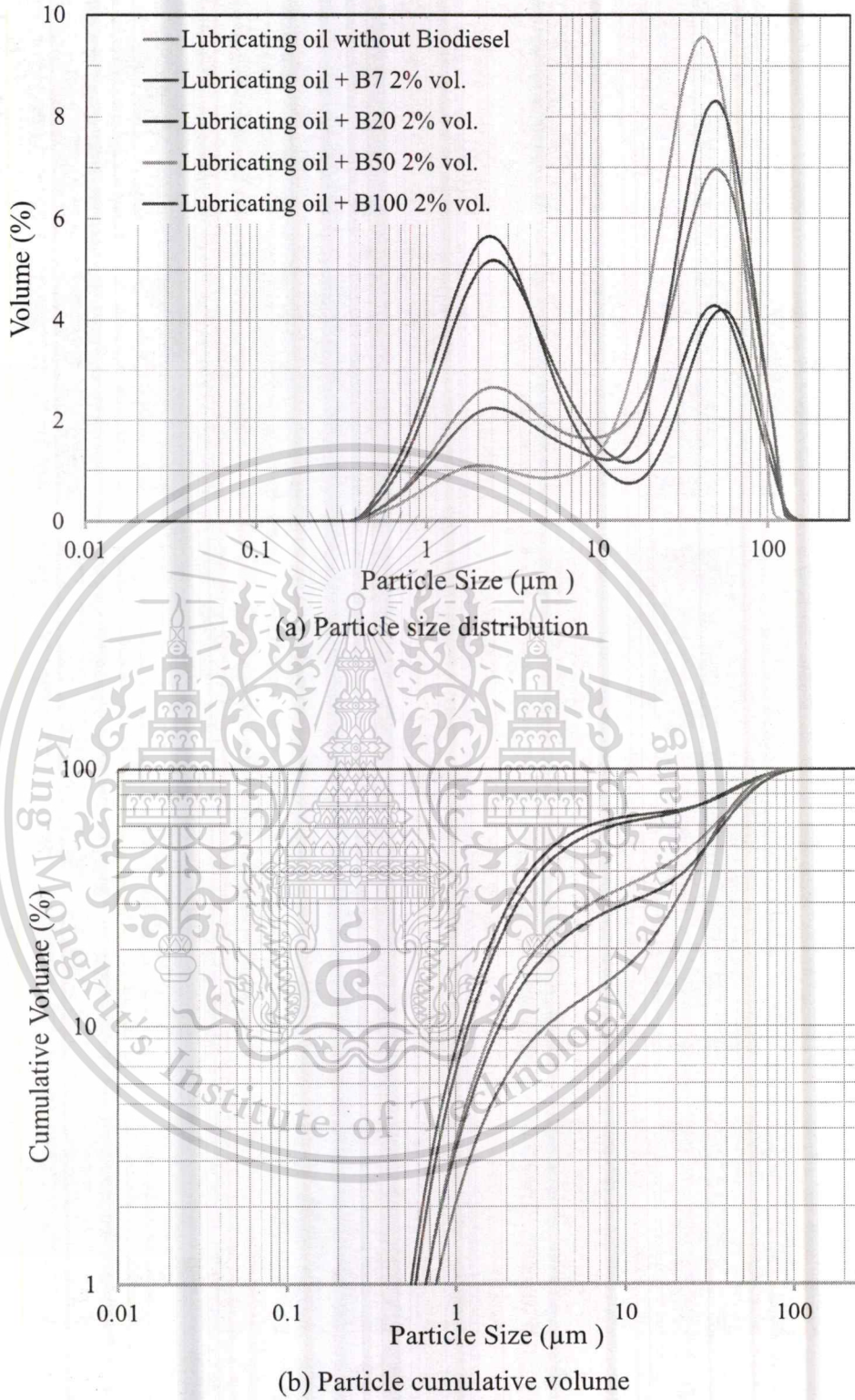

Figure 4.6 Wear metal (a) size distribution and (b) cumulative volume in lubricating oil before Four-ball wear test using Laser Particle Diffraction Spectroscopy.

4.3 The effect of soot contamination on metal wear

4.3.1 Commercial carbon blacks primary particle size distribution

Figures 5 shows TEM micrographs of Commercial Carbon Black (a) N220, (b) N330, (c) N550 and (d) N660. The samples were prepared by using the ethanol solvent extraction technique and were put on the copper grid plates. These images of primary particle are quite difficult to measure the primary size of single particle because they are stacking together, so we cannot determine diameter of all particulates. The idea is just only measuring some of them that clearly appear. After that, the TEM micrographs of CB was used to determine the primary particle size distribution by using measurement program. The area of primary particle were measured by using an elliptical shape selection and convert that area to diameter. It might be the fallibility from the uncertainly of measurement technique such as the unclear image from TEM and the accuracy of measurement technique. These reasons cause to not too much different on size distribution of the diesel and biodiesel primary particulate matter.

Finally, more than 600 particles of each CB samples were investigated. Figure 5-14 presents shows Carbon Black's primary nanoparticle size distribution. The primary nanoparticle diameters were in the range of 5-90 nm. It was clearly observed much amount of particle diameters were in the range of 20-65 nm. The average primary nanoparticles of CB N660 was significant larger than that of N220.

The statistical data has been concluded in Table 5-7. It showed that the average primary particle size of CB N660 was largest and the average primary particle of CB N220 was smallest. The average primary particle size of CB N220, N330, N550 and N660 were 28.1, 30.5, 40.3 and 49.8 nm, respectively.

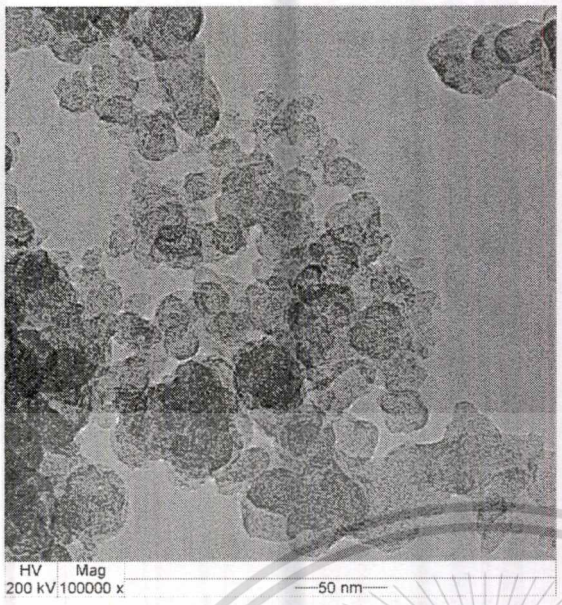

(a) Carbon black N220.

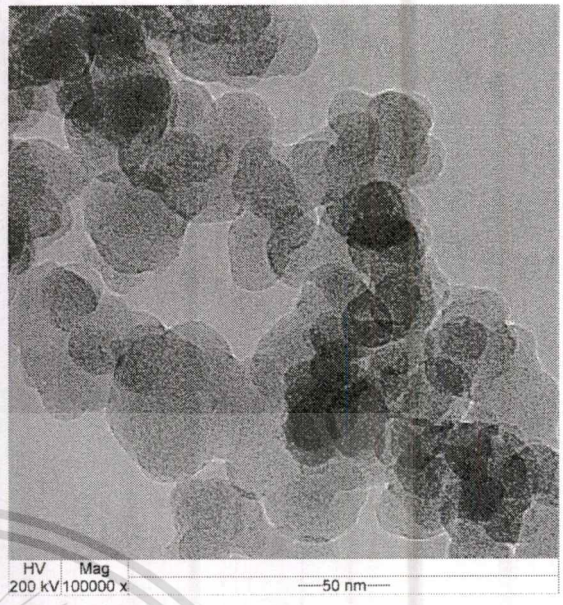

(b) Carbon black N330.

(c) Carbon black N550.

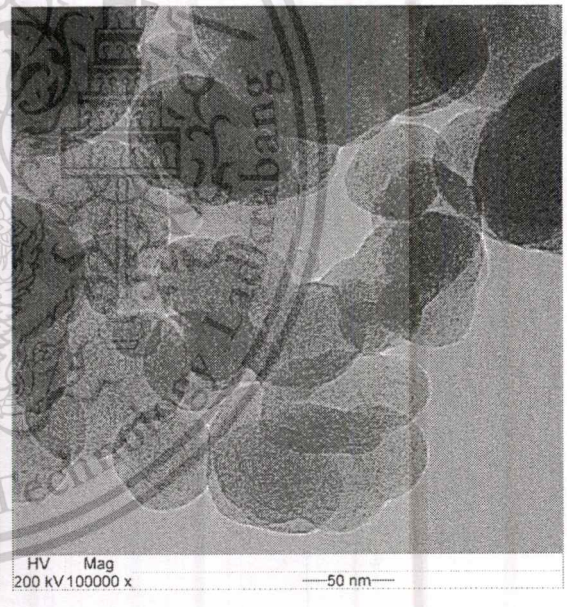

(d) Carbon black N660.

Figure 4.7 TEM micrographs of commercial carbon black

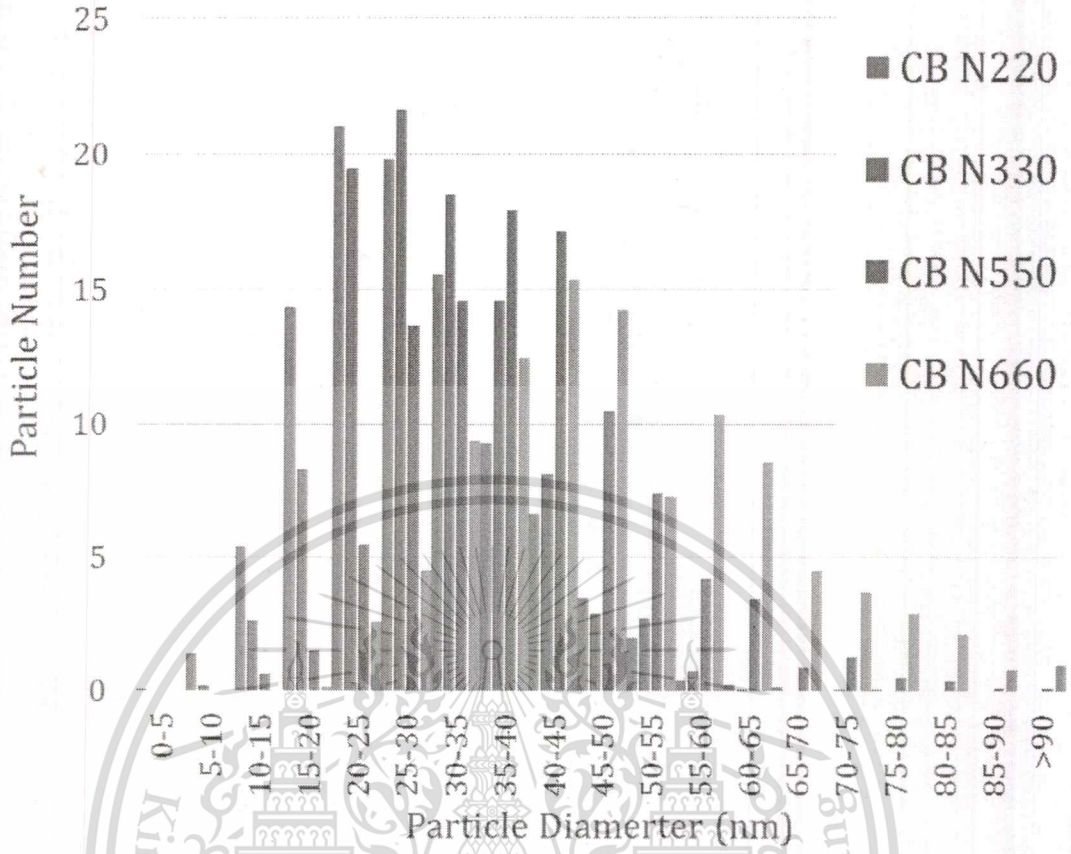

Figure 4.8 Size distribution of commercial carbon black's Nano particles

Table 4.3 Statistical data of Commercial Carbon Black

Statistical Data	Carbon Black			
	N220	N330	N550	N660
Particle Count	1204	1070	784	625
Maximum (nm)	76.5	70.7	107.6	102.9
Minimum (nm)	6.4	7.9	11.7	15.9
Average (nm)	28.1	30.5	40.3	49.8
SD	10.0	9.2	12.6	15.7

4.3.2 Soot Particle Distributing in Liquid

Figure 2a shows size distribution of different types of carbon black mixing in the engine oil which measured before Four-ball wear test. There were CB N220, N330, N550 and N660, respectively. The results showed that the different types of soot dispersing in the engine oil were not significantly different. They were in the range of 0.01 – 300 microns, which were small particle that have size of 10 - 100 nm. The first and second groups of agglomerate were in the range of 0.1 - 2 micron and 2 – 300 micron, respectively.

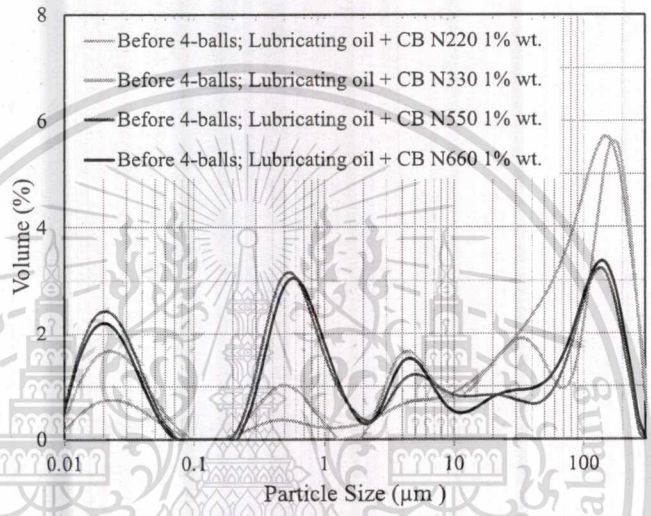

(a) Particle size distribution

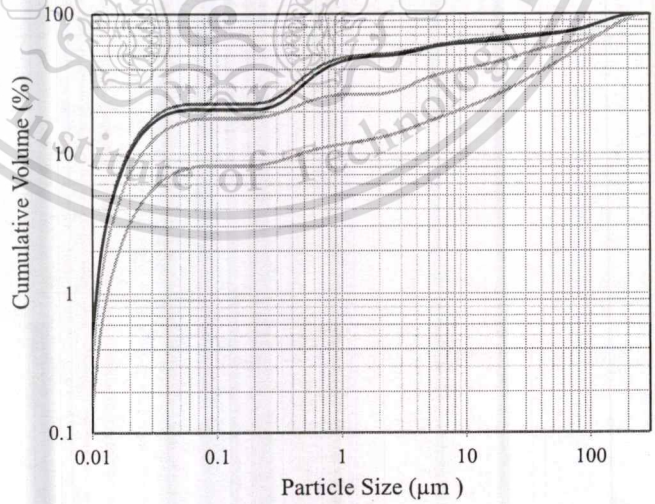

(b) Particle cumulative volume

Figure 4.9 Carbon black (a) size distribution and (b) cumulative volume in lubricating oil before Four-ball wear test using Laser Particle Diffraction Spectroscopy.

4.3.3 The effect of soot contamination on metal wear

The objective of using lubricating oil is to get advantage from ability of film layer forming by lubricant, whereas film thickness is depended on viscosity at operating temperature. Then the viscosity of SAE 0W 30 was used to estimate oil film thickness. Minimum and mean film thickness were calculated according to the following equation (2.1, 2.2):

$$\frac{h_{mean}}{R} = 2.69\left(\frac{U\eta_0}{ER}\right)^{0.67}(\alpha E)^{0.53}\left(\frac{W}{ER^2}\right)^{-0.067}(1-0.61e^{-0.73k}) \quad (2.1)$$

$$\frac{h_{min}}{R} = 3.63\left(\frac{U\eta_0}{ER}\right)^{0.68}(\alpha E)^{0.49}\left(\frac{W}{ER^2}\right)^{-0.073}(1-e^{-0.68k}) \quad (2.2)$$

Where:

h_{mean} is mean oil film thickness [m].

h_{min} is minimum oil film thickness [m].

η_0 is viscosity at atmospheric pressure of the lubricant [Pa.s].

R is Radius of curvature [m].

U is Entering surface velocity [ms^{-1}].

E is Young's modulus, E=210 [GPa].

α is Pressure-viscosity coefficient, $\alpha = 0.44 \times 10^{-8}$ [$\frac{m^2\,Pa}{N}$].

W is contract load [N].

K is Elasticity parameter, k = 1.03.

After calculation, the oil film thickness of lubricant A and B are shown in **Table 5-10.**

Table 4.4. Estimation of oil film thickness of lubricant A and B

Items	SAE 0W40	
	40 °C	100 °C
kinematic Viscosity (cSt)	44.5	9.6
Mean oil film thickness (nm)	57.67	20.48
Minimum oil film thickness (nm)	36.42	12.73

The predicted values of film thickness were so low that it was inconceivable for the contacting surfaces to be separated by a viscous liquid film. In fact, the calculated

film thicknesses suggested that the surfaces were lubricated by films only one molecule in thickness. In experiments specifically designed to permit only lubrication by monomolecular films, much higher wear rates and friction coefficients were obtained.

4.3.4 Impact of soot on metal wear using four ball wear tester

To understand the effect of soot Nano particle size on metal wear the four ball wear tester was used. In this study the commercial carbon black was used to simulate engine soot. The several types of commercial carbon blacks (CB) which have different primary particle size were mixed with the engine oil at 1% by weight per volume for simulating soot different primary particle size contaminated engine oil. After the four ball tests, the three lower balls used to measure wear scar diameter (WSD) using a high-resolution optical microscope (OM). Testing formulations were compared using average diameter of the wear scar diameter on the three lower balls. Two measurements were made on each lower ball at 90 degree to each other. If wear were elliptical, then first measurement was made in direction of striations and other was made across the striations. An average of 3 wear scars readings is reported as scar diameters. The surface roughness was also measured using 3D rendering system of that OM.

Figure 4.10 shows the average wear scar diameter and surface roughness the engine oil without soot and engine oil containing 1% wt. of N220, N330, N550 and N660 Carbon Black. **Figure 4.11** shows the corresponding microscopy image of wear scars and 3D-rendering image found on three lower balls and one upper ball after 60 min running time. The results showed that the ball wear scar diameter (WSD) increased when the primary particle size of the carbon black was increased, but the surface roughness was not significantly change. This result suggests that the wear was affected not only soot concentration but some relation between primary soot diameter and oil film thickness. **Figure 4.8** shows the particle size distributions of primary soot. The mean diameter and mean oil film thickness are shown in **Table 4.4**. In case of the engine oil containing CB N550 and N660, primary soot particle diameter were very larger than the oil film thickness. It is suggested that the existence of soot particles of which diameter is larger than the oil film thickness, contributes the acceleration of wear, and not only the concentration of soot but the relation between primary soot diameter and oil film thickness are very important to discuss the wear by soot.

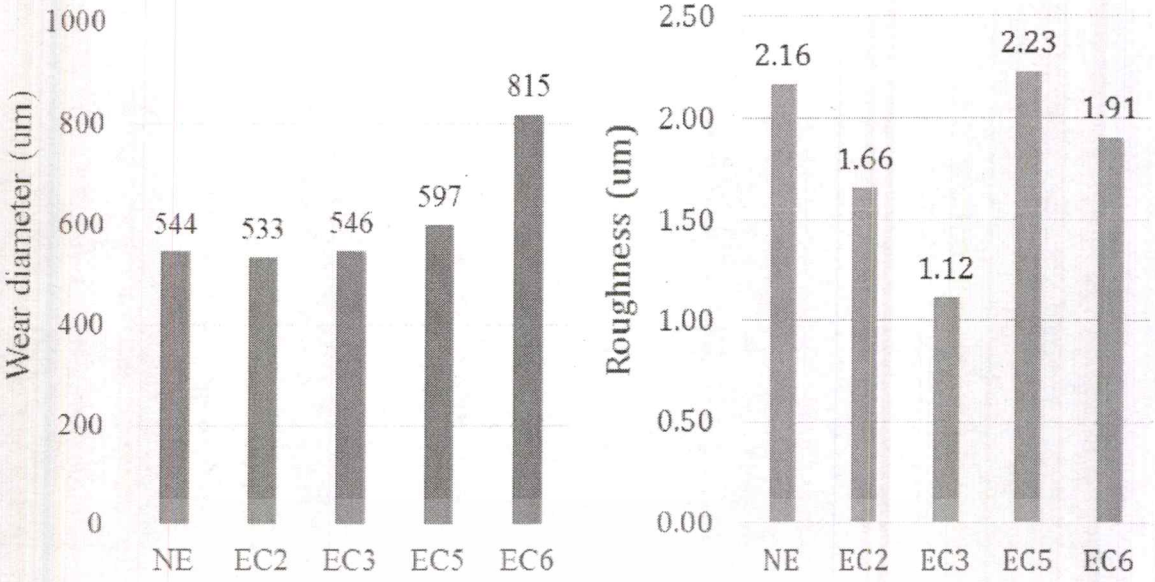

Figure 4.10 Average wear scar diameter and surface roughness on lower

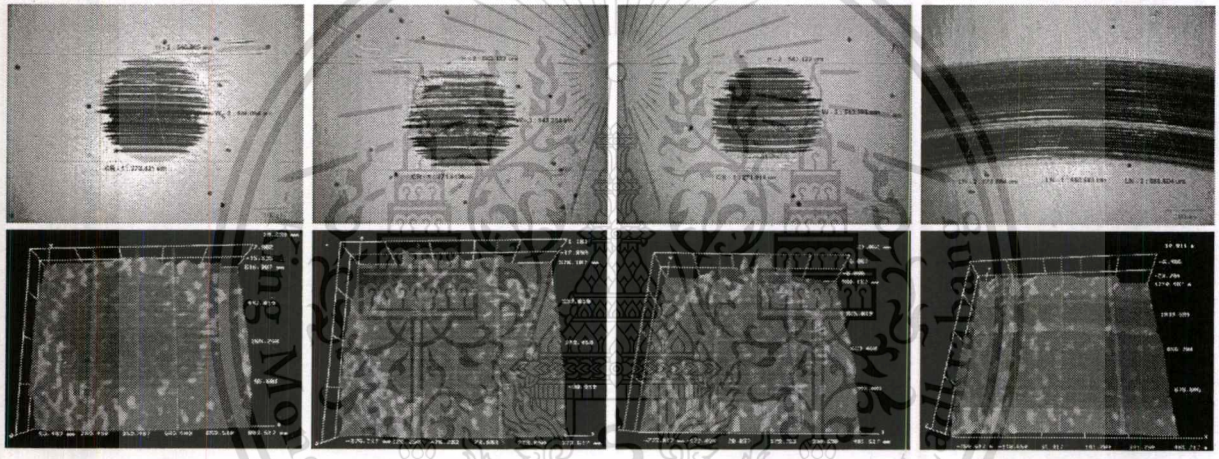

(a) Engine oil without CB

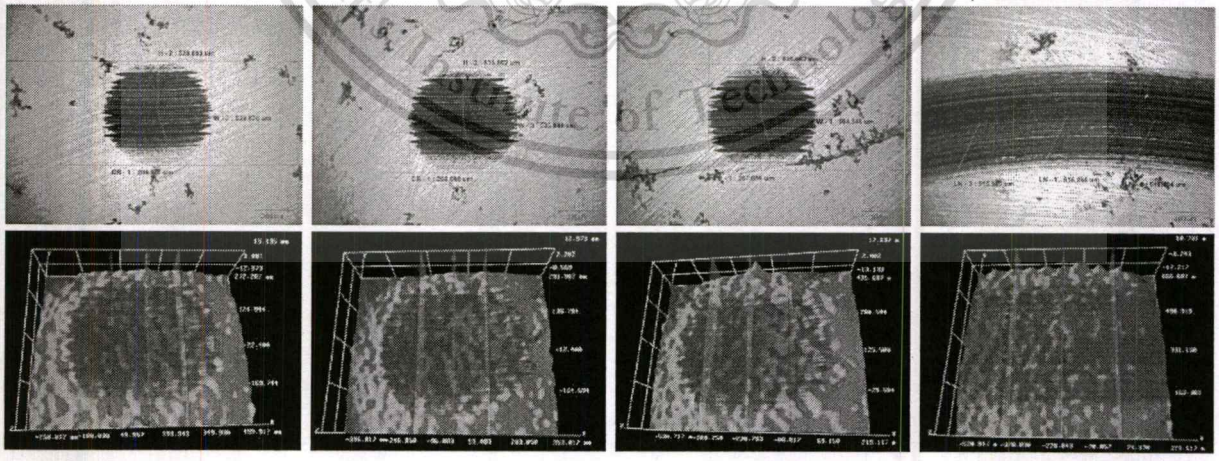

(b) Engine oil with CB N220

Figure 4.11 Wear scar and surface roughness of the ball from (a) the engine oil without soot and the engine oil containing 1% wt. of (b) CB N 220, (c) CB N330, (d) CB N550 and (e) CB N660

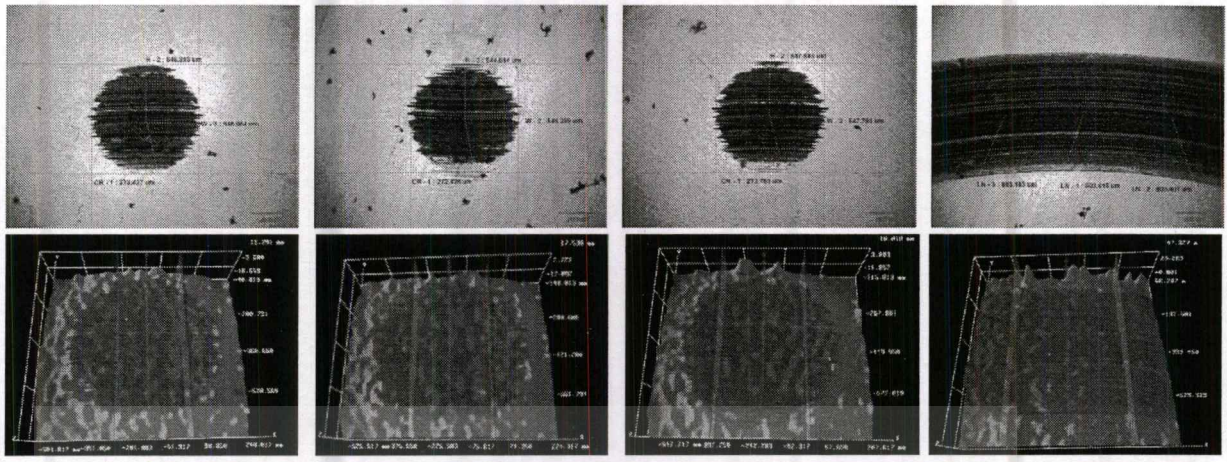

(c) Engine oil with CB N330

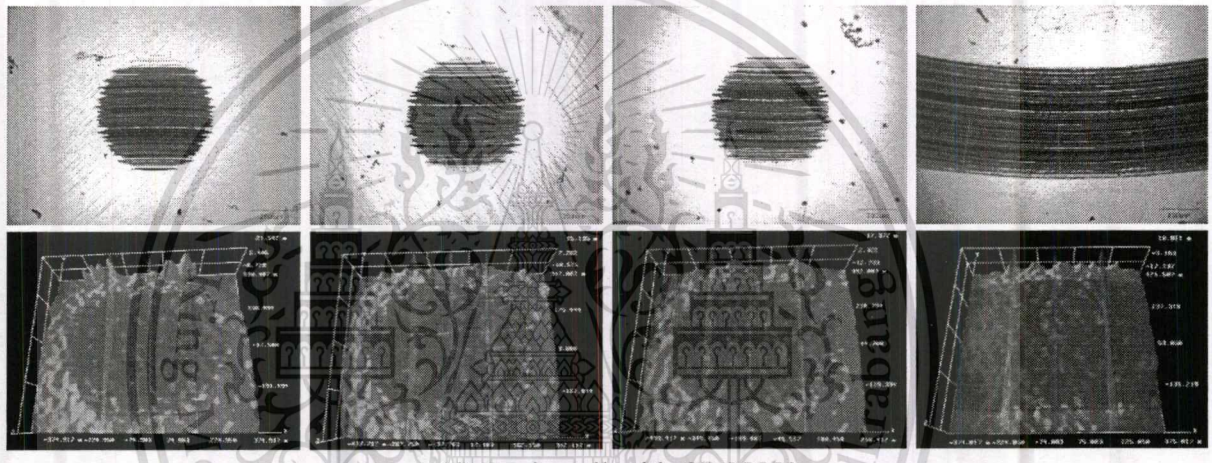

(d) Engine oil with CB N550

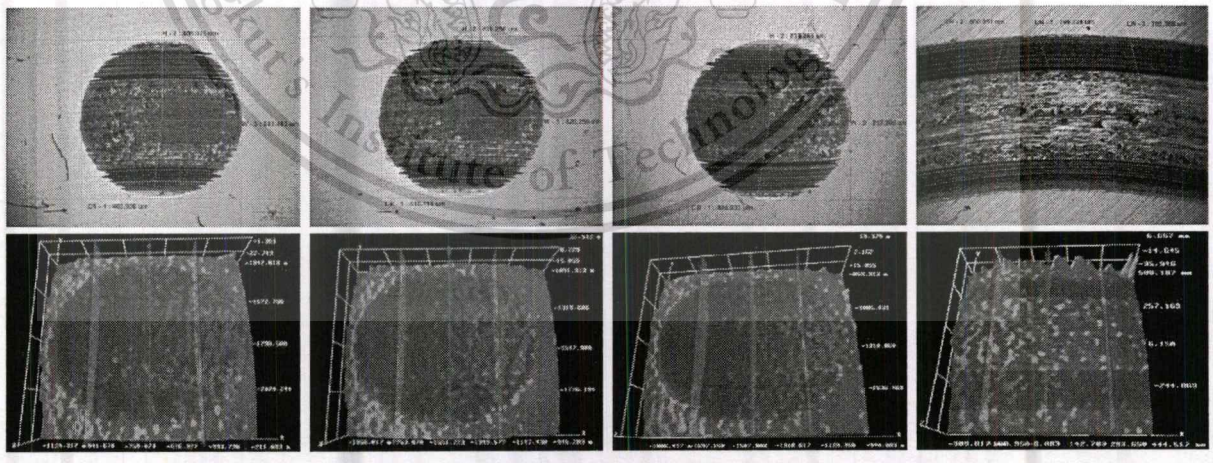

(e) Engine oil with CB N660

Figure 4.11 Wear scar and surface roughness of the ball from (a) the engine oil without soot and the engine oil containing 1% wt. of (b) CB N 220, (c) CB N330, (d) CB N550 and (e) CB N660 (continuous)

4.3.5 Particle size distribution after wear test

After Four-ball wear test, the tested oils were also measured size distribution. They were the wear metal without CB and wear metal with CB N220, N330, N550 and N660. **Figure 7** shows size distribution of particles inside the tested oils. They were in the range of 0.01 – 200 micron. The size of wear metal without CB was in the range of 1-100 microns. On the other hand, the size of wear metal with CB were in the range of 0.01 – 300 microns. It might be expected that the size of soot particle might be in the 0.01-300 microns. The small particle should be soot primary and agglomerate particles.

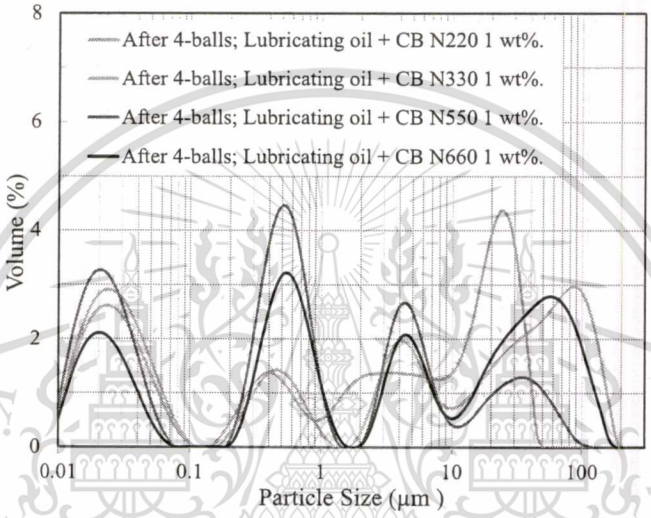

(a) Particle size distribution

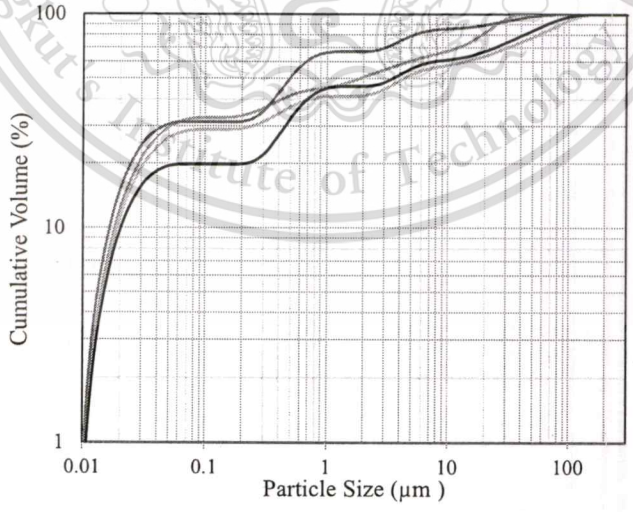

(b) Particle cumulative volume

Figure 4.13 Carbon black (a) size distribution and (b) cumulative volume in lubricating oil before Four-ball wear test using Laser Particle Diffraction Spectroscopy.

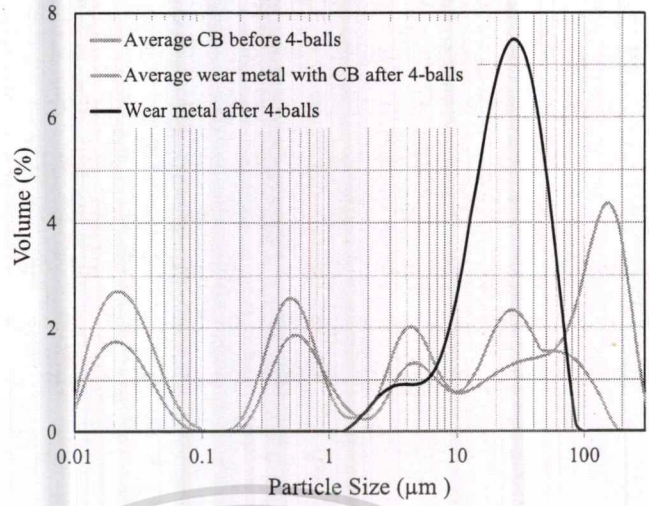

(a) Particle size distribution

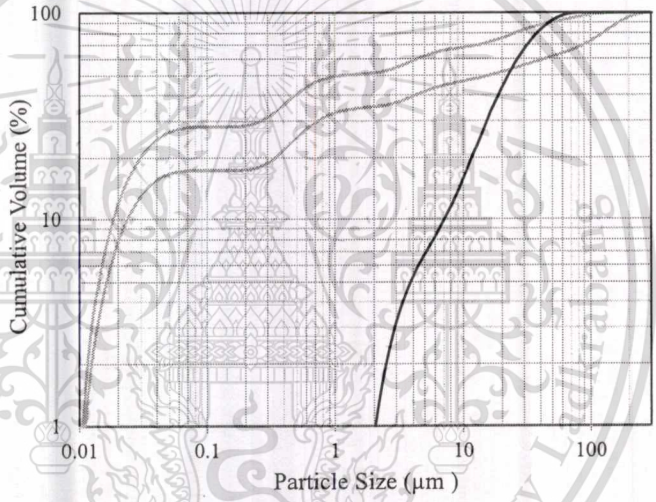

(b) Particle cumulative volume

Figure 4.14 Carbon black (a) size distribution and (b) cumulative volume in lubricating oil before Four-ball wear test using Laser Particle Diffraction Spectroscopy.

Moreover, the comparison between particle size distribution before and after Four-ball wear tests are shown in **Figure 4.14**. The average CB size distribution before Four-ball wear test of the 4 samples including CB N220, N330, N550 and N660 in engine oil is represented by blue line. The wear metal without CB size distribution is represented by black dash line. In addition, the average wear metal with CB size distribution after Four-ball wear is represented by orange line with circle marker type. The average size distribution before Four- ball wear test were in the range of 0.01-300 microns. The average wear metal without CB and wear metal with CB particle size distribution after Four-ball wear test were in the range of 1-100 microns and 0.01-200

microns. It can be considered that the shape and diameter of primary soot particles changes when they behave as abrasive media. The size of CB with wear metal seems smaller than those particles before the wear test. It suggests that the primary soot particle is hard and scrapes the metal surface directly.

Analysis of worn surfaces by SEM

Figure 4.15 shows SEM micrographs of wear scar found on the ball of (a) the engine oil without soot and engine oil containing 1% wt. of (b) N220, (c) N330, (d) N550 and (e) N660 Carbon Black. This figure presents the wear scar worn surface of stationary ball under the same test conditions according to ASTM D4172. The wear scar diameter of the engine oil containing CB N660 and N550 are larger than the other, with the increasing of carbon black primary particle size the wear scar also increases. The metal layers from the worn surfaces conducted by the rotating balls in a sliding direction are shown by the surface morphology.

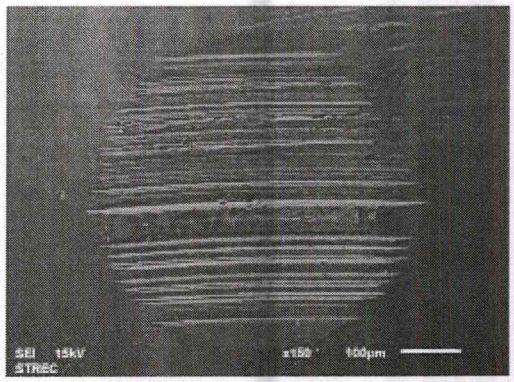

(a) The engine oil without soot

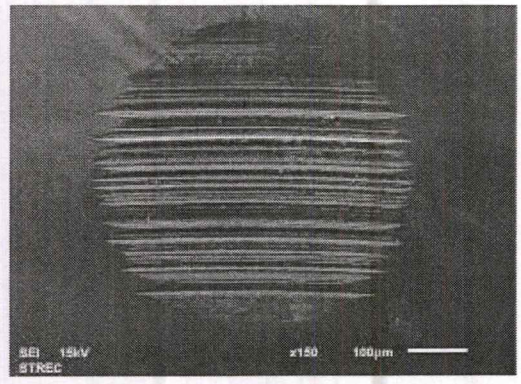

(b) The engine oil containing CB N220.

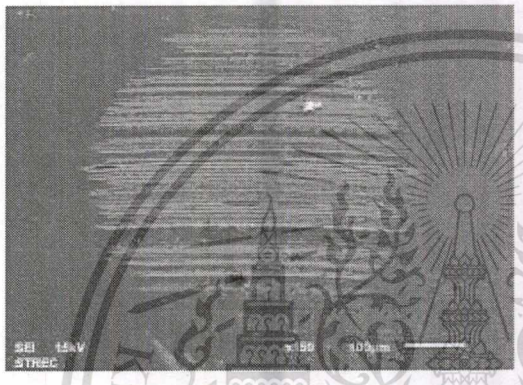

(c) The engine oil containing CB N330.

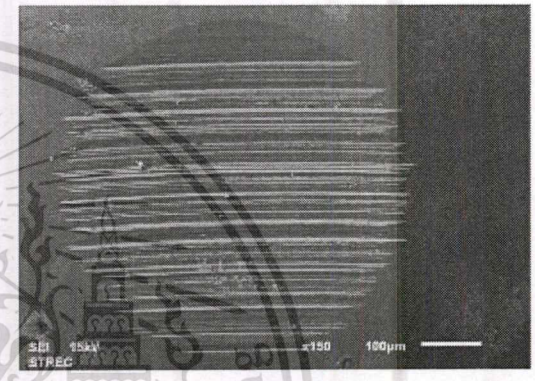

(d) The engine oil containing CB N550.

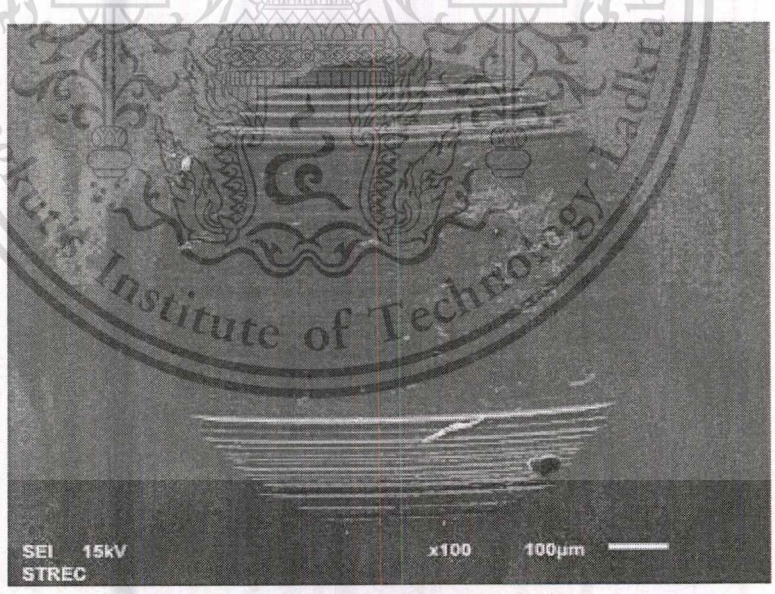

(e) The engine oil containing CB N660.

Figure 4.15 SEM micrographs taken using Secondary electron of the ball surface from (a) the engine oil without soot and the engine oil containing 1% wt. of (b) CB N 220, (c) CB N330, (d) CB N550 and (e) CB N660

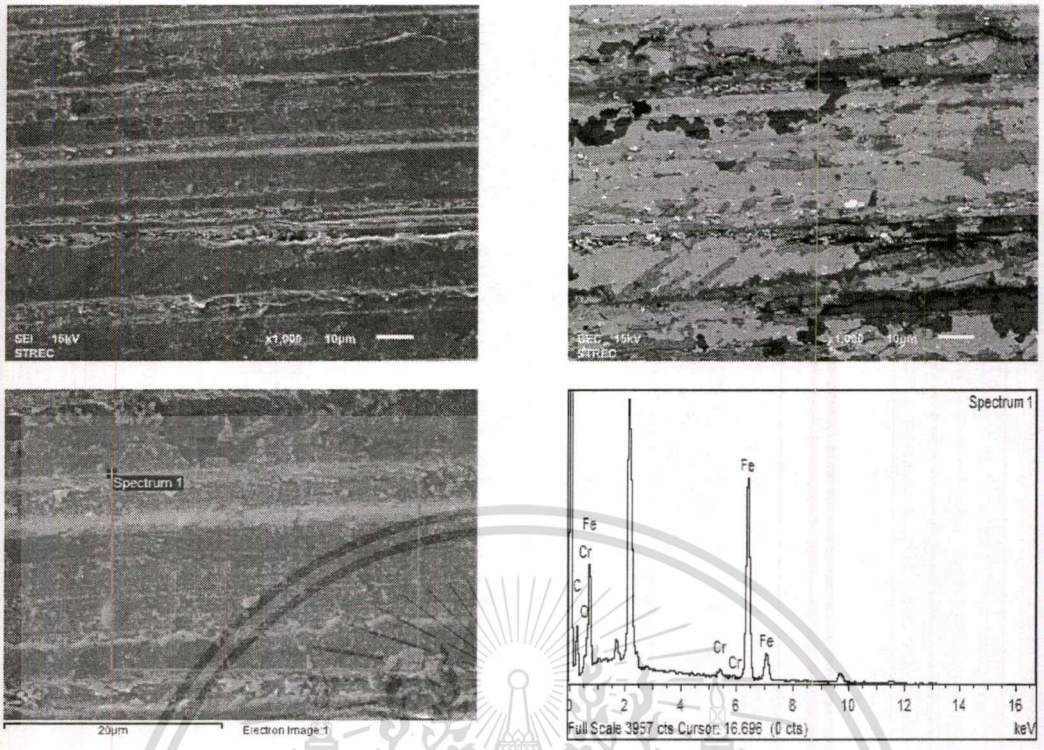

(a1) The engine oil without soot.

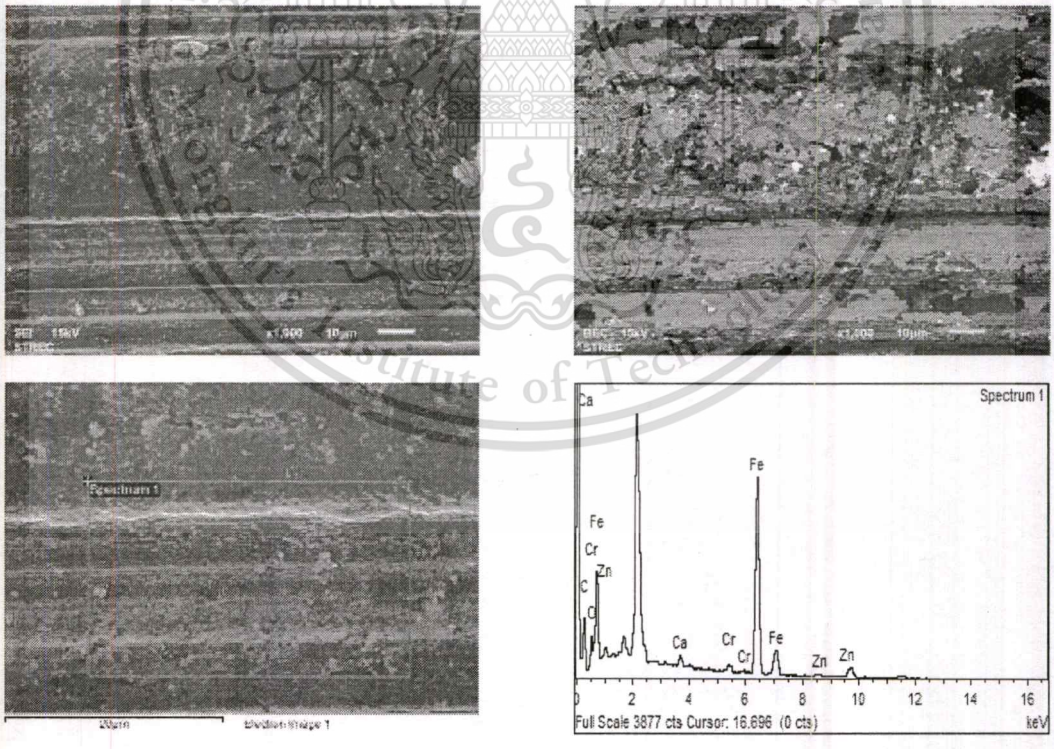

(a2) The engine oil without soot.

Figure 4.17 SEM micrographs taken using secondary and backscattered electron and EDX spectra of the ball surface

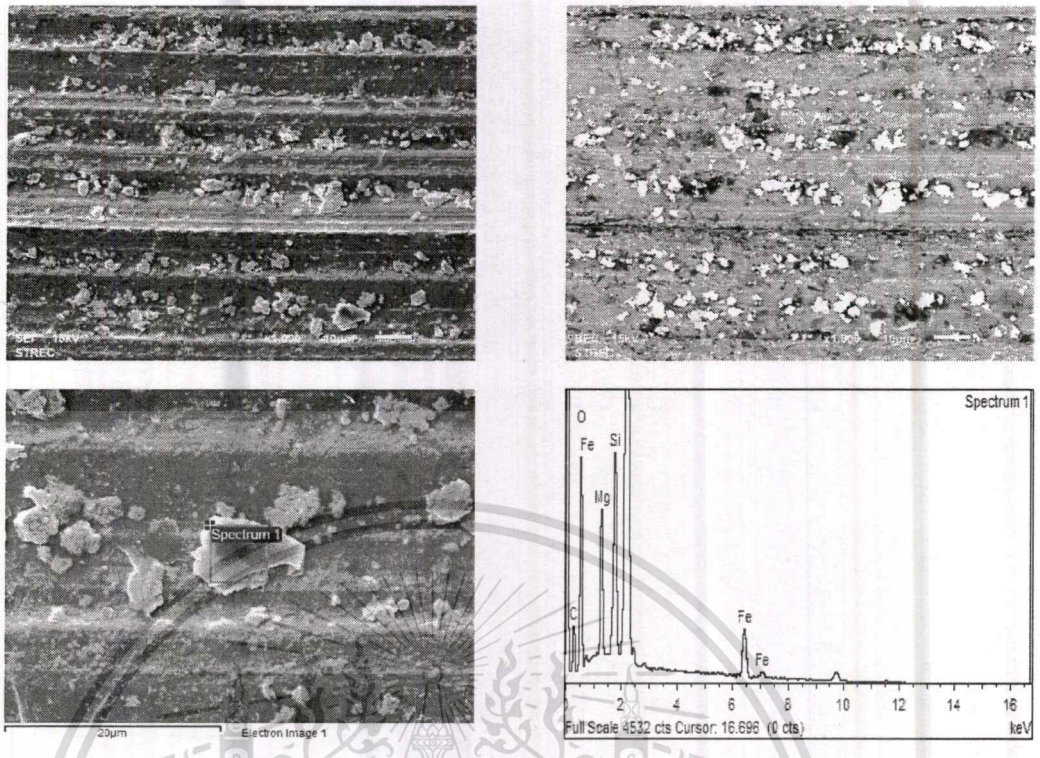

(b1) The engine oil containing CB N220.

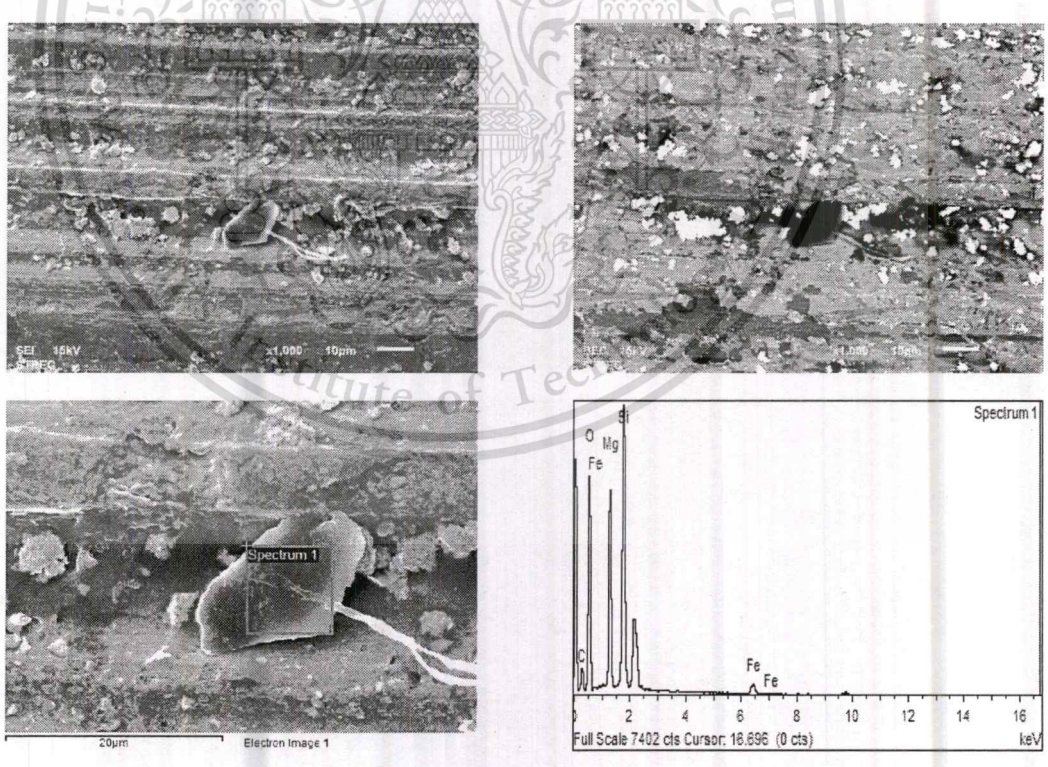

(b2) The engine oil containing CB N220.

Figure 4.17 SEM micrographs taken using secondary and backscattered electron and EDX spectra of the ball surface (continous)

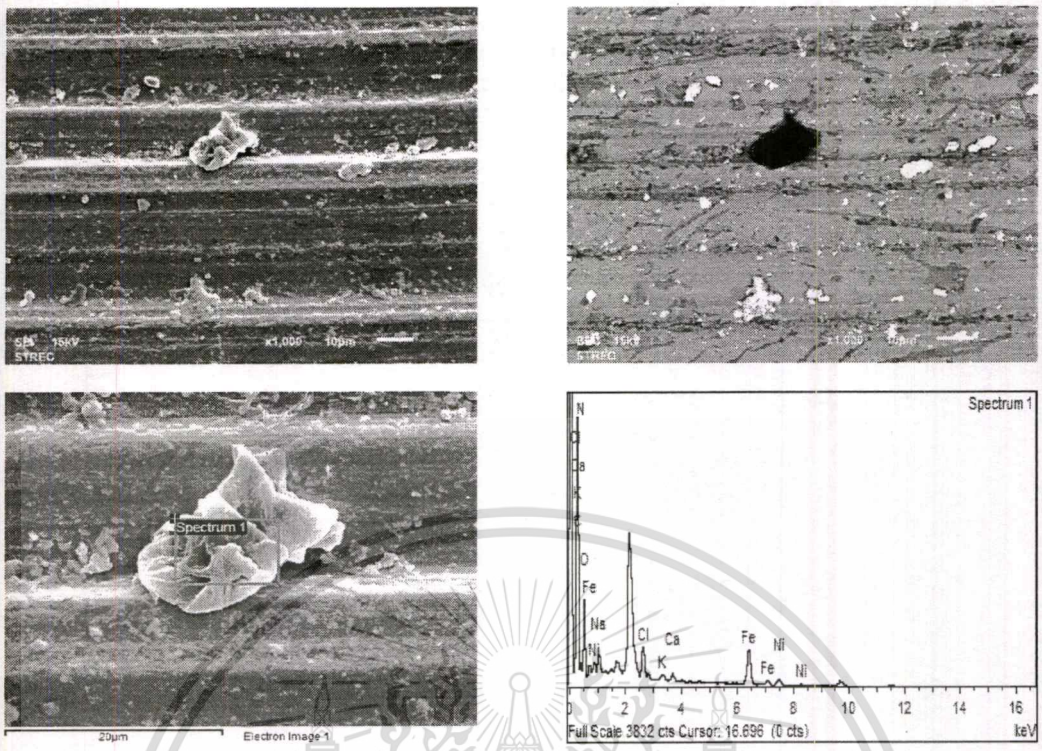

(c1) The engine oil containing CB N330.

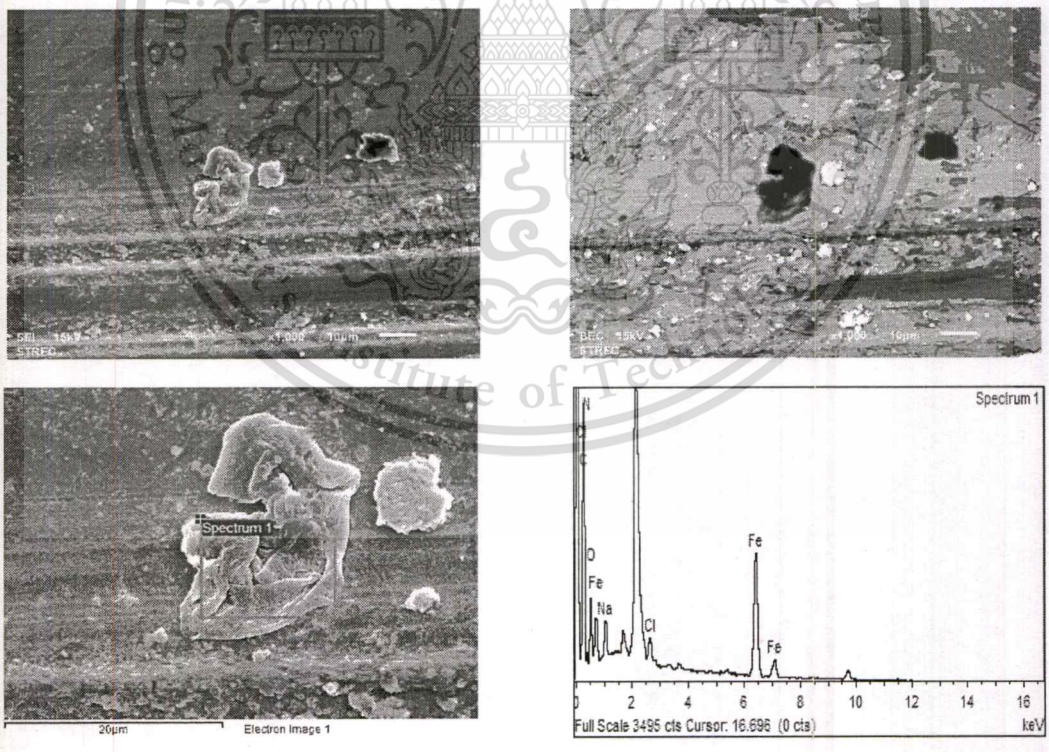

(c2) The engine oil containing CB N330.

Figure 4.17 SEM micrographs taken using secondary and backscattered electron and EDX spectra of the ball surface (continous)

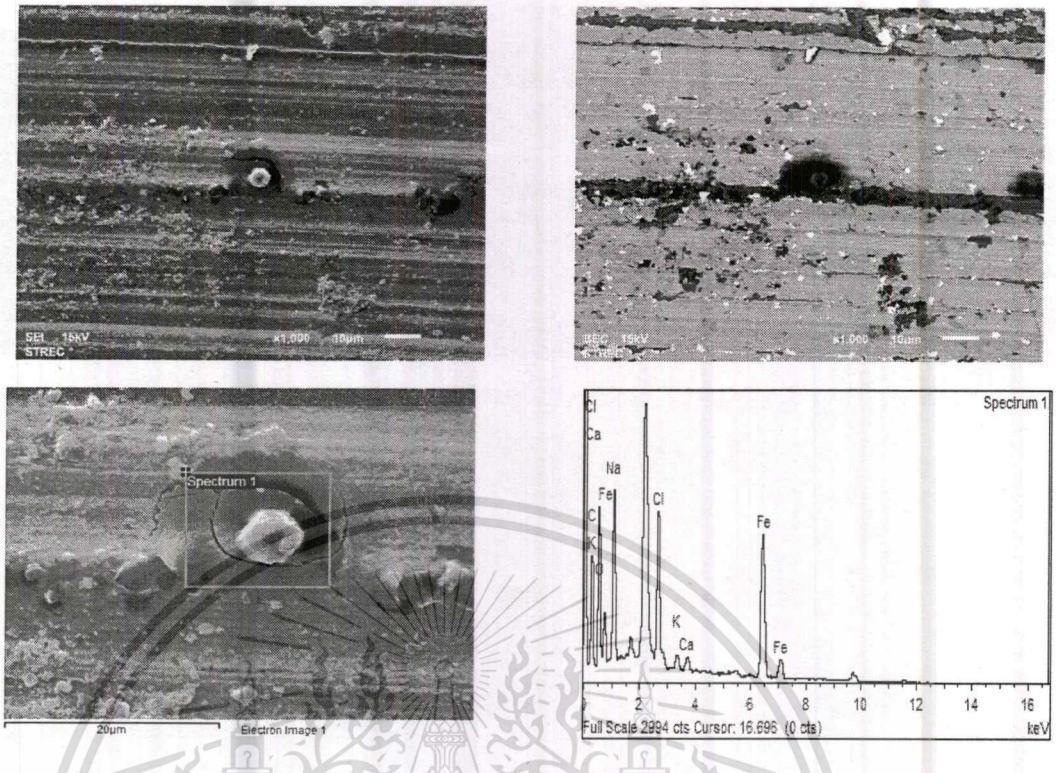

(d1) The engine oil containing CB N550.

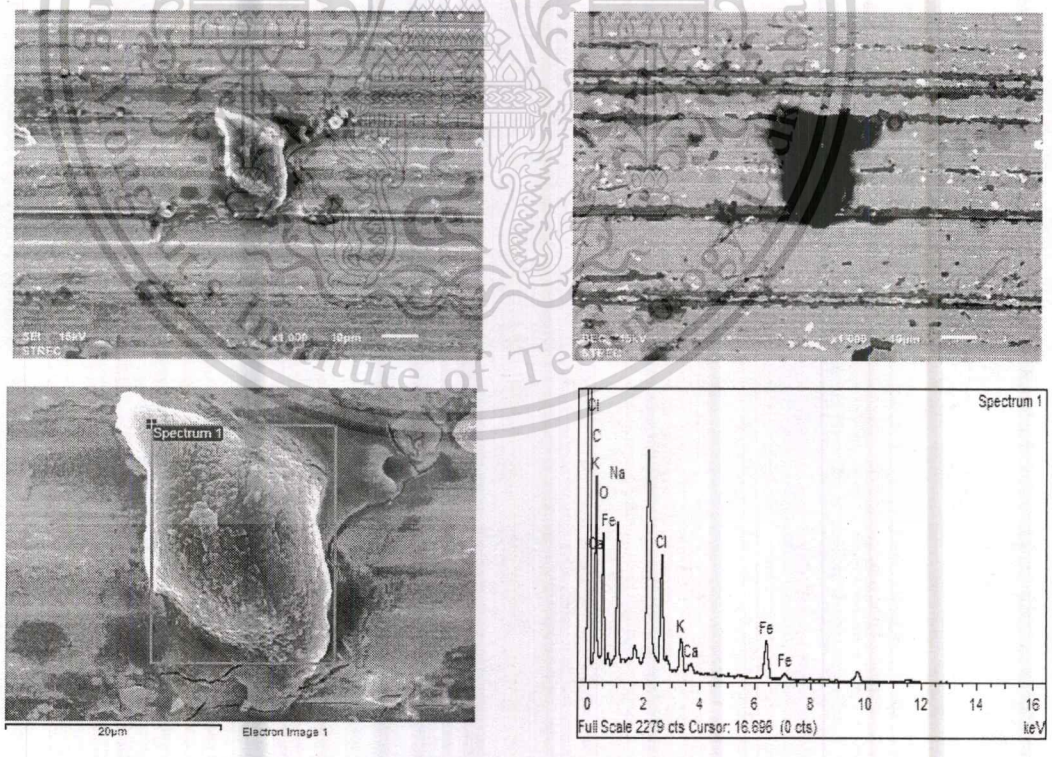

(d2) The engine oil containing CB N550.

Figure 4.17 SEM micrographs taken using secondary and backscattered electron and EDX spectra of the ball surface (continous)

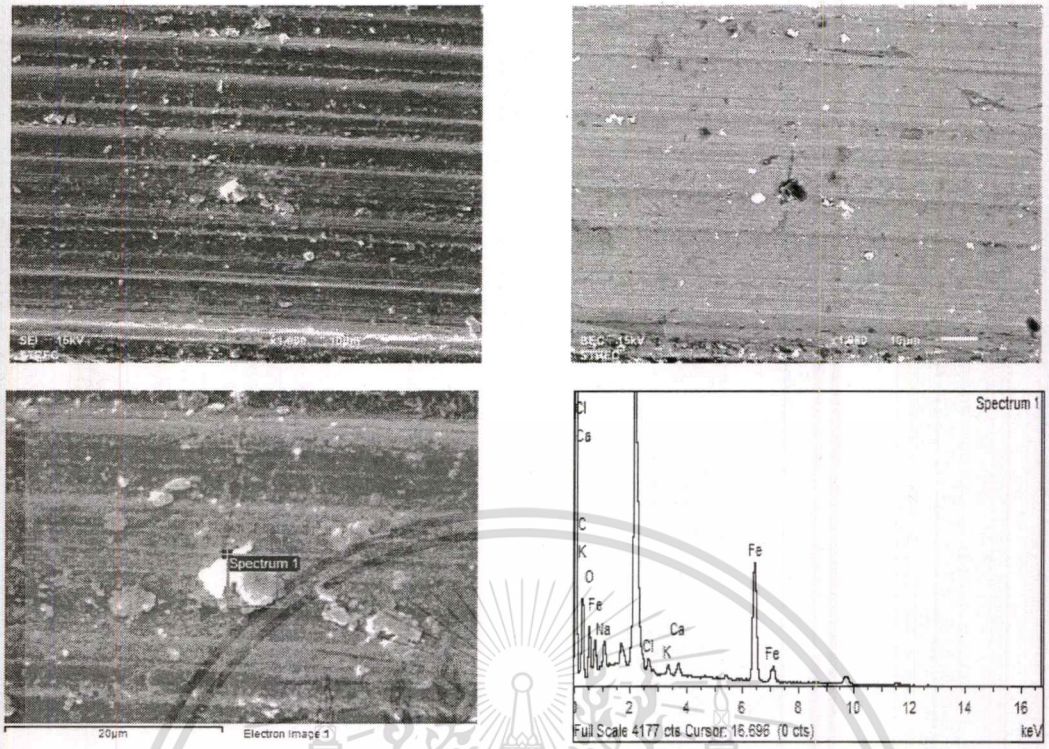

(e1) The engine oil containing CB N660.

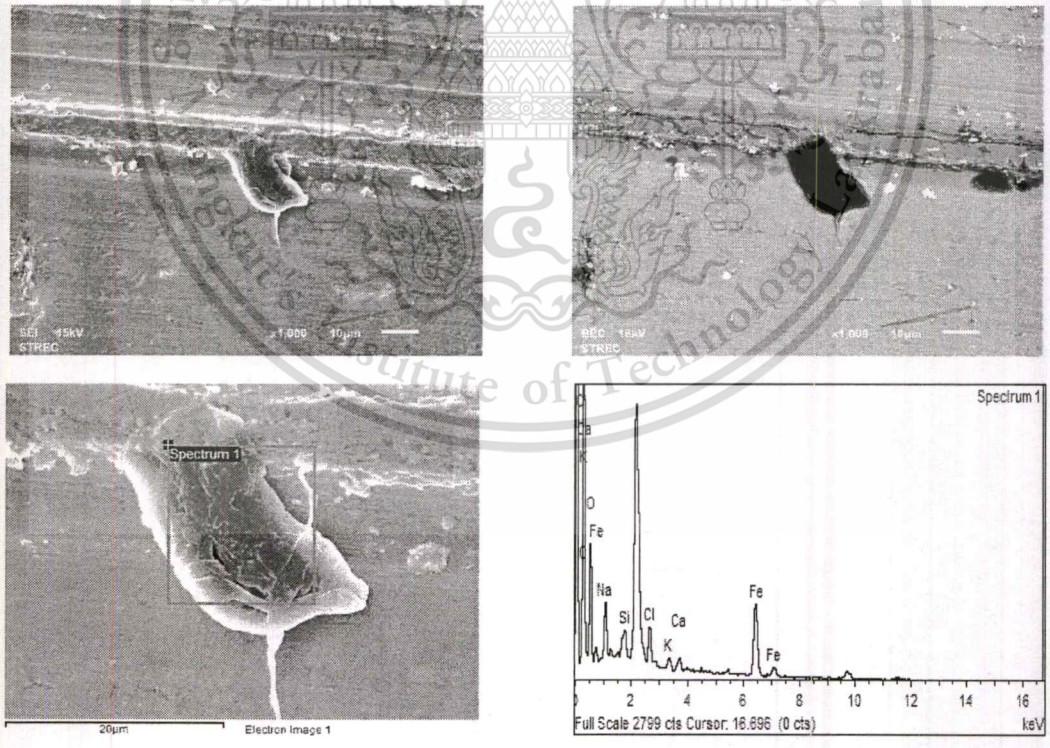

(e2) The engine oil containing CB N660.

Figure 4.17 SEM micrographs taken using secondary and backscattered electron and EDX spectra of the ball surface (continous)

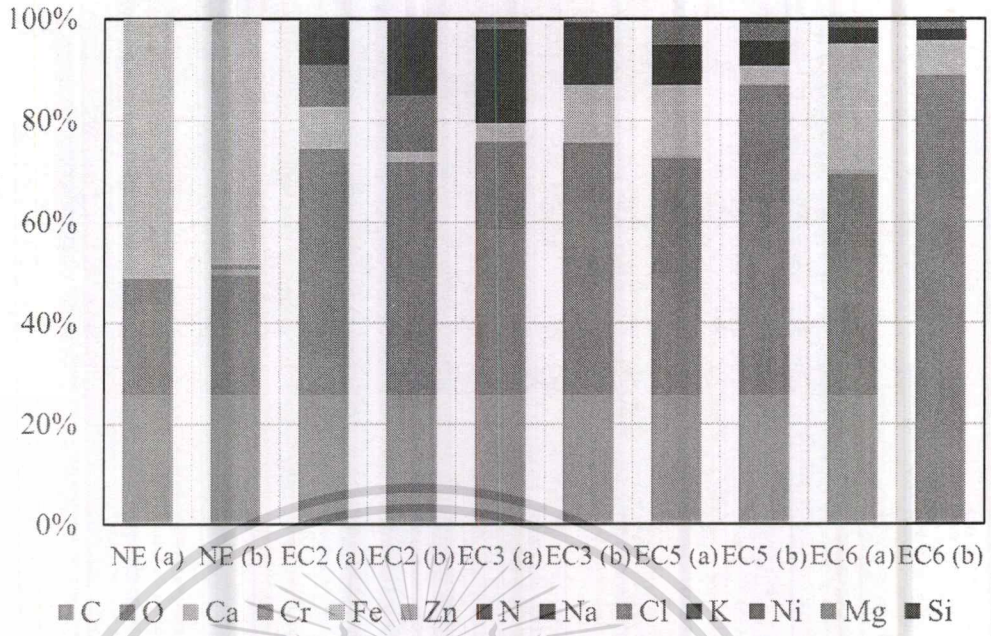

(a) Stacked bar chart of elements analysis of the wear on each steal ball using EDX

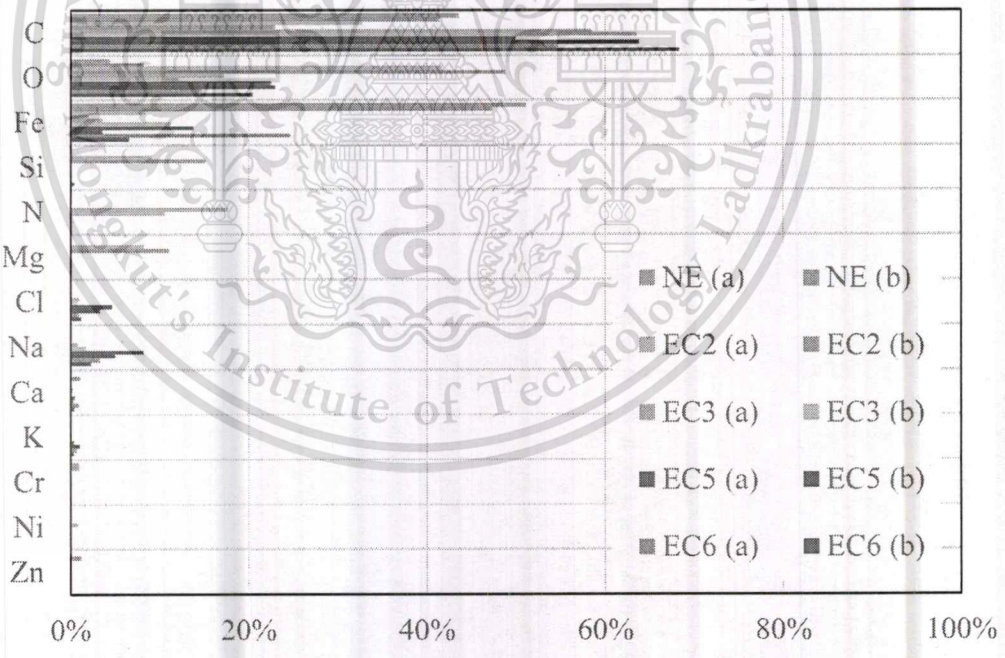

(b) Clustered bar chart of elements analysis of the wear on each steal ball using EDX

Figure 4.18 Stacked bar chart and clustered bar chart of elements analysis of the wear on each steal ball using EDX analysis

CHAPTER 5

CONCLUSION

According to the study of the impact of soot on lubricating oil properties and on metal wear, it can be concluded as following:

In case of investigating used engine from small diesel engine vehicles, the results have been showed that soot contamination was about 0.78 percent by weight. Fuel contamination was about 2.0 percent by weight. The particle size in the used oil and in the used filter were in the range of 0.1 – 20 microns and 1 - 100 microns, respectively.

Based on the four-ball tribology test, the effect of biodiesel contamination were increasing in wear scar diameter However, the surface roughness was decrease. It might be expected that hetero atom of bio- oxygenate fuel promote more heterogeneous oil film. Wear particle size distribution in the Four-ball tested oils occurred as a bimodal distribution. Moreover, the low biodiesel-blended fraction (B7 and B20) produce more amount of smaller size of metal wear particles.

Moreover, Soot particle distributions in liquids were observed by Laser Diffraction Spectroscopy. It was found that there were highly agglomerated in water, a smaller group of agglomeration in palm oil and well distribution in formulated lubricant. The impact of soot nanoparticle affecting on metal wear was investigated by Four-ball wear tester. It was found that the ball WSD increased proportionally to the soot primary particle size. It is expected that the soot particle which is larger than the oil film thickness can increase the metal wear.

In this research, soot wear mechanisms might be expected as three-body abrasive wear. The role of lubricating oil is to generate an oil film between two surfaces and trap soot particles. If the soot particle size is smaller than the oil film, the surface can be separated, and no wear should occur. Further, if the soot particle size is larger the oil film thickness, then soot might occur as three body abrasion. Therefore, viscosity improver additives would be a key to preventing soot abrasive wear.

REFERENCES

1. S. Daido, Y. K, T. I, N. O, and T. S, Analysis of Soot Accumulation inside Diesel Engines, *JSAE Review*, Vol. 21, 303-308 (2000).
2. W. M. Needelman, and P. V. Madhavan, Review of Lubricant Contamination and Diesel Engine Wear, *SAE papers*, 881827 (1988).
3. P. Kamsrisuk, P. Karin, K. Sriprapha, and H. KOSAKA. An Investigation on Physical and Chemical Properties in Used Lubricating Oil of Diesel Engine, Master Of Engineering Thesis *IC KMITL* (2016).
4. M. Gautam, S. George, S. Balla, and V. Gautam, Effect of diesel soot on lubricant oil viscosity, *Tribology International*, Vol. 40. 809–818 (2007).
5. D. A. Green, and R. Lewis. The effects of soot-contaminated engine oil on wear and friction: A review. *Proc Inst Mech Eng Pt D: J Automobile Eng,* Vol. 222, 1669-89 (2008).
6. P.R. Ryason, I. Chan, and J.T. Gilmore, Polishing Wear by Soot, *Wear*, Vol.137, 15-24 (1990).
7. P. Karin, C. SUPANAMOK and K. Hanamura, Impact of Soot on Metal Wear Characteristics Using Laser Diffraction Spectroscopy. *JRAME*, Vol. 4. No.2, 126-134 (2016).
8. E. Hu, X. Hu, T. Liu, L. Fang, K.D. Dearn, and H. Xu, The role of soot particles in the tribological behavior of engine lubricating oils, *Wear*, Vol. 304, 152-161 (2013).
9. P. Karin, J. Boonsakda, K. Siricholathum, E. Saenkhumvong, C. Charoenphonphanich, and K. Hanamura, Morphology And Oxidation Kinetics Of Ci Engine's Biodiesel Particulate Matters On Cordierite Diesel Particulate Filters Using TGA, *KSAE,* Vol. 18, 31-40 (2017).
10. M. Torbacke, A.K. Rudolphi, and E. Kassfeldt, Lubricants: Introduction to Properties and Performance: *John Wiley & Sons*, First Edition (2014).
11. P.A. Lakshminarayanan, N.S. Nayak, Critical Component Wear in Heavy Duty Engines: *Wiley* (2011).
12. G.W. Stachowiak, A.W. Batchelor, Engineering Tribology, *Elsevier Inc.* (2013).
13. M.M. Maricq: Chemical characterization of particulate emissions from diesel engines – A review, *Aerosol Science*, vol. 38, p.1079-1118 (2007).

14. C. Supanamok, P. Karin, C. Benyajati, and K. Hanamura, Impact of Soot in Engine Lubricating Oil on Metal Wear Using Four-Ball Testing, *JSAE Annual Congress Proceedings* (spring), p.1673-1679 (2015).
15. Crea Laboratory Technolgies Pty Ltd, SpectroT2FM Q500 Analytical Ferrography Laboratory Application, [Online]. Available : http://www.crealt.co.nz/oilanalysis/onsite/q5200/pulp-and-paper/spectrot2fm-q500-analytical-ferrography-laboratory/ (2559)
16. S. Raadnui, Analytical Ferrography Analysis, [Online]. Available : http://www.machinerylubrication.com/Read/672/grease-analysis-bearings (2559)
17. Trico Corporation, TYPICAL FERROGRAPHIC WEAR PARTICLES, [Online]. Available : https://www.tricocorp.com (2559)
18. G. Chandra, SCANNING ELECTRON MICROSCOPE (SEM), [Online]. Available: http://www.iaszoology.com/sem/ (2559)
19. Schematics of transmission electron microscopy operation, [Online]. Available : http://www.hk-phy.org/atomic_world/tem/tem02_e.html
20. Particle Analytical, Laser diffraction theory, [Online]. Available : http://particle.dk/methods-analytical-laboratory/particle-size-by-laser-diffraction/laser-diffraction-theory/ (2559)
21. FG. Rounds, Carbon: Cause of diesel engine wear?, *SAE Technical Paper*, Paper Number 770829.
22. Ryason PR, et al. Polishing wear by soot - Presented before the Division of Petroleum Chemistry, ACS, Boston Meeting, April 22, 1990 - April 272 1990; 35:250.
23. Nagai I, Endo H, Nakamura H, Yano H. Soot and valve train wear in passenger car diesel engines. Lubricant and Additive Effects on Engine Wear. 1983:87-101.
24. Needelman, W. and Madhavan, P., Review of Lubricant Contamination and Diesel Engine Wear, SAE Technical Paper 881827, 1988
25. P. Khamsrisuk, P. karin, K. Sriprapha and H. Kosaka, An Investigation on Physical and Chemical Properties of Lubricant Used in Diesel Engine, The 6th TSME International Conference on Mechanical Engineering (6th TSME ICoME) 16th December - 18th December 2015, Regent Cha-Am Beach Resort, Petchburi, Thailand

APPENDIX A

InS Thai Ltd.
Thai-French Innovation Institute (8th Floor),
King Mongkut's University of Technology North Bangkok,
1518 Pracharat 1 Rd., Wongsawang, Bangsue, Bangkok 10800, Thailand.
Tel: +66 (0)2 585 9946, +66 (0)2 585 9964, +66 (0)2 585 9982, Fax: +66 (0)2 585 9951
www.ins-thai.com

ANALYSIS REPORT:
King Mongkut's Institute of Technology Ladkrabang
Four ball – Wear resistance according to ASTM D4172

Sample description	Lubricants
Customer Sample Reference	See table 1
Internal Sample Reference	See table 1
Date of Receipt	12/01/2017
Date of Analysis	12/01/2017-03/02/2017
Analysis Report Reference	R1701204KMI

TESTS & SAMPLES

TEST	STANDARD	CONDITIONS	CUSTOMER SAMPLE REF.	INTERNAL SAMPLE REF.
4-Ball Method	ASTM D4172	– *Rotational speed: 1200±10 rpm* – *Load: 392±2 N (40±2 kgf)* – *Duration per load: 60±1 min* – *Temperature: 75±2 °C*	See Table 1	See Table 1

Table 1: List of samples reference

Customer Reference	InS Thai Reference
SAEOW3O	S1701204KMI-01
N220	S1701204KMI-02
N330	S1701204KMI-03
N660	S1701204KMI-04
N550	S1701204KMI-05

APPENDIX A

(Continuous)

InS Thai Ltd.
Thai-French Innovation Institute (8th Floor),
King Mongkut's University of Technology North Bangkok,
1518 Pracharat 1 Rd., Wongsawang, Bangsue, Bangkok 10800, Thailand.
Tel: +66 (0)2 585 9946, +66 (0)2 585 9964, +66 (0)2 585 9982, Fax: +66 (0)2 585 9951
www.ins-thai.com

SAMPLE PREPARATION & TESTING

According to the four balls testing standard (ASTM D4172), the samples are tested at 75°C. The normal load applied is 392 N. Running time is 60 minutes.

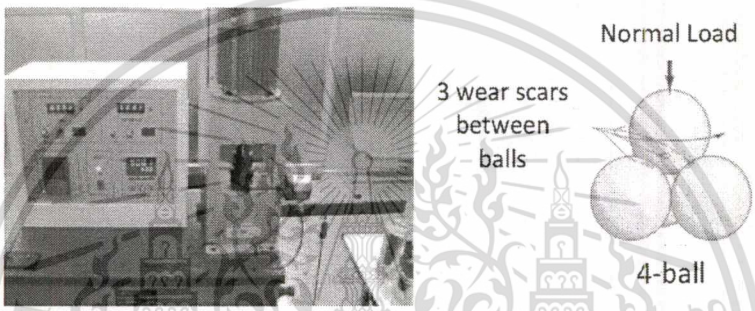

Figure 1: Four balls testing machine and direction of applied load

Figure 2: samples images received from the customer

After the test, the diameter of wear scar is measured by optical microscope at ×100 and ×200 magnifications. The wear scar diameters of the three lower balls are measured and the average values are calculated. The friction torque during the test is recorded every 5 minute and reported also.

APPENDIX A

(Continuous)

InS Thai Ltd.
Thai-French Innovation Institute (8th Floor),
King Mongkut's University of Technology North Bangkok,
1518 Pracharat 1 Rd., Wongsawang, Bangsue, Bangkok 10800, Thailand.
Tel: +66 (0)2 585 9946, +66 (0)2 585 9964, +66 (0)2 585 9982, Fax: +66 (0)2 585 9951
www.ins-thai.com

RESULTS

Table 2 presents the wear scars diameter measured on the three lower balls. The variation of wear scar diameter is small indicating a good sample installation. Figure 3 shows the comparison of wear scar size between different samples.

Table 2: Wear scars diameter measured by microscope

Sample	Ball 1		Ball 2		Ball 3		Average (µm)	Ball 4			Average (µm)
	d_1 (µm)	d_2 (µm)	d_1 (µm)	d_2 (µm)	d_1 (µm)	d_2 (µm)		d_1 (µm)	d_2 (µm)	d_3 (µm)	
SAEOW30	546.29	546.06	543.12	543.30	543.12	543.30	**544.20**	550.58	550.68	550.68	**550.65**
N220	529.69	529.87	535.66	535.84	535.66	534.35	**533.51**	516.26	516.40	515.99	**516.22**
N330	546.29	546.06	546.29	544.61	547.60	547.78	**546.44**	603.62	603.41	603.16	**603.40**
N660	808.08	808.40	820.26	820.26	817.27	817.27	**815.25**	799.34	800.95	799.57	**799.95**
N550	582.73	596.14	606.60	579.63	599.13	605.14	**579.90**	573.73	573.38	569.89	**572.34**

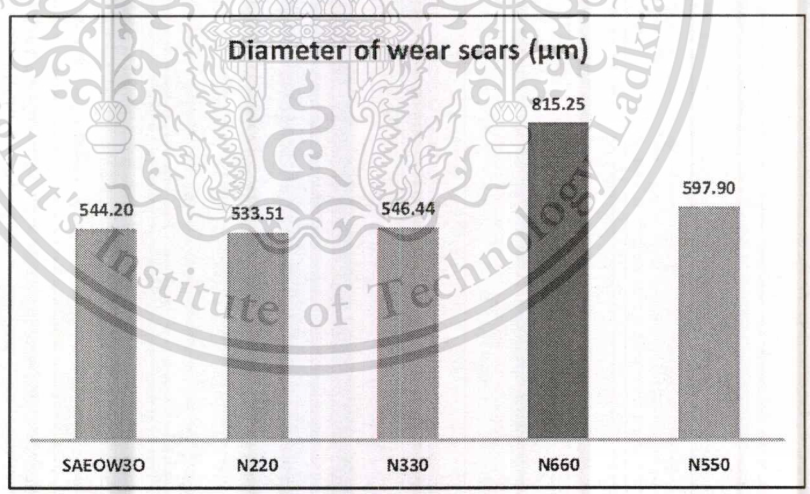

Figure 3: Average wear scar size of three lower balls after testing

APPENDIX A

(Continuous)

InS Thai Ltd.
Thai-French Innovation Institute (8th Floor),
King Mongkut's University of Technology North Bangkok,
1518 Pracharat 1 Rd., Wongsawang, Bangsue, Bangkok 10800, Thailand.
Tel: +66 (0)2 585 9946, +66 (0)2 585 9964, +66 (0)2 585 9982, Fax: +66 (0)2 585 9951
www.ins-thai.com

Table 3 showed the mass loss of each ball after testing of all lubricant samples.

Table 3: Mass loss measured by high precision balance (4 digit)

Sample	Customer Reference		Weight (g)		
			Before	After	Weight loss (g)
Sample 1	SEAOW30	Ball 1	8.3506	8.3506	0.0000
		Ball 2	8.3550	8.3549	0.0001
		Ball 3	8.3530	8.3528	0.0002
		Ball 4	8.3524	8.3522	0.0002
Sample 2	N220	Ball 1	8.3548	8.3548	0.0000
		Ball 2	8.3508	8.3508	0.0000
		Ball 3	8.3533	8.3532	0.0001
		Ball 4	8.3543	8.3542	0.0001
Sample 3	N330	Ball 1	8.3540	8.3539	0.0001
		Ball 2	8.3521	8.3520	0.0001
		Ball 3	8.3549	8.3548	0.0001
		Ball 4	8.3542	8.3540	0.0002
Sample 4	N660	Ball 1	8.3546	8.3545	0.0001
		Ball 2	8.3522	8.3521	0.0001
		Ball 3	8.3546	8.3545	0.0001
		Ball 4	8.3535	8.3533	0.0002
Sample 5	N550	Ball 1	8.3515	8.3514	0.0001
		Ball 2	8.3536	8.3535	0.0001
		Ball 3	8.3512	8.3511	0.0001
		Ball 4	8.3525	8.3524	0.0001

General conclusion:

- The lowest and highest wear scar diameters were found on N220 and N660, respectively.
- The mass loss of each ball for all samples were less than or equal to 0.0002 g.

Prepared by:
Mr.Panumas Songvut
Miss. Alisa Jukra
R&D Scientist
Panumas Songvut
Alisa Jukra
2017-02-03

Approved by:
Dr. Pornsit Lorkit
Project Leader, Material Science Laboratory
Pornsit L.
2017-02-03

APPENDIX B

Eval2 V2.5.500 Admin 3/16/2017 4:28:44 PM
Sample: 601503-9876-Mazda sae0w30
Measured on 3/15/2017 2:18:03 PM
Sample measured by Admin
Measurement method: Best Detection-He34mm

Sum	S	Ca	Zn	P	Mo	K
0.60 %	0.214 %	0.166 %	847 PPM	779 PPM	454 PPM	74.0 PPM

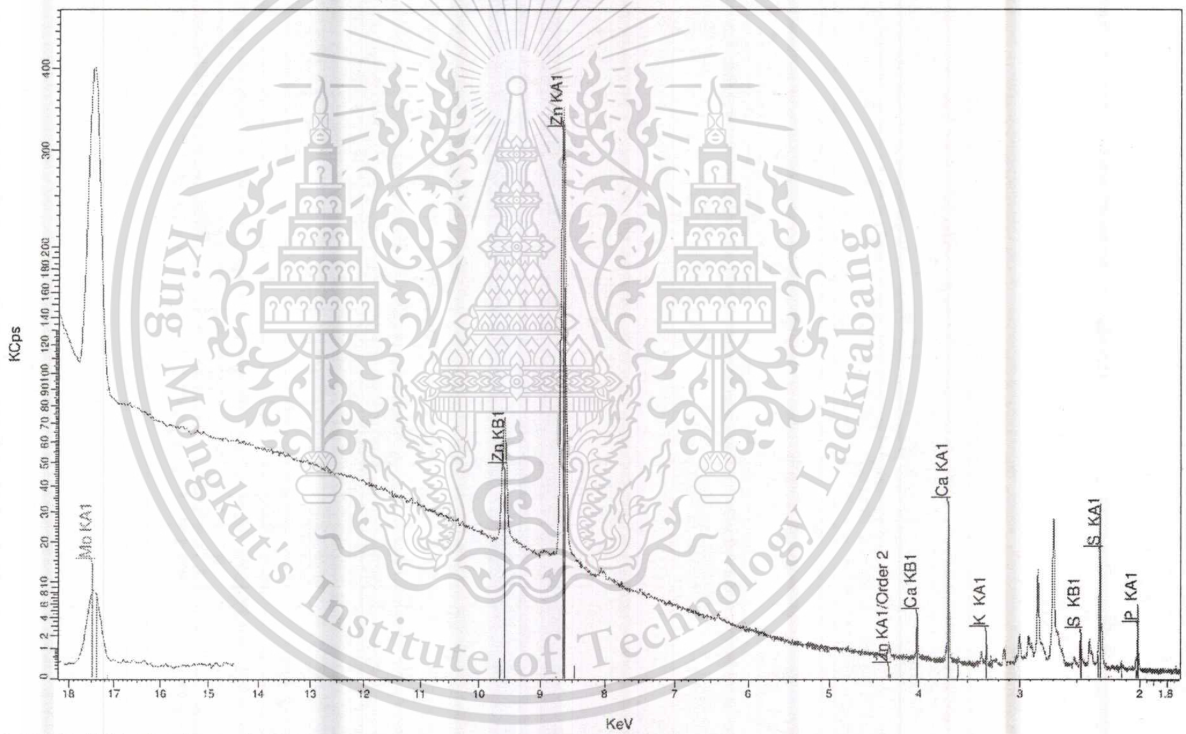

601503-9876-Mazda sae0w30
Eval2 V2.5.500 Admin 3/16/2017 4:28:02 PM

APPENDIX C

ศูนย์เครื่องมือวิจัยวิทยาศาสตร์และเทคโนโลยี จุฬาลงกรณ์มหาวิทยาลัย
อาคารสยามบิน 3 ชั้น 3 จุฬาซอย 62 ถนนพญาไท เขตปทุมวัน กรุงเทพฯ 10330 โทร. (662) 218-8101, 218-8033 โทรสาร (662) 218-8101, 254-0211
SCIENTIFIC AND TECHNOLOGICAL RESEARCH EQUIPMENT CENTRE CHULALONGKORN UNIVERSITY
CHULALONGKORN SOI 62 PHAYA-THAI ROAD PHATUMWAN BANGKOK 10330 THAILAND TEL. (662) 218-8101, 218-8033 FAX : (662) 218-8101, 254-0211

Report No. 601601-3766

Analysis Report

Sample Carbon black
Sample owner Warawut Amornprapa
International College King Mongkut's Institute of Technology Ladkrabang
Objective To determine particle size distribution
Instrument Laser Particle Size Analyzer (Mastersizer 3000)
Analysis date February 6, 2017
Results (Refer also to data in the attached statistical results)

Sample name	Particle size (Micron)					
	Particle size distribution	Measured values			Mean	SD
		#1	#2	#3		
II	10 percentile, D(v,0.1)	0.2280	0.3640	0.4870	0.3597	0.1296
	50 percentile, D(v,0.5)	2.8100	3.0000	3.1200	2.9767	0.1563
	90 percentile, D(v,0.9)	8.5500	8.5900	8.3800	8.5067	0.1115
	Average D[4,3]	6.7600	6.9800	6.6500	6.7967	0.1680
III	10 percentile, D(v,0.1)	0.0184	0.0186	0.0190	0.0187	0.0003
	50 percentile, D(v,0.5)	0.3200	0.3500	0.3850	0.3517	0.0325
	90 percentile, D(v,0.9)	2.7200	2.9600	3.2000	2.9600	0.2400
	Average D[4,3]	0.8680	0.9620	1.0600	0.9633	0.0960
V	10 percentile, D(v,0.1)	0.0245	0.0255	0.0268	0.0256	0.0012
	50 percentile, D(v,0.5)	0.7620	0.8860	1.0400	0.8960	0.1393
	90 percentile, D(v,0.9)	10.4000	10.3000	10.1000	10.2667	0.1528
	Average D[4,3]	3.4000	3.4100	3.3800	3.3967	0.0153
VI	10 percentile, D(v,0.1)	0.0207	0.0215	0.0222	0.0215	0.0008
	50 percentile, D(v,0.5)	0.5020	0.5650	0.6400	0.5690	0.0691
	90 percentile, D(v,0.9)	4.8200	5.0800	5.2500	5.0500	0.2166
	Average D[4,3]	1.9400	1.9700	2.0400	1.9833	0.0513

(Miss Kaew Kajornchaiyakul) Analyst
(Mrs. Sunan Rangseekansong) Chief Scientist
(Assoc. Prof. Dr. Amorn Petsom) Director

APPENDIX D

ศูนย์เครื่องมือวิจัยวิทยาศาสตร์และเทคโนโลยี จุฬาลงกรณ์มหาวิทยาลัย
อาคารสถาบัน 3 ชั้น 5 จุฬาซอย 62 แขนพญาไท เขตปทุมวัน กรุงเทพฯ 10330 โทร. (662) 218-8101, 218-8023 โทรสาร (662) 218-8101, 254-0211

SCIENTIFIC AND TECHNOLOGICAL RESEARCH EQUIPMENT CENTRE CHULALONGKORN UNIVERSITY
CHULALONGKORN SOI 62 PHAYA-THAI ROAD PHATUMWAN BANGKOK 10330 THAILAND TEL. (662) 218-8101, 218-8023 FAX : (662) 218-8101, 254-0211

Report No. 600902-1263

Analysis Report

Sample: Carbon blacks mixed with new sae0w30 engine oil

Sample owner: Warawut Amornprapa
International College King Mongkut's Institute of technology ladkrabang

Objective: To determine particle size distribution

Instrument: Laser Particle Size Analyzer (Mastersizer 3000)

Analysis date: March 2-3, 2017

Result (Refer also to data in the attached statistical results)

Sample name	Particle size (Micron)					
	Particle size distribution	Measured values			Mean	SD
		#1	#2	#3		
Sample 1	No result of particle size distribution because the samples amount was not enough for the measurement.					
Sample 2	10 percentile, D(v,0.1)	0.6180	0.5060	0.5180	0.5473	0.0615
	50 percentile, D(v,0.5)	79.4000	75.9000	74.4000	76.5667	2.5658
	90 percentile, D(v,0.9)	218.0000	214.0000	217.0000	216.3333	2.0817
	Average D[4,3]	95.5000	92.8000	93.4000	93.9000	1.4177
Sample 3	10 percentile, D(v,0.1)	0.0288	0.0282	0.0282	0.0284	0.0003
	50 percentile, D(v,0.5)	33.4000	29.6000	29.3000	30.7667	2.2855
	90 percentile, D(v,0.9)	232.0000	217.0000	217.0000	222.0000	8.6603
	Average D[4,3]	83.6000	76.3000	77.2000	79.0333	3.9804
Sample 4	10 percentile, D(v,0.1)	0.0224	0.0226	0.0227	0.0226	0.0002
	50 percentile, D(v,0.5)	2.1300	2.8000	3.0800	2.6700	0.4882
	90 percentile, D(v,0.9)	163.0000	159.0000	161.0000	161.0000	2.0000
	Average D[4,3]	44.9000	44.3000	45.6000	44.9333	0.6506
Sample 5	10 percentile, D(v,0.1)	0.0215	0.0216	0.0223	0.0218	0.0004
	50 percentile, D(v,0.5)	1.2000	1.3800	3.3200	1.9667	1.1755
	90 percentile, D(v,0.9)	150.0000	156.0000	169.0000	158.3333	9.7125
	Average D[4,3]	39.4000	40.9000	47.9000	42.7333	4.5369

APPENDIX D

(Continuous)

Sample name	Particle size (Micron)					
	Particle size distribution	Measured values			Mean	SD
		#1	#2	#3		
Sample 1A	10 percentile, D(v,0.1)	8.3800	7.9500	7.9300	8.0867	0.2542
	50 percentile, D(v,0.5)	26.2000	25.1000	25.4000	25.5667	0.5686
	90 percentile, D(v,0.9)	55.6000	52.6000	55.4000	54.5333	1.6773
	Average D[4,3]	29.5000	28.1000	28.9000	28.8333	0.7024
Sample 2A	10 percentile, D(v,0.1)	0.0207	0.0207	0.0207	0.0207	0.0000
	50 percentile, D(v,0.5)	2.0300	2.1600	2.1900	2.1267	0.0850
	90 percentile, D(v,0.9)	27.9000	29.2000	29.6000	28.9000	0.8888
	Average D[4,3]	8.9100	9.2900	9.4400	9.2133	0.2732
Sample 3A	10 percentile, D(v,0.1)	0.0217	0.0215	0.0217	0.0216	0.0001
	50 percentile, D(v,0.5)	5.0700	4.7000	4.9200	4.8967	0.1861
	90 percentile, D(v,0.9)	99.1000	97.5000	99.0000	98.5333	0.8963
	Average D[4,3]	30.1000	29.0000	29.5000	29.5333	0.5508
Sample 4A	10 percentile, D(v,0.1)	0.0228	0.0232	0.0236	0.0232	0.0004
	50 percentile, D(v,0.5)	3.5700	3.9700	4.3200	3.9533	0.3753
	90 percentile, D(v,0.9)	76.5000	75.8000	75.5000	75.9333	0.5132
	Average D[4,3]	22.8000	22.8000	23.5000	23.0333	0.4041
Sample 5A	10 percentile, D(v,0.1)	0.0187	0.0187	0.0189	0.0188	0.0001
	50 percentile, D(v,0.5)	0.5590	0.5580	0.5750	0.5640	0.0095
	90 percentile, D(v,0.9)	25.5000	24.2000	26.3000	25.3333	1.0599
	Average D[4,3]	6.6900	6.6300	6.7300	6.6833	0.0503

(Miss Kaew Kajornchaiyakul) Analyst

(Mrs. Sunan Rangseekansong) Chief Scientist

(Assoc. Prof. Dr. Amorn Petsom) Director

Remark: The results are good only for those samples analyzed.

PUBLICATION

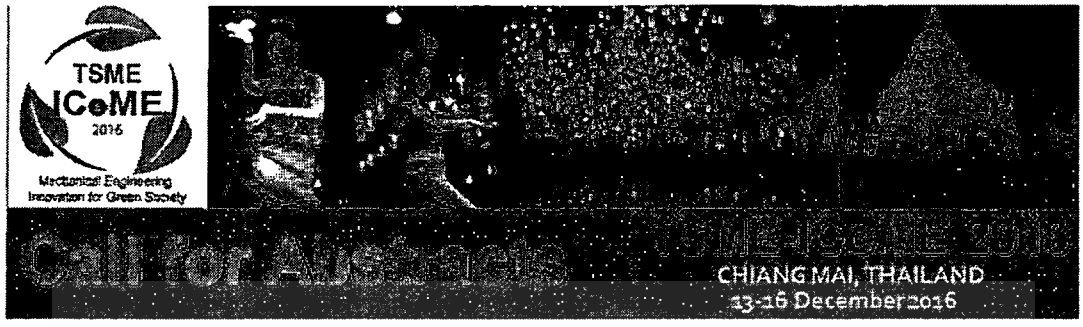

AME0008

Impact of Biodiesel Contamination on Engine Wear using Four-ball Wear Tester and Laser Particle Size Analyzer

Warawut Amornprapa[1,*], Phiranat Khamsrisuk[1], Preechar Karin[1], Kobsak Sriprapha[2] and Katsunori Hanamura[3]

[1] International college, King Mongkut's Institute of Technology Ladkrabang,Bangkok, 10520, Thailand
[2] National Electronics and Computer Technology Center (NECTEC), Pathumthani, 12120, Thailand
[3] Departments of Mechanical Engineering, Tokyo institute of technology, Japan
[*] Corresponding Author: Warawut_Amo@hotmail.co.th, 02-329-8261.

Abstract

The diesel engine is a compression ignition engine which converts chemical energy into mechanical energy. The energy forces the piston to perform up and down movement. The sliding movement of the components surfaces produces friction and wear. The lubricant protects an engine by producing the oil film to minimize the contacting surfaces. An incomplete combustion leads to fuel contamination, the contamination effect to oil degradation and lubrication breakdown. This research is aimed to investigate the effects of biodiesel contamination on the engine oil properties and wear characteristics. The used SAE0W30 engine oils were collected from diesel engine vehicles (B5-7). The amount of fuel contamination and particle size were measured by FT-IR and laser particle size analyzer, respectively. The results showed that the average amount of fuel contamination in used oils from the diesel engine vehicles was about 2% by weight. In addition, the new SAE0W30 engine oils were blended with biodiesel fuel to simulate fuel contamination. Friction torque and wear characteristics were evaluated by Four-ball wear tester and the worn surfaces of the balls were examined by scanning electron microscope (SEM) and 3D optical microscope. The particles in the Four-ball tested oil were also measured. The biodiesel contamination shows the negative effect on lubricating oil such as wear scar diameter and friction torque increase. On the other hand, it shows the positive effect to reduce surface roughness.

Keywords: Lubricant, Friction and Wear, Engine, Biodiesel, Four-Ball wear tester

1. Introduction

Recently, diesel engine is widely used as the powertrain in many fields. The advantage of the diesel engine is high efficiency due to high compression ratio. The engine converts chemical energy into mechanical energy. The contacting of metal to metal surfaces inside the engine generate heat and friction that can resulted in increases wear. Lubricant has an advantage in reducing friction prevent wear and removing frictional heat. It has an ability to minimize metal to metal contact by generating a lubricating film between the surfaces. The lubrication regimes can be divided into a boundary lubrication, mixed film lubrication, and full film lubrication [1, 2].

Biodiesel is an alternative fuel which is produced from vegetable oil or animal fat which plays an important role in petroleum diesel replacement. Biodiesel is an oxygenated fuel that makes more completely combustion process which resulted in lower carbon monoxide and unburned hydrocarbon. Khongdet [3] investigated performance and wear of the diesel engine which used diesel, biodiesel blends as a fuel. The results showed that the engine power and torque were similar to diesel engine. However, the amount of wear from biodiesel engine was higher than the diesel engine. Fazal et al. and Haseeb et al. [4, 5] studied the tribological properties of the palm biodiesel blends by using Four-ball wear tester. The tests were tested at different rotating speeds and temperatures. The results showed that wear scar diameter (WSD) and friction torque were increased proportionally to rotational speeds and temperature. Fuel film thickness was reduce, when the heat and rotational speeds increase, resulting in larger WSD. On the other hand, the WSD was decreased when biodiesel blends was increased, because of higher viscosity.

Jame et al. [6] reviewed the types of diesel engine lubricant contaminations. The fuel contamination are driven into the crank case engine oil by the high pressure during the combustion process. The solid particle which is larger than lubricant film thickness can lead to abrasive and fatigue wear. Water and fuel contamination can corrosive the component surface and makes lubricant breakdown. Kiatkong et al. [7] investigated the effect of fuel contamination on engine oil properties by using high frequency reciprocating rig. The results showed that the increasing of fuel contamination decreases oil viscosity. However, the contamination of biodiesel fuel resulted in increased lubricity, which resulted in decreases wear.

This research is aimed to investigate the effects of biodiesel contamination on the engine oil properties and wear characteristics.

2. Experiment Setup

2.1 Physical and Chemical Properties of Used Oil

The main purpose of this part was to measure the amount of fuel contamination in used engine oils from the real situations. The oils were collected from diesel engine vehicles. The engine displacement volume and

AME0008

the rate output were 1,500 cc and 105 HP, respectively. It was four cylinder, four strokes, used commercial diesel (B5-7) as a fuel. The engines were used SAE0W30 as an engine oil. The technical properties of the oil are shown in Table 1. The used engine oils were kept from the real diesel engine vehicles. The oils had the mileage and oil aged in a range of 3,000-20,000 and 0-10,000 km, respectively.

The amount of fuel contamination was measured by Fourier Transform Infrared (FT-IR) Spectrometry followed ASTM E-2412. The amount of total wear metal was measured by rotating disc electrode atomic emission spectroscopy (RDE-AES) followed ASTM D-6595. The morphology of wear particle was investigated by ferrogram and filtragram analysis. The particle sizes in the used oils were measured by laser particle size analyzer.

Table. 1 Properties of SAE0W30 engine oil

Properties	Specification
Viscosity @ 40 °C, (cSt)	44.5
Viscosity @ 100 °C, (cSt)	9.6
Viscosity Index	207
Oxidation, (Abs)	18.1
TBN, (mg KOH/g)	5.6

2.2 Effect of Fuel Contamination on Metal Wear

The main purpose of this test was to investigate the effect of fuel contamination on engine wear by using Four-ball wear tester and laser particle size analyzer. The commercial diesel (B5-7) and palm biodiesel blends (B20, B50 and B100) were blended with the new SAE0W30 engine oil at concentration of 2% by weight. The fuel properties and the list of different biodiesel blends mixed with new engine oil are shown in Table. 2 and Table. 3, respectively.

The Four-ball wear tester is used to determine wear preventive properties of lubricant in sliding contact. This machine consists of four 12.7 mm diameter steels ball which covered with lubricating oil, the three lower balls are held in a steel cup with fixed position and the fourth ball is rotating ball that held in the upper chunk. The test methods and conditions are followed standard test ASTM D4172 [8]. The fourth ball is pressed with a force of 392 N and it is rotated at 1,200 rpm. The temperature of lubricant and the operating time are 75 °C and 60 min. During the test, the friction torque is recorded by load cell sensor. After the test, the Four-ball tested oils were measured particle size by using laser particle size analyzer. The wear scar diameter and the surface roughness of the balls were measured by using scanning electron microscope and 3D optical microscope.

Laser particle size analyzer is used to determine the size distribution of the particles. It was measured by Malvern Mastersizer 2000 particle size analyzer. The machine is capable for measuring particles between 0.01 and 20000 μm.

Table. 2 Fuel Properties

Fuel properties	Biodiesel	Diesel
Cetane Number	70	55
Heating Value, (kJ/kg)	39,550	46,800
Density, (kg/m3)	847.73	844.78
Viscosity @ 40 °C, (cSt)	4.5	3.0
Flashpoint, (°C)	70	64

Table. 3 Fuels mixed with the engine oils

Samples	% SAE0W30	Fuel Type	% Fuel
NE	100 %	-	-
EB7	98 %	Commercial diesel (B7)	2 %
EB20	98 %	B20	2 %
EB50	98 %	B50	2 %
EB100	98 %	B100	2 %

Table. 4 Mileage and Oil aged of the used engine oils

Samples	Mileage (Km)	Oil age (Km)
1	19,046	9,362
2	19,500	9,800
3	19,779	9,811

3. Result and Discussion

3.1 Fuel contamination

Figure 1 shows the amount of (a) total wear metal and (b) fuel contamination by using oil analysis methods in the condition of 2,000 – 20,000 km of mileage and 2,000 - 10,000 km of oil aged. Total wear metal and fuel contamination were measured by using FT-IR and RDE-AES, respectively. The result showed that the total wear metal and fuel contamination increased with the increasing in mileage and oil aged. The average amount of fuel contamination was about 2% by weight.

Figure 2 shows the image of ferrogram and filtergram analysis. They are used to analysis the wear particles inside the used oil. A used oil from real diesel engine vehicle which had the oil aged around 9,800 km was chosen for ferrographic analysis. The results showed that the wear particles were 50% normal rubbing wear, 30% fatigue bearing wear, 10% black and red oxides, 5% white metal and 5% dirt and dust.

The three used engine oils from real diesel engine vehicles, which has similar mileage and oil aged as shown in Table. 4. It were collected and measured the particle size distribution by using the laser particle size analyzer. Fig. 3 shows particle size distribution of used oil. It occurs as a bimodal distribution. The particle sizes were in the range of 0.1 – 23 μm. The first and the second fraction were in the range of 0-1.4 μm and 1.4 – 23 μm, respectively. It might be expected that the particle sizes in this range were not trapped by the oil filter. The small and large particle might be soot and metal wear debris, respectively.

AME0008

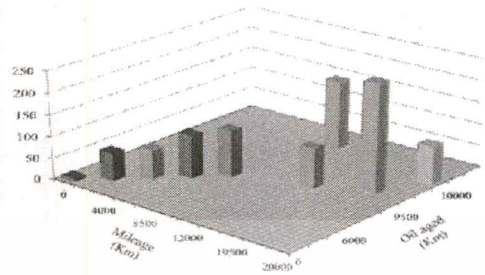

(a) Total wear metal (ppm)

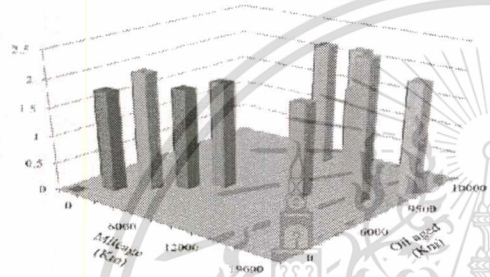

(b) Fuel contamination (%wt)

Fig. 1 (a) total wear metal and (b) fuel contamination on mileage and oil age from real diesel engine vehicles

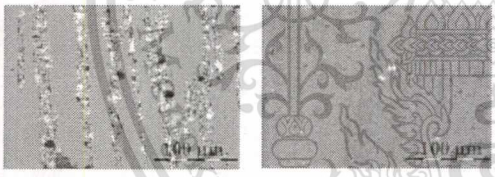

(a) Ferrogram image (b) Filtergram image

Fig.2 Image of (a) ferrogram and (b) filtergram analysis from real diesel engine vehicles

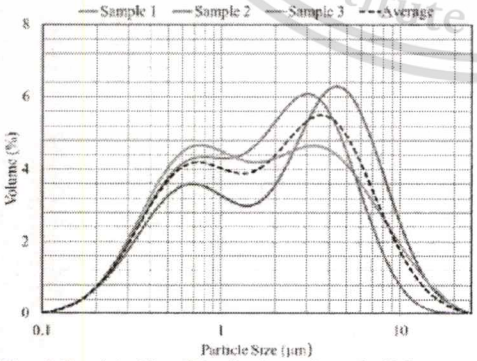

Fig. 3 Particle Size Distribution of used oil from real diesel engine vehicles by using laser particle size analyzer

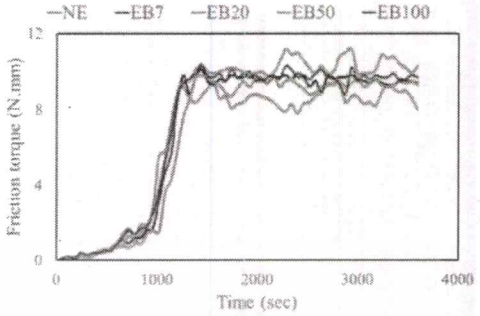

Fig. 4 Behavior of friction torque respect to times during using Four-ball wear tester

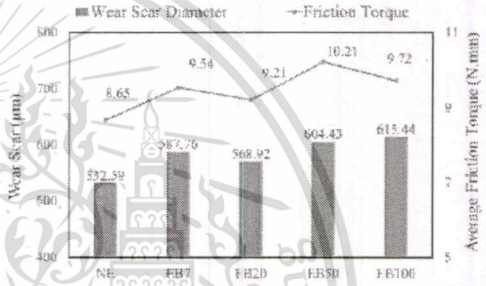

Fig. 6 Average Friction Torque and Average Wear Scar Diameter of each sample

3.2. Friction and wear properties

Figure 4 shows the behavior of friction torque respect to times of each sample, which recorded during using Four-ball wear tester. At the beginning of each test, the friction torque was increased with time. And a few minute later, the friction torque was almost stable. It might be expected that the removing of peak asperities makes the surfaces become smoother and increased the friction torque to the steady state condition.

Figure 6 shows the average friction torque from the steady state condition. The steady state condition was in the range of 1,200 - 3,600 second. The results showed that the average friction torque increased with the increasing in the percentage of biodiesel blends. However, EB20 gives the average lowest amount of friction torque as compared to other biodiesel blends contamination. The average wear scar diameters of each sample are shown in Fig. 5. The results showed that the average WSD increased with the increasing in the percentage of biodiesel blends. This trend was also similar to the friction torque.

After the Four-ball tests, the lower ball of each sample was collected for measure the surface roughness. The surface roughness were measured three places along the surface of the ball, as shown in Fig.5. Fig. 7 (a) shows the surface profiles of the tested balls, and (b) the average surface roughness of Four-ball tested balls.

AME0008

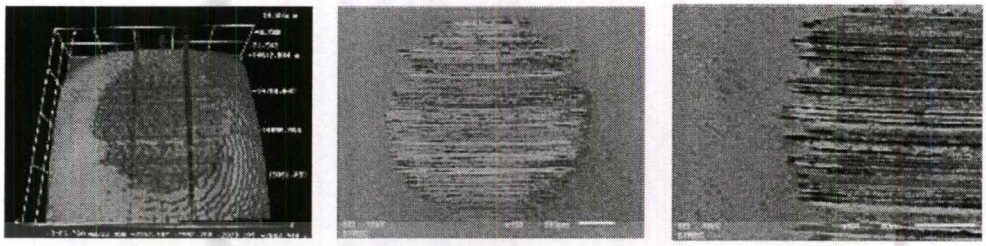

(a) NE

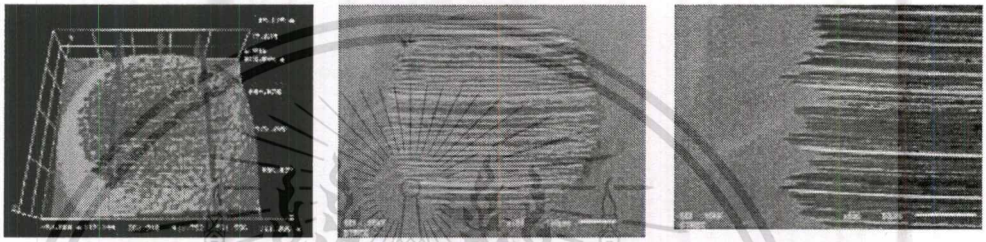

(b) EB7

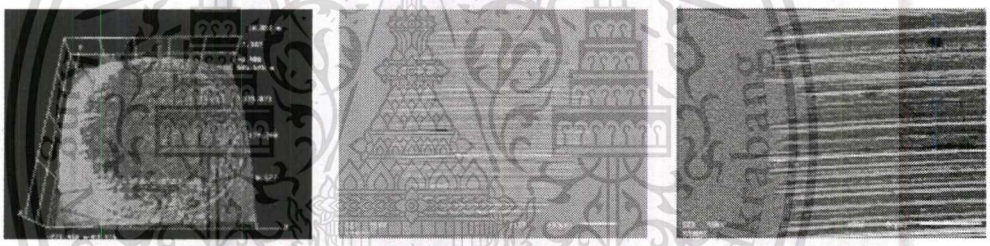

(c) EB20

(d) EB50

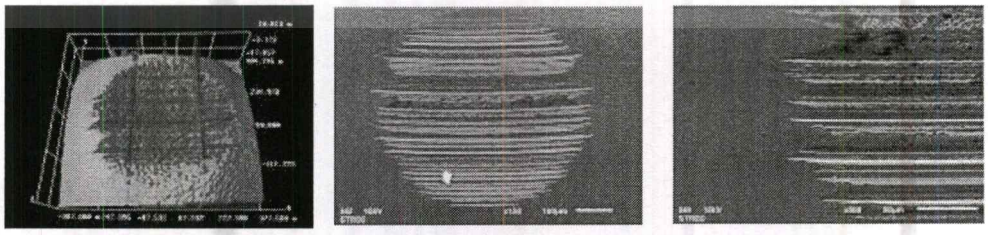

(e) EB100

Fig. 5 The wear surfaces under 3D optical microscope and scanning electron microscope of (a) New SAE 0w30 engine oil (b) Commercial diesel (B7)-2% (c) B20-2% (d) B50-2% (e) B100-2%

AME0008

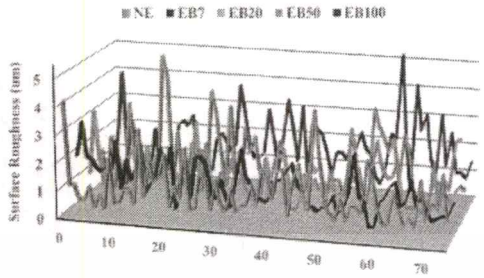

(a) Surface Profile

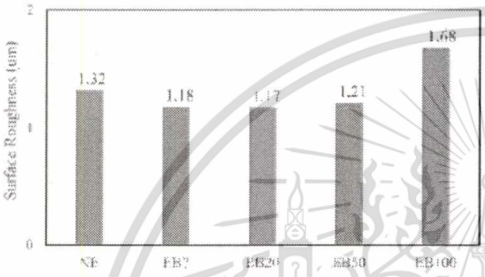

(b) Average surface roughness

Fig. 7 (a) Surface Profiles and (b) Average surface roughness of Four-ball tested balls

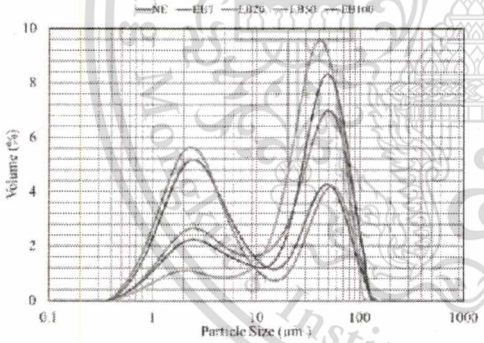

(a) Wear particle size distribution

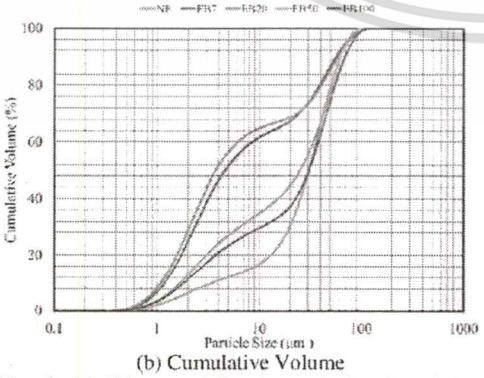

(b) Cumulative Volume

Fig. 8 (a) Wear particle size and (b) Cumulative particles volume of Four-ball tested oils

The results showed that the average surfaces roughness of the biodiesel blends contamination (EB7, EB20 and EB50) were lower than the pure engine oil (NE). However, the surface roughness of EB100 was higher than NE.

3.3. Laser particle size analyzer

After Four-ball tests, the Four-ball tested oils were measured the particle size distribution by using laser particle size analyzer. Fig. 8 shows (a) Particle size distribution and (b) Cumulative Volume of Four-ball tested oils. The particles sizes were in the range of 0-125 µm. The size distributions occur as bimodal distribution. The first and the second fraction were in the range of 0-15 µm and 15-125 µm, respectively.

The results showed that the EB7 and EB20 consist mostly of the small particles. However, the NE, EB50 and EB100 consist mostly of the large particles. At 20 % cumulative volume of NE, EB7, EB20, EB50 and EB100, the particle sizes were in the range of 0-3.2, 0-1.9, 0-1.6, 0-13.7 and 0-4.0 µm, respectively. At 40% cumulative volume, the particle sizes of each sample were in the range of 0-15.9, 0-3.2, 0-2.7, 0-25.3 and 0-23.3 µm, respectively. At 80% cumulative volume, the particle sizes of each sample were in the range of 0-54.4, 0-39, 0-40.7, 0-50.2 and 0-54.4 µm, respectively.

4. Conclusions

This study has been investigated the effect of fuel contamination on lubricating oil properties and wear characteristics.

The fuel contamination in used engine oils of diesel engine vehicles was about 2% by weight. The particles size in the oil pan of the engine were in the range of 0.1 – 23.3 µm. The soot and metal wear particle sizes might be in the range of 0 - 1 µm and 1-23.3 µm, respectively.

The effect of biodiesel contamination were increasing in wear scar diameter and friction torque. However, the surface roughness was decrease. It might be expected that hetero atom of bio-oxygenate fuel promote more heterogeneous oil film.

Wear particle size distribution in the Four-ball tested oils occurred as a bimodal distribution. Moreover, the low biodiesel-blended fraction (B7 and B20) produce more amount of smaller size of metal wear particles.

5. Acknowledgement

The authors would like to acknowledge Energy Policy & Planning Office (EPPO), Thailand Research Fund (TRF) and FOCUSLAB Ltd. for providing facility and research funding.

6. References

[1] Mang, T., Dresel, W. (2007). Lubricants and Lubrication. Weinheim: WILEY-VCH Verlag GmbH & Co. KGaA.

AME0008

[2] Syed Q. A. Rizvi. (2009). A Comprehensive Review of Lubricant Chemistry, Technology, Selection, and Design. West Conshohocken: ASTM international.
[3] Phasinam, K. (2009). Wearing Study of Medium Speed Diesel Engine Using Blended Biodiesel Fuel. Master Degree of Energy Management Engineering Thesis. Suranaree University of Technology.
[4] Fazal, M.A., Haseeb, A.S.M.A., Masjuki, H.H. (2013). Investigation of Friction and Wear Characteristics Of Palm Biodiesel, Energy Conversion and Management 67: 251–256.
[5] A.S.M.A. Haseeb, S.Y. Sia, M.A. Fazal*, H.H. Masjuki. (2010). Effect of temperature on tribological properties of palm biodiesel, Energy 35: 1460–1464.
[6] James A. Addison: Diesel Engine Lubricant Contamination and Wear: p 1-12 NY 11542.
[7] Kiatkong, S., Baitiang, T.,Tongroon, M., Chunhakitiyanon, S., and Chollacoop, N. (2011). Biodiesel Contamination in Engine Lube Oil. TSME AEC-02.
[8] ASTM D4172 -94 Standard test method for wear preventive characteristics of lubricating fluid (Four-ball method).

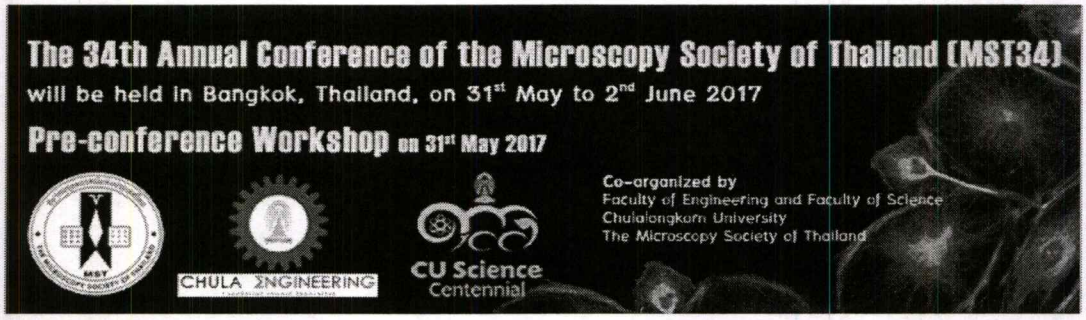

VENUE & TRAVEL INFORMATION

The 34th Annual Conference of the Microscopy Society of Thailand (MST34) is held at Grand Mercure Bangkok Fortune, Bangkok, Thailand.
The hotel located only 30 minutes from Suvarnabhumi International Airport, just a few steps from the MRT Rama 9 subway station.

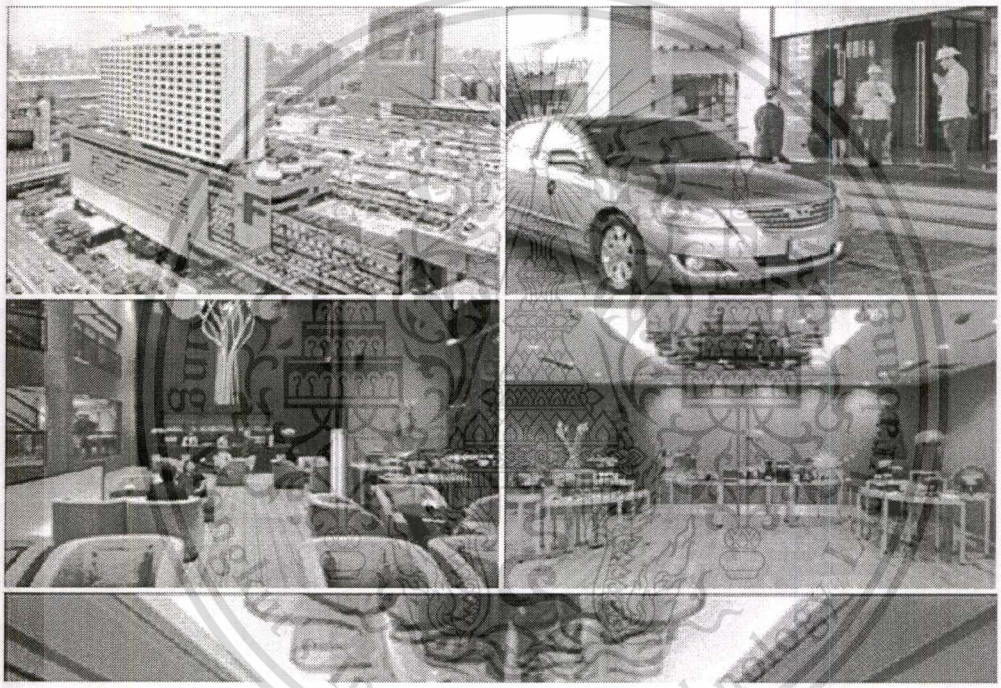

The Effect of Soot Nanoparticle Size on Metal Wear Using Electron Microscopy

Warawut Amornprapa[1*], Preechar Karin[1], Kobsak Sriprapha[2] and Katsunori Hanamura[3]
[1] International college, King Mongkut's Institute of Technology Ladkrabang, Bangkok, 10520, Thailand
[2] National Electronics and Computer Technology Center (NECTEC), Pathumthani, 12120, Thailand
[3] Departments of Mechanical Engineering, Tokyo institute of technology, Japan
*Presenter e-mail address: Warawut_Amo@hotmail.co.th

Abstract

The impact of soot nanoparticles affecting metal wear was investigated. Several types of Commercial Carbon Black was used to simulate an engine soot. The wear tests were evaluated by using Four-ball wear tester. After the tests, the ball surfaces were examined by using High-Resolution Optical Microscope and Scanning Electron Microscope (SEM). The results showed that the ball wear scar diameter (WSD) increased when the primary particle size of carbon black was increased. In conclusion, it might be expected that the soot particle which was larger than the oil film thickness can increase the metal wear.

Keywords: Lubricant; Wear; Soot; Four-Ball wear tester; Electron microscopy; Laser diffraction spectroscopy

Background

Diesel engine is a compression ignition engine which converts chemical energy within the fuel into mechanical energy. Diesel fuel is injected under high pressure into the combustion chamber where the combustion process occurs. Soot is remain of incomplete combustion which consists mostly of carbon, hydrocarbon and metallic ash. The primary and agglomerated soot particles observed by Transmission Electron Microscopy (TEM) are in the range of 20 - 80 nm and 100 - 300 nm, respectively [1]. Soot can be entered into the engine oil through the piston ring clearance during the combustion process [2].

Khamsrisuk *et al.* [3] performed the used oil analysis by collecting the engine oil from the small diesel engine vehicles. The results showed that the percentage of wear metal, soot and fuel contamination increased as the engine mileage increase. The average of soot contamination was about 0.69 percent by weight. Guatam *et al.* [4] investigated the effect of soot contamination on engine oil viscosity by increasing the percentage of soot contamination. The results showed that the engine oil viscosity increased with the increase of soot contamination. The engine testing for evaluated soot tribological properties is challenging, because of the uncontrolled test parameter and the difficulty of wear measurement [5]. The specimen bench test which is easy to control test parameter and good repeatable results are used. Carbon black is a synthesis soot which has similar particle size and physical properties to engine soot. It can be used as soot representative. Ryason *et al.* [6] performed wear tests on a ball-on-flat-disk wear tester using carbon black, alumina and silica. The results showed that the balls were worn similarly in three different kinds of the samples. Karin *et al.* [7] performed wear tests on Four-Ball Wear Tester. He found that the Wear Scar Diameter (WSD) of the ball in the oil containing carbon black was higher than that of the oil alone. Hu *et al.* [8] also performed Four-Ball Wear Tester using base oil and formulated lubricant. The results showed that the WSD was high when carbon black levels increased. But, the WSD of the formulated lubricant was lower than that of the pure base oil. They suggested that the wear mechanism of soot-contaminated lubricant might be abrasion.

Biodiesel is an alternative fuel that plays an importance role in replacement using petroleum diesel. It is an oxygenated fuel that promotes more completely combustion. The soot diameter size and quantity from biodiesel engine emission is lower than that of diesel [9]. However, soot induced wear mechanisms are still not fully understood. This research aimed to investigate the effects of soot Nanoparticles on metal wear characteristics using Four-Ball Wear Tester, Laser Diffraction Spectroscopy, and Electron Microscopy.

Materials and Methods

A formulated engine oil which had the same grade as SAE0W30 was used in this research. The engine oil condition including viscosity, oxidation, nitration and total base number were measured according to ASTM standard test methods. Oil additives were measured by x-ray fluorescence.

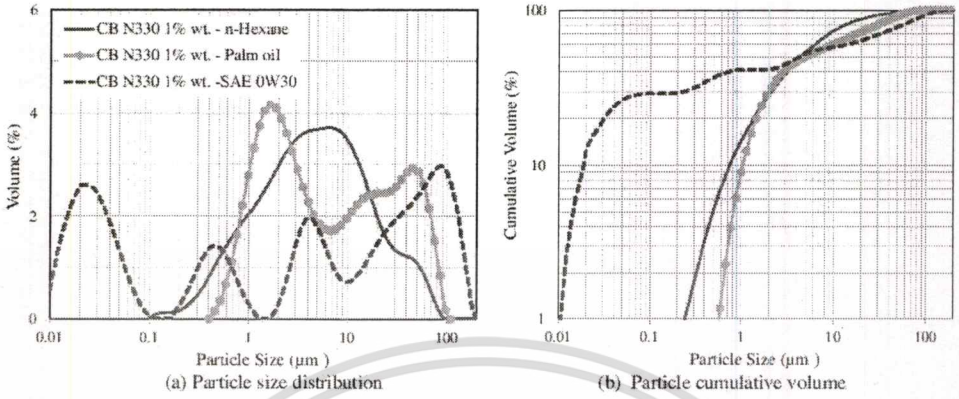

(a) Particle size distribution (b) Particle cumulative volume

Figure 1 Carbon black N330 (a) size distribution and (b) cumulative volume in different type of liquids by Laser Diffraction Spectroscopy.

Table 1 CB mixed with the engine oils.

Samples	Carbon Black	Average Primary Particle diameter (nm)*[10]	% CB (wt. / vol.)
NE	-	-	-
EC2	N220	21	1 %
EC3	N330	31	1 %
EC5	N550	53	1 %
EC6	N660	63	1 %

After that, the different types of carbon blacks (CB) were mixed with the engine oil at 1% by weight per volume for simulating soot contamination. They were Carbon black N220, N330, N550 and N660. The details of oil samples and CB average particle size [10] were shown in **Table 1.**

In order to investigate the effect of soot contamination on wear, the Four-Ball Wear Tester was chosen. The test methods and conditions followed the standard test ASTM D4172 [11]. The machine consists of four 12.7 mm. diameter steel balls, the three lower balls held in a steel cup with fixed position and the fourth ball was held in the upper chunk. The top ball was pressed with a force of 392 N and rotated at 1,200 rpm. The lubricant temperature and operating time were 75 °C and 60 min, respectively. After the tests, the three lower balls used to measure wear scar diameter (WSD) using a high-resolution optical microscope (OM). It was the average value of these balls. The surface roughness was also measured using 3D rendering system of that OM. The worn surface analysis was investigated by using Scanning Electron Microscopy (SEM). Moreover, the particle size distribution was measured using Laser Diffraction Spectroscopy.

Table 2 Properties of SAE0W30 engine oil

Oil conditions		Oil additives (ppm)	
Viscosity @ 40 °C	44.5 cSt	S	214.0
Viscosity @ 100 °C	9.6 cSt	Ca	166.0
Oxidation (Abs)	18.1	Zn	847.0
Nitration (Abs)	6.1	P	779.0
TBN (mgKOH/g)	5.6	Mo	454.0

Table 3 WSD and Roughness of each sample

Samples	Wear Scar Diameter (Micron)	Roughness (Micron)
NE	544	2.06
EC2	533	1.35
EC3	546	1.44
EC5	597	2.11
EC6	815	1.53

Results and Discussion

Soot particle size distribution

Table 2 shows oil properties of SAE 0W30 engine oil which is a diesel formulated lubricating oils. The several oil condition including viscosity, oxidation, nitration, and total base number were investigated. Oil additive elements were also analyzed by using X-ray fluorescence (XRF). **Figure 1** shows the size distribution of CB N330 mixing in n-Hexane, Palm oil and SAE 0W30 engine oil at 1% by weight. These tests were investigated by using laser diffraction technique. The results showed that soot dispersing in different liquids were significantly different. The results of carbon black dispersing in formulated lubricant seem better than those of n-hexane and palm oil that might be expected that the additives in an engine oil can help to disperse soot particle.

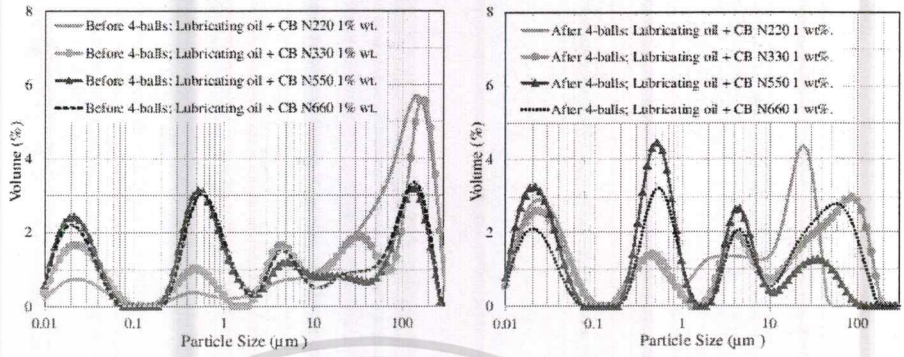

(a) Before Four-ball wear test (b) After Four- ball wear test

Figure 2 Particle size distribution of (a) Carbon black and (b) Carbon black with wear metal particles in lubricating oil before and after Four- ball wear test by Laser Diffraction Spectroscopy.

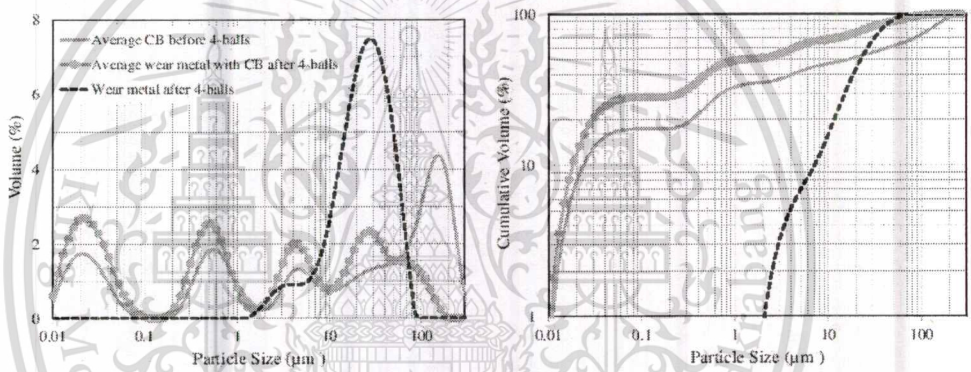

(a) Particle size distribution (b) Particle cumulative volume

Figure 3 Average Carbon black and wear metal particles (a) size distribution and (b) cumulative volume in lubricating oil before and after Four-ball wear test by Laser Particle Diffraction Spectroscopy.

Figure 2a shows size distribution of different types of carbon black mixing in the engine oil which were measured before Four-ball wear test. There were CB N220, N330, N550 and N660, respectively. The results showed that the different types of soot dispersing in the engine oil were not significantly different. They were in the range of 0.01 – 300 microns, which were small particle that have size of 10 - 100 nm. The first and second groups of agglomerate were in the range of 0.1 - 2 micron and 2 – 300 micron, respectively.

Impact of soot on metal wear

The wear scar diameters (WSD) and surface roughness were measured by using an optical microscope and 3D rendering analysis. They were the average value of the three lower balls. Additionally, the micro surface analyses were investigated by using Scanning Electron Microscopy (SEM). **Figure 4** shows microscopy image of wear scar found on the ball of (a) the engine oil without soot and engine oil containing 1% wt. of (b) N220, (c) N330, (d) N550 and (e) N660 Carbon Black. The average wear scar diameter and surface roughness were shown in **Table 3.** The results showed that the ball wear scar diameter (WSD) increased when the primary particle size of the carbon black was increased, but the surface roughness decreased. After Four-ball wear test, the tested oils were also measured size distribution. **Figure 2b** shows size distribution of particles inside the tested oils. They were in the range of 0.01 – 200 micron. **Figure 3** shows the comparison of particles size distribution before and after Four-ball wear test. After Four-ball test, the wear metal sizes were about of 1- 100 micron and the size of CB with wear metal seems smaller than those particles before the wear test.

The morphological and elemental composition of wear scar were studied. **Figure 5** shows SEM secondary and backscattered electron micrographs and energy dispersive X-ray (EDX) analysis.

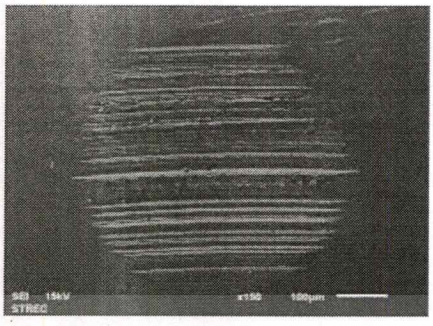

(a) The engine oil without soot

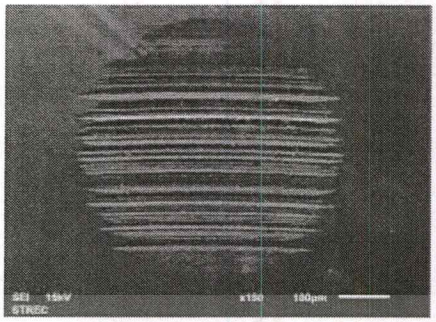

(b) The engine oil containing CB N220.

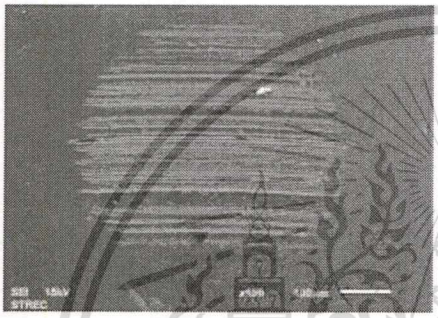

(c) The engine oil containing CB N330.

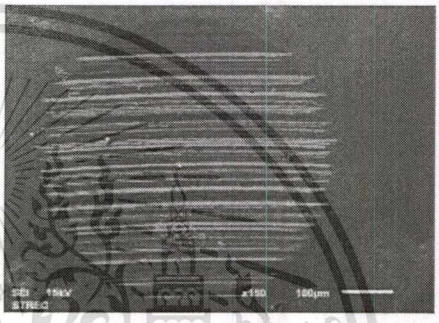

(d) The engine oil containing CB N550.

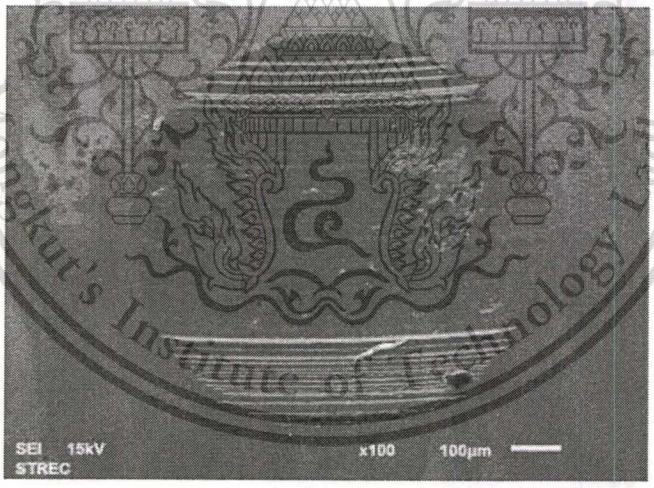

(e) The engine oil containing CB N660.

Figure 4 SEM micrographs taken using Secondary electron of the ball surface from (a) the engine oil without soot and the engine oil containing 1% wt. of (b) CB N 220, (c) CB N330, (d) CB N550 and (e) CB N660

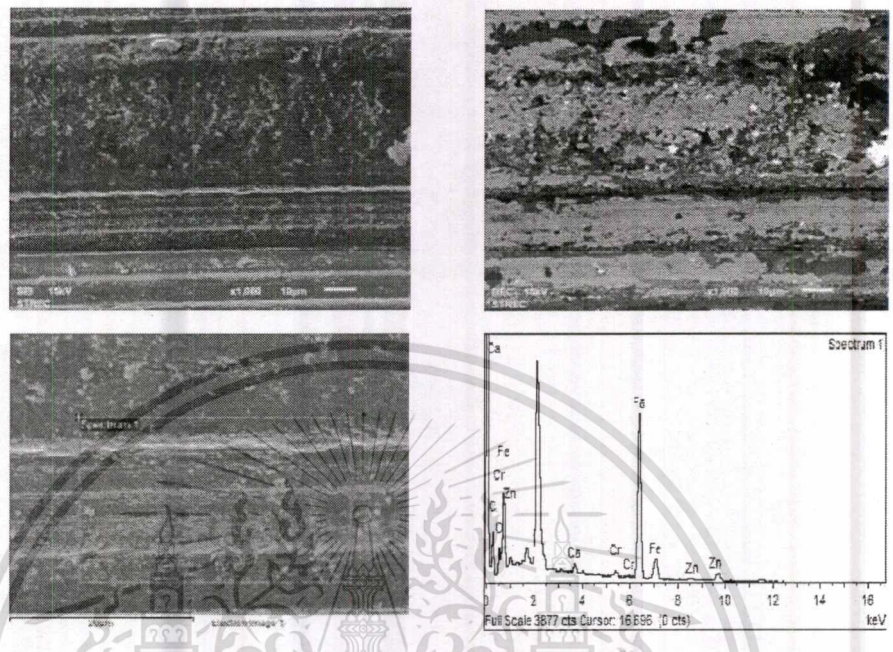

(a) The engine oil without soot.

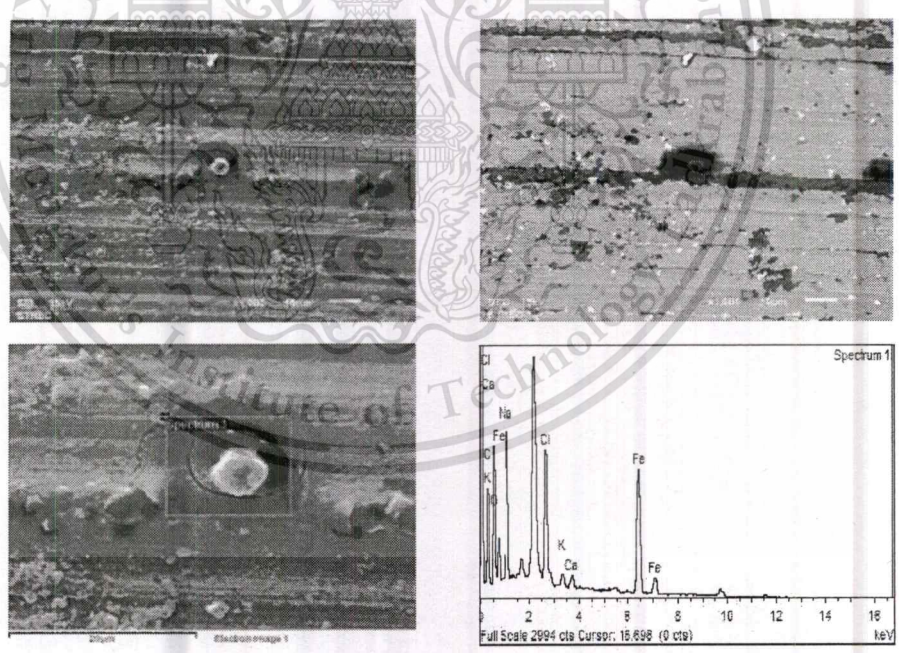

(b) The engine oil containing CB N550.

Figure 5 SEM micrographs taken using secondary and backscattered electron and EDX spectra of the ball surface from (a) the engine oil without soot and (b) the engine oil containing CB N550

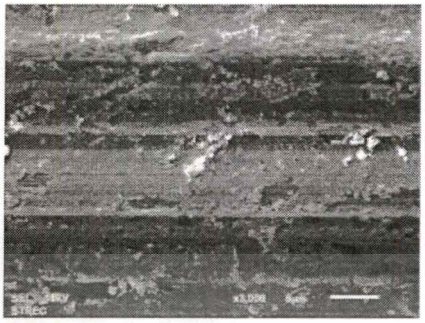

(a) The engine oil without soot.

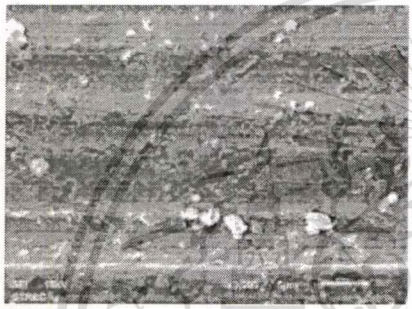

(b) The engine oil containing CB N330.

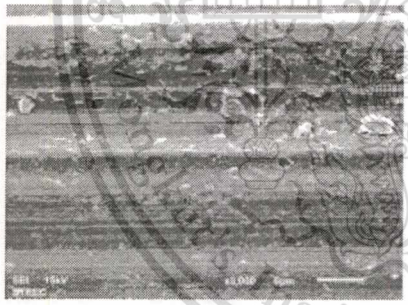

(c) The engine oil containing CB N550.

Figure 6 SEM micrographs taken using secondary electron at 3,000 magnification of the ball surface from (a) the engine oil without soot and (b) the engine oil containing CB N330 and (c) CB N550.

The EDX analysis indicated a composition of 41C-8O-1Ca-0.9Cr-47Fe-1Zn (in at. %) for the ball from the engine oil without soot and a composition of 50C-23O-8Na-5Cl-0.5K-0.5Ca-14Fe for the ball from the engine oil containing CB N550. **Figure** 6 shows the ball wear surface from (a) the engine oil without soot, (b) the engine oil containing CB N330 and CB 550. The ball surface of the engine oil containing CB N550 (**Figure 6c**) shows very clear wear trace that might be the result of soot abrasive wear.

Four-ball soot wear mechanisms

In this research, soot wear mechanisms might be expected as three-body abrasive wear. The role of lubricating oil is to generate an oil film between two surfaces and trap soot particles. If the soot particle size is smaller than the oil film, the surface can be separated, and no wear should occur. Further, if the soot particle size is larger the oil film thickness, then soot might occurr as three body abrasion. Therefore, viscosity improver additives would be a key to preventing soot abrasive wear

Conclusion

Soot particle distributions in liquids were observed by Laser Diffraction Spectroscopy. It was found that there were highly agglomerated in water, a smaller group of agglomeration in palm oil and well distribution in formulated lubricant. The impact of soot nanoparticle affecting on metal wear was investigated by Four-ball wear tester. It was found that the ball WSD increased proportionally to the soot primary particle size. It is expected that the soot particle which is larger than the oil film thickness can increase the metal wear.

Acknowledgements

The authors would like to acknowledge King Mongkut's Institute of Technology Ladkrabang, National Science and Technology Development Agency, Bangchak Corporation Pub Co., Ltd. and FOCUSLAB Ltd.

References

1. S. Daido, Y. K. T. I. N. O, and T. S, Analysis of Soot Accumulation inside Diesel Engines, *JSAE Review*, Vol. 21, 303-308 (2000).
2. W. M. Needelman, and P. V. Madhavan, Review of Lubricant Contamination and Diesel Engine Wear, *SAE papers*, 881827 (1988).
3. P. Kamsrisuk, P. Karin, K. Sriprapha, and H. KOSAKA, An Investigation on Physical and Chemical Properties in Used Lubricating Oil of Diesel Engine, Master Of Engineering Thesis *IC KMITL* (2016).
4. M. Gautam, S. George, S. Balla, and V. Gautam, Effect of diesel soot on lubricant oil viscosity, *Tribology International*, Vol. 40, 809–818 (2007).
5. D. A. Green, and R. Lewis, The effects of soot-contaminated engine oil on wear and friction: A review, *Proc Inst Mech Eng Pt D: J Automobile Eng*, Vol. 222, 1669-89 (2008).
6. P.R. Ryason, I. Chan, and J.T. Gilmore, Polishing Wear by Soot, *Wear*, Vol.137, 15-24 (1990).
7. P. Karin, C. SUPANAMOK and K. Hanamura, Impact of Soot on Metal Wear Characteristics Using Laser Diffraction Spectroscopy, *JRAME*, Vol. 4, No.2, 126-134 (2016).
8. E. Hu, X. Hu, T. Liu, L. Fang, K.D. Deam, and H. Xu, The role of soot particles in the tribological behavior of engine lubricating oils, *Wear*, Vol. 304, 152-161 (2013).
9. P. Karin, J. Boonsakda, K. Siricholathum, E. Saenkhumvong, C. Charoenphonphanich, and K. Hanamura, Morphology And Oxidation Kinetics Of Ci Engine's Biodiesel Particulate Matters On Cordierite Diesel Particulate Filters Using TGA, *KSAE*, Vol. 18, 31-40 (2017).
10. Carbon Black. *IARC MONOGRAPHS*, Vol. 93, 43-191 (2010).
11. Standard test method for wear preventive characteristics of lubricating fluid (Fourball method). *ASTM D4172 -94* (2016).

The 23rd Small Engine Technology Conference

Call for Papers

SETC 2017 JOGJAKARTA

Society of Automotive Engineers of Japan, Inc. | SAE INTERNATIONAL | IATO SAE-INDONESIA | Patronage of FISITA

VENUE : JAKARTA CONVENTION CENTER
PERIOD : November 15 to 17, 2017

DUE DATES
Abstracts due : January 31, 2017
Draft manuscripts due : April 14, 2017
Final manuscripts due : July 31, 2017

FOREWORD
JSAE, Society of Automotive Engineers of Japan, Inc., is pleased to announce that the 23rd Small Engine Technology Conference (SETC2017) will be held in Jakarta, Indonesia from November 15 to 17, 2017.

The conference is jointly organized by JSAE and SAE International with the support of Society of Automotive Engineers Indonesia (IATO) and Japan Land Engine Manufacturers Association (LEMA). We kindly ask prospective researchers and engineers in a diversified field of technologies and products with power source to submit electronic abstracts.

The conference offers up-to-date and new information in the development of technologies concerned in an exchange of participants from the globe. The events include technical visits, keynote speech, plenary session, exhibition and poster sessions besides ceremonial events of opening and awards & closing. Lunch & coffee-break for networking, welcome reception and banquet will be served as well.

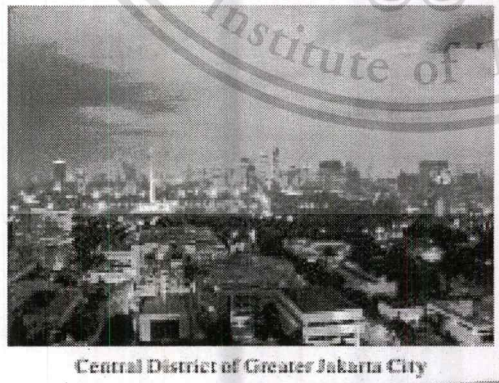

Central District of Greater Jakarta City

MAIN SUBJECT AREAS

- **Product Categories focused in this conference are:**

  Vehicles with power source such as ATV, Motorcycles, Scooters, Personal Mobility, Marine, Snowmobiles, Recreational Vehicles, Utility Vehicles, Power Assist Devices, Power Assist Bicycles and Unmanned Vehicles.

  ***Automobiles, Large Vessels, Large Aircraft, Locomotives and Spaceships are inapplicable.**

  Machines with power source such as Snow Removal Equipment, Portable Power Generators, Agricultural Equipment, Garden Equipment, Hand Tools and Powered Exoskeleton.

  Technologies applicable for the products above are to be presented in this conference.

- **Technological Areas focused in this conference are:**

  Combustion Engines such as 4 stroke Engines, 2 stroke Engines, SI Engines, Diesel Engines, HCCI Engines, Unconventional Engines and Competition Engines.

  New Energy Sources such as Hybrid Drives, Electric Drives, Fuel Cells and Solar Cells.

  Components such as Chassis, Suspensions, Brakes, Transmissions, Drivetrains, Electrical Systems, Electronic Systems, Fuel Supply Systems and Wheels & Tires.

  Development Technologies such as Numerical Simulations, Measurements and Production Technologies.

  Fuels, Lubricants, and Tribology such as Alternative Fuels, Fuel Reformations, Additives, Friction Loss and Wear.

  Vehicle Technologies such as Dynamics, Handling, Drivability, Safety Technology & Functional Safety and Human Factors & Ergonomics.

  Environmental Impacts such as Noise, Vibration, Emissions, Aftertreatment and Life Cycle & Recyclability.

  Materials such as Composites, Metal Alloys, Heat & Surface Treatment, New Material and Material Processing.

JSAE 20179095 / SAE 2017-32-0095

Effect of Biofuel and Soot on Metal Wear Characteristic using Electron Microscopy and 3D Image Processing

Preechar Karin, Warawut Amornprapa, Phiranat Khamsrisuk, Pol-ake Budsayahem, Pattara Chammana
King Mongkut's Institute of Technology Ladkrabang

Kobsak Sriprapha
National Science and Technology Development Agency

Katsunori Hanamura
Tokyo Institute of Technology

ABSTRACT

The soot contamination in used engine oils of diesel engine vehicles was about 1% by weight. The soot and metal wear particle sizes might be in the range of 0-1 μm and 1-25 μm, respectively. The characteristics of soot affecting on metal wear was investigated. Soot particle contamination in diesel engine oil was simulated using carbon black. Micro-nanostructure of soot particles were studied by scanning electron microscopy (SEM), transmission electron microscopy (TEM) and laser diffraction spectroscopy (LDS). The metal wear behavior was studied by means of a Four-Ball tribology test with wear measured. Wear roughness in micro-scale was investigated by high resolution optical microscopy (OM), 3D rendering optical technique and SEM image processing method. It was found that the ball wear scar diameter increased proportionally to the soot primary particle size. The effect of biodiesel contamination were also increasing in wear scar diameter.

INTRODUCTION

Diesel engine is a compression ignition engine which converts chemical energy within the fuel into mechanical energy. Diesel fuel is injected under high pressure into the combustion chamber where the combustion process occurs. Soot is remain of incomplete combustion which consists mostly of hydrocarbon, carbon and metallic ash. The primary and agglomerated soot particles observed by TEM are in the range of 20-80 nm and 100-300 nm, respectively [1]. Soot can be entered into the engine oil through the piston ring clearance during the combustion process [2].

Khamsrisuk *et al.* [3] performed the used oil analysis by collecting the engine oil from the small diesel engine vehicles. The results showed that the percentage of wear metal, soot and fuel contamination increased as the engine mileage increase. The average of soot contamination was about 0.69 percent by weight. Guatam *et al.* [4] investigated the effect of soot contamination on engine oil viscosity by increasing the percentage of soot contamination. The results showed that the engine oil viscosity increased with the increase of soot contamination. The engine testing for evaluated soot tribological properties is challenging, because of the uncontrolled test parameter and the difficulty of wear measurement [5]. The specimen bench test which is easy to control test parameter and good repeatable results are used. Carbon black is a synthesis soot which has similar particle size and physical properties to engine soot. It can be used as soot representative. Ryason *et al.* [6] performed wear tests on a ball-on-flat-disk wear tester using carbon black, alumina and silica. The results showed that the balls were worn similarly in three different kinds of the samples. Karin *et al.* [7] performed wear tests on Four-Ball Wear Tester. He found that the wear scar diameter (WSD) of the ball in the oil containing carbon black was higher than that of the pure oil without carbon black. Hu *et al.* [8] also performed Four-Ball wear tester using base oil and formulated lubricant. The results showed that the WSD was high when carbon black levels increased. But, the WSD of the formulated lubricant was lower than that of the pure base oil. They suggested that the wear mechanism of soot-contaminated lubricant might be abrasion.

Biodiesel is an alternative fuel that plays an importance role in replacement using petroleum diesel. It is an oxygenated fuel that promotes more completely combustion. The soot diameter size and quantity from biodiesel engine emission is lower than that of diesel [9]. However, soot induced wear mechanisms are still not fully understood. This research aimed to investigate the effects of soot Nanoparticles on metal wear characteristics using Four-Ball wear tester, laser diffraction spectroscopy, and electron microscopy.

EXPERIMENTAL SETUP

A formulated engine oil which had the same grade as SAE0W30 was used in this research. The engine oil condition including viscosity, oxidation, nitration and total base number (TBN) were measured according to ASTM standard test

methods. Oil additives were measured by x-ray fluorescence. The used engine oils were collected from the small diesel engine vehicles with different oil changed interval. The engine oil's mileage and oil aged were in the range 3,000-20,000 and 0-10,000 km, respectively. After that, the contaminants including fuel, soot and metal wear particles were measured. In order to investigate the effect of biodiesel contamination on metal wear, the different types of palm biodiesel blend were mixed with the engine oil at 2% by volume. The types of biodiesel were conventional diesel (B7), B20, B50 and B100. Moreover, the effect of soot contamination on metal wear were also investigated. The different types of commercial carbon blacks (CB) were mixed with the engine oil at 1% by weight per volume for simulating soot contamination. They were carbon black N220, N330, N550 and N660. The details of engine oil samples mixing with difference blend of biodiesel and carbon black are shown in Table 1.

In order to investigate the effect of soot contamination on wear, the Four-Ball wear tester was chosen. The test methods and conditions followed the standard test ASTM D4172 [11]. The machine consists of four 12.7 mm diameter steel balls, the three lower balls held in a steel cup with fixed position and the fourth ball was held in the upper chunk. The top ball was pressed with a force of 392 N and rotated at 1,200 rpm, as shown in Figure 1. The lubricant temperature and operating time were 75 °C and 60 min, respectively. After the tests, the three lower balls used to measure WSD using a high-resolution optical microscope (OM). It was the average value of these balls. The surface roughness was also measured using 3D rendering system of that OM. The worn surface analysis was investigated by using SEM. Moreover, the particle size distribution was measured using LDS.

Table 1. Fuel and carbon black mixed with the engine oils for four ball test.

Samples	% SAE0W30 (Volume)	Fuels or CB Types	% Fuel (vol.) %CB (wt.)
NE	100 %	-	-
EB7	98%	B7	2 %
EB20	98%	B20	2 %
EB50	98%	B50	2 %
EB100	98%	B100	2 %
EC2	100 %	N220	1 %
EC3	100 %	N330	1 %
EC5	100 %	N550	1 %
EC6	100 %	N660	1 %

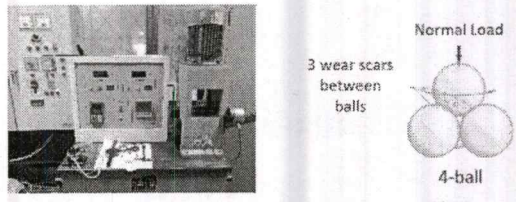

Figure 1. Four-Ball Wear Tester (ASTM D4172)

RESULTS AND DISCUSSION

Soot and Fuel in Diesel Engine Oil

A formulated engine oil which had the same grade as SAE0W30 was used in this research. The engine oil condition including viscosity, oxidation, nitration and TBN were measured according to ASTM standard test methods. Oil additives were measured by x-ray fluorescence. The oil conditions and additives are shown in Table 2. The used oil analysis showed that the fuel and soot contamination increased as the mileage and oil age increase. Fuel and soot are remain of the incomplete combustion process that can be transported to the engine oil during combustion process. The average fuel contamination in the small diesel engine vehicles was about 2 % by weight and the average soot was about 0.7 % by weight as shown in Table 3.

Figure 2 show TEM micrographs of commercial carbon black (CB) (a) N220, (b) N330, (c) N550 and (d) N660. Most of CB's primary nanoparticle diameter is smaller than 90 nm. The average primary nanoparticles of CB N660 was significant larger than that of N220. After that, primary nanoparticles of those CB were measured using image processing method. Figures 2 (e) shows carbon black's primary nanoparticle size distribution. The primary nanoparticle diameters are in the range of 5-90 nm. It was clearly observed much amount of particle diameters are in the range of 20-65 nm.

Table 2. Properties of SAE0W30 engine oil.

Oil conditions		Oil additives (ppm)	
Viscosity @ 40 °C	44.5 cSt	S	214.0
Viscosity @ 100 °C	9.6 cSt	Ca	166.0
Oxidation (Abs)	18.1	Zn	847.0
Nitration (Abs)	6.1	P	779.0
TBN (mgKOH/g)	5.6	Mo	454.0

Table 3. Fuel, soot and metal wear contaminations in conventional diesel vehicle's used oil.

Contaminations		
Fuel	% by weight	2.0
Soot	% by weight	0.7
Wear	Total metal (ppm)	111.0
	Iron (ppm)	74.38
	Normal rubbing wear (%)	65
	Fatigue bearing wear (%)	20
	White metal (%)	5
	Black oxide (%)	5
	Dirt and dust (%)	5

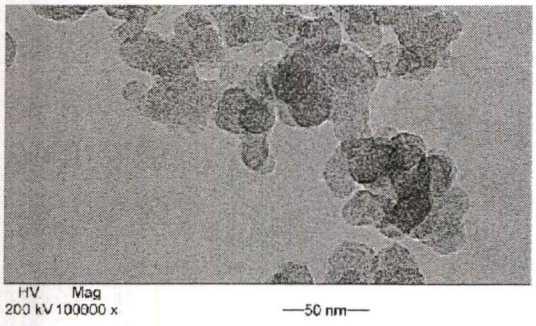

(a) CB N220

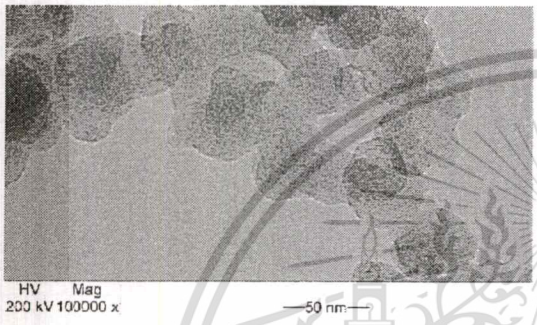

(b) CB N330

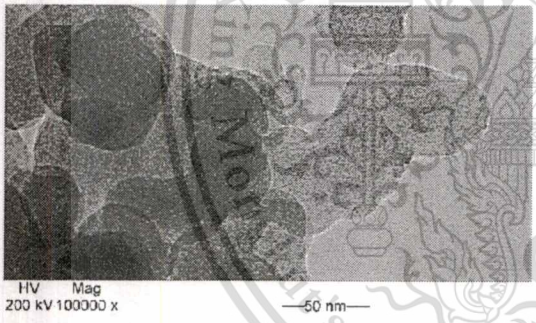

(c) CB N550

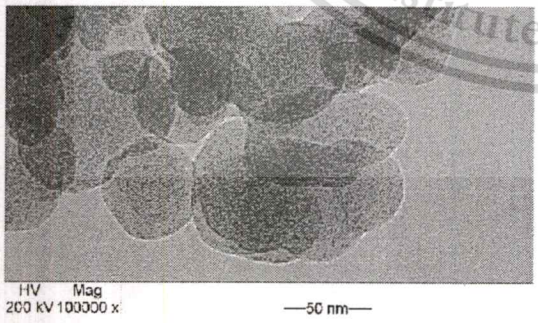

(d) CB N660

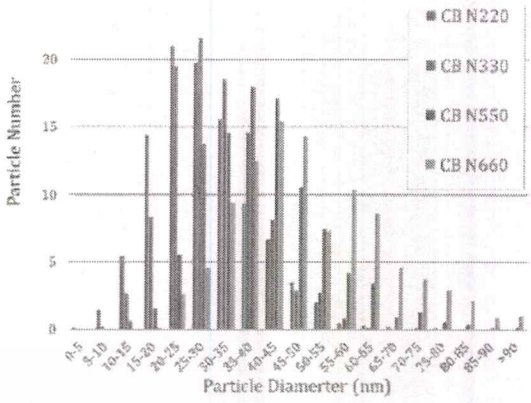

(e) Size distributions of CB's nanoparticle

Figure 2. TEM images of carbon black (a) N220, (b) N330, (c) N550 and (d) N660 and (e) size distributions of CB's nanoparticle using TEM image processing method.

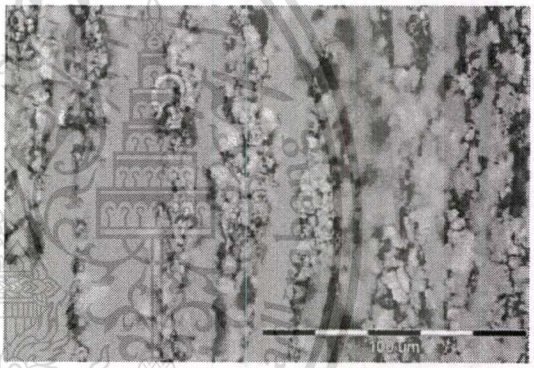

(a) Metal wear particles

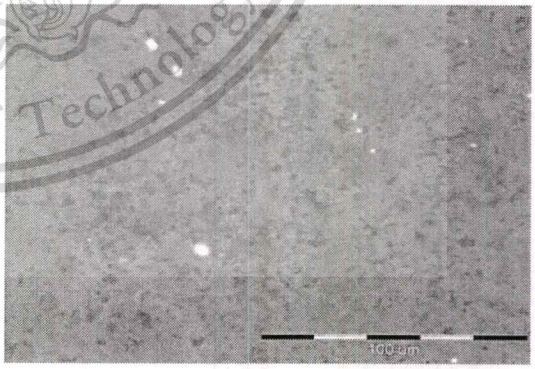

(b) Soot particles

Figure 3. Images of (a) metal wear and (b) soot particles contamination in the diesel engine's used lubricating oil using OM.

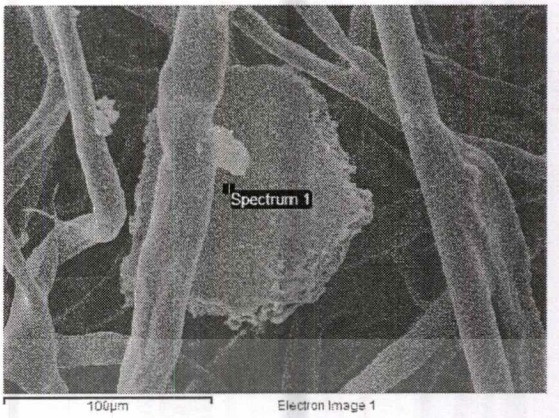

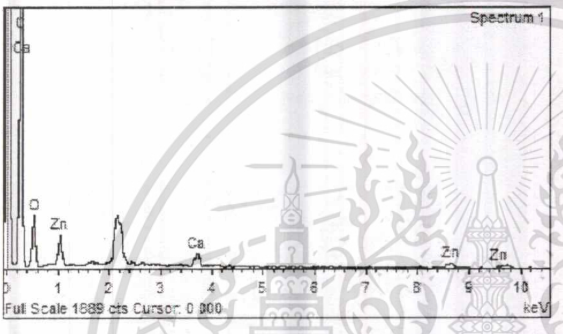

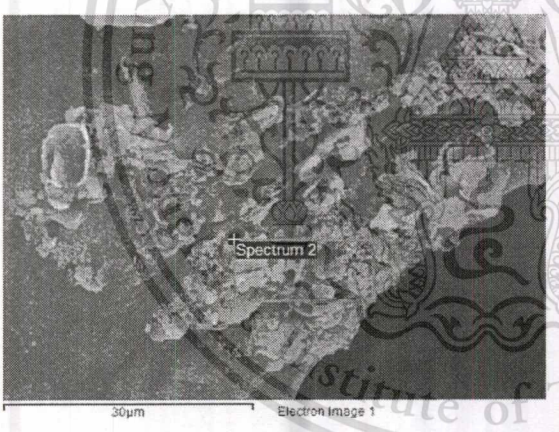

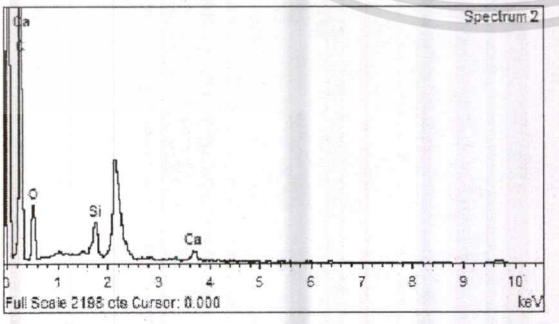

Figure 4. Metal wear and soot particles contamination in the diesel engine's used oil filter using SEM-EDX.

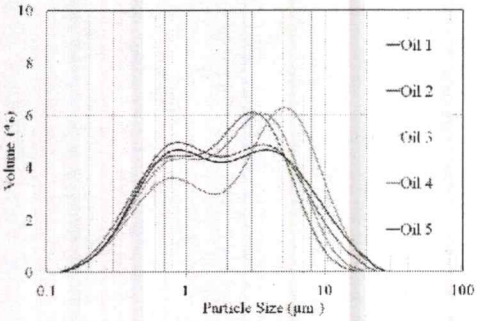

(a) Particle size distribution of the diesel engine's used lubricating oil

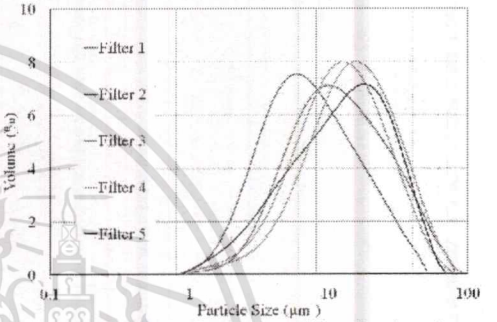

(b) Particle size distribution of the diesel engine's used oil filter

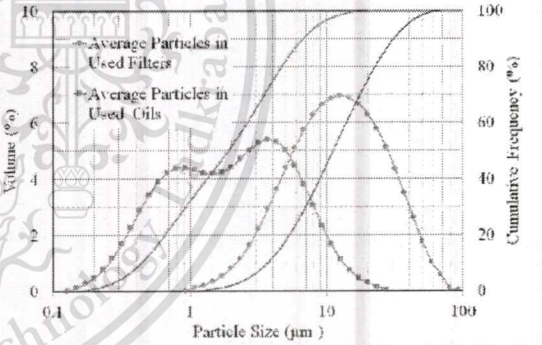

(c) The average particle size distribution of the diesel engine's used lubricating oil and used filter

Figure 5. Particle size distribution of the diesel engine's used (a) lubricating oil, (b) oil filter, and (c) the average particle size distribution inside used oil and used oil filter using LDS.

The main metal wear particles are normal rubbing wear and fatigue bearing wear of iron parts. Figures 3 and 4 show optical and SEM-EDX images of soot and wear particles. SEM-EDX analysis indicated a composition of 76C-22O-1Ca-1Zn (in at. %) for a big wear particle and a composition of 76C-21O-2Si-1Ca for a small wear particle. Figure 5 shows particle size distributions of used lubricating oils and used oil filters. They were both collected from the small diesel engine vehicles at the oil end interval. The used oil particles were in the range of 0.1-30 microns and the particles inside the filter were in the range of 1-100 microns.

(a) NE-A

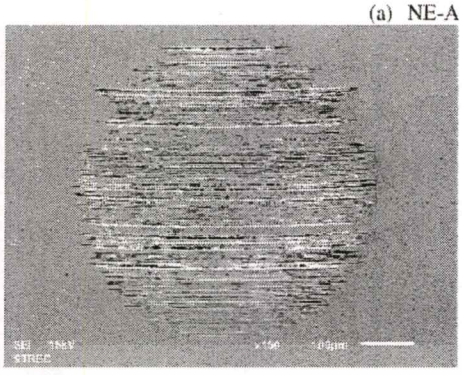

(b) EB7

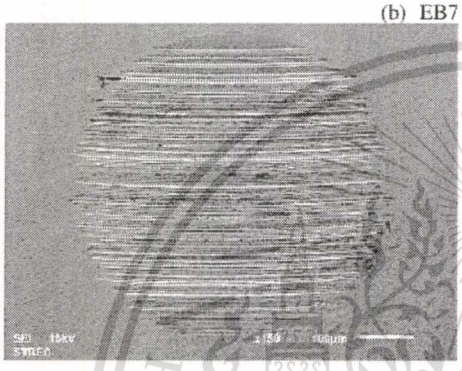

(c) EB20

(d) EB50

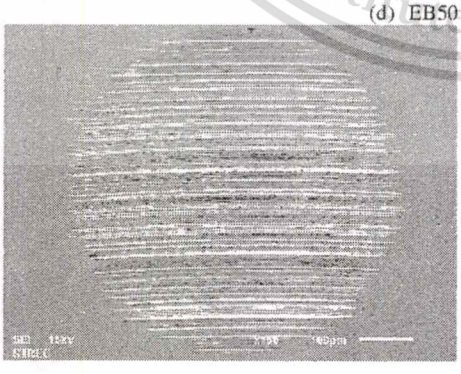

(e) EB100

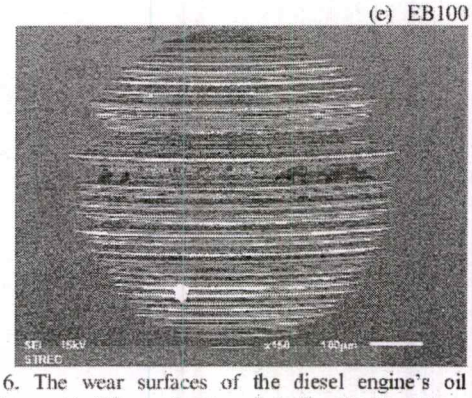

Figure 6. The wear surfaces of the diesel engine's oil contaminate with different fraction of biodiesel in diesel fuels using SEM.

Table 4. WSD and roughness of the diesel engine's oil contaminate with different fraction of biodiesel in diesel fuels.

Samples	WSD (micron)	Roughness (micron)
NE-A	533	1.32
EB7	588	1.18
EB20	569	1.17
EB50	604	1.21
EB100	625	1.68

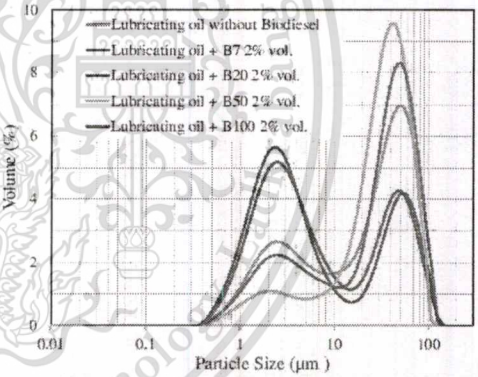

Figure 7. Wear particle size distribution of Four-Ball tested oils using LDS.

Impact of Biodiesel and Soot on Metal Wear

Figure 6 shows SEM micrographs of wear scar found on the ball of (a) the engine oil without fuel and engine oil containing 2% wt. of (b) B7, (c) B20, (d) B50 and (e) B100. The average wear scar diameter and surface roughness were shown in Table 4. The results showed that the ball WSD of the oil containing B100 was higher than that of the pure oil without fuel and it increased when the concentration of biodiesel was increased but the surface roughness is not significant different. Fuel contamination may decreases the viscosity of the engine oil that resulting in reducing oil film thickness. It might decreases the strength of anti-wear additives that make higher wear on metal surface. Figure 7 shows size distribution of particles inside the tested oils. They were in the range of 0.3-125 micron.

(a) NE-B

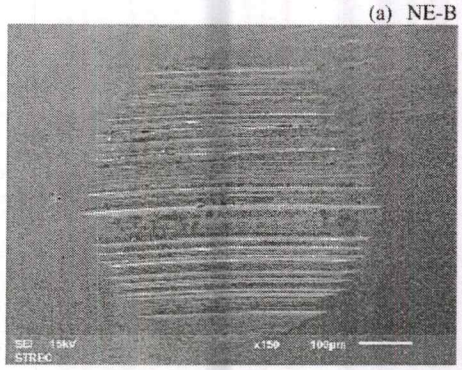

(b) EC2

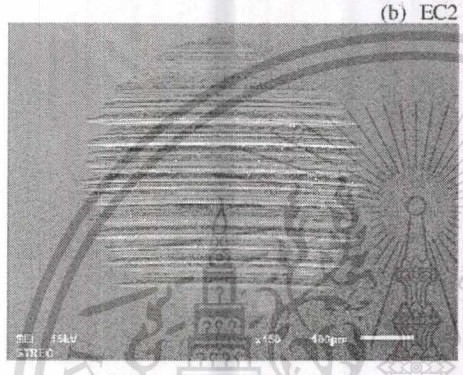

(c) EC3

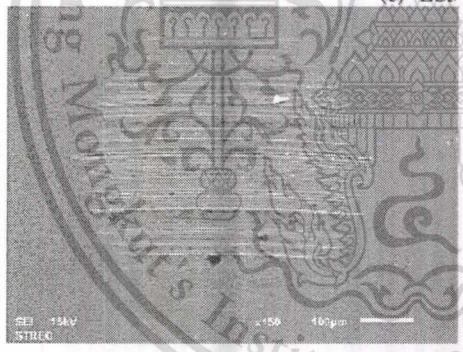

(d) EC5

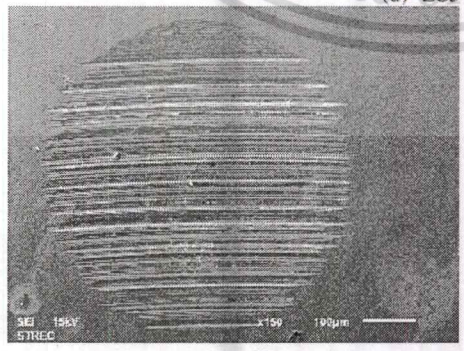

(e) EC6

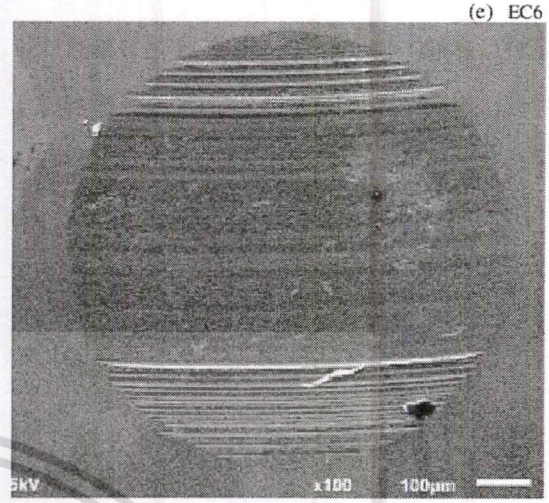

Figure 8. The wear surfaces of the diesel engine's oil contaminate with different size of primary particle size of carbon black.

Table 5. WSD and roughness of the diesel engine's oil contaminate with different size of primary particle size of carbon black.

Samples	WSD (micron)	Roughness (micron)
NE-B	544	2.06
EC2	533	1.35
EC3	546	1.44
EC5	597	2.11
EC6	815	1.53

Figure 8 shows microscopy image of wear scar found on the ball of (a) the engine oil without soot and engine oil containing 1% wt. of (b) N220, (c) N330, (d) N550 and (e) N660 carbon black. The average wear scar diameter and surface roughness were shown in Table 5. The results showed that the ball WSD of the oil containing CB N600 was higher than that of the pure oil without carbon black and it increased when the primary particle size of the carbon black was increased. However, the surface roughness is not significant different.

In this research, soot wear mechanisms might be expected as three-body abrasive wear. The role of lubricating oil is to generate an oil film between two surfaces and trap soot particles. If the soot particle size is smaller than the oil film, the surface can be separated, and no wear should occur. Further, if the soot particle size is larger the oil film thickness, then soot might occur as three body abrasion. Therefore, oil viscosity improver and soot agglomerate dispersant additives would be a key to preventing soot abrasive wear.

After Four-Ball wear test, the tested oils were also measured size distribution. Figure 9 shows size distribution of different types of carbon black and wear particles which were measured after Four-Ball wear test. They were in the range of 0.01-300 microns, which were small particle that have size of 10-100 nm. Figure 10 shows the average size distribution of particles inside the tested oils. They were in the range of 0.01-300 micron. It was clearly observed that metal wear particles size are larger than that of carbon black.

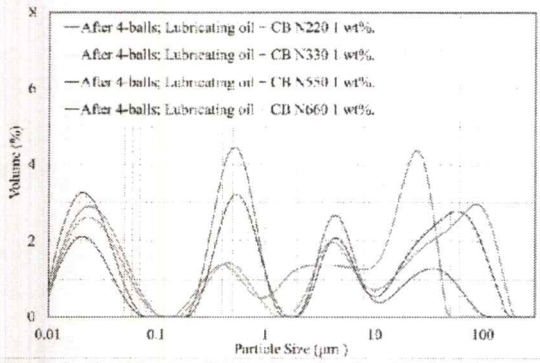

Figure 9. Particle size distribution of carbon black with wear particles in lubricating oil after Four-Ball tested by LDS.

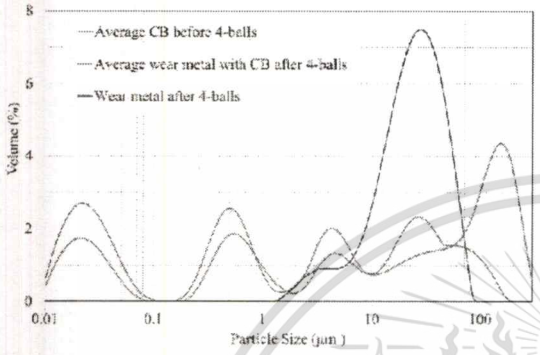

Figure 10. The average particle size distribution of carbon black with wear particles in lubricating oil before and after Four-Ball tested by LDS compared to wear particle without carbon black.

SUMMARY

The fuel and soot contamination in used engine oils of diesel engine vehicles was about 2% and 1% by weight, respectively. The particles size in the oil pan of the engine were in the range of 0.1-25 µm. The soot and metal wear particle sizes might be in the range of 0-1 µm and 1-25 µm, respectively.

It was clearly observed that the effect of biodiesel contamination were increasing in wear scar diameter. It might be expected that fuel contamination may decreases the viscosity of the engine oil and the strength of anti-wear additives that make higher wear on metal surface.

Moreover, the ball wear scar diameter increased proportionally to the soot primary particle size. It is expected that the soot particle which is larger than the oil film thickness can increase the metal wear.

The impact of biodiesel contamination and carbon black particle size could not observed in micro-scale of surface roughness. Submicron- and nano-scales of metal wear surface analysis is needed to characterize for more understanding of metal wear mechanisms.

REFERENCES

1. S. Daido, Y. Kodamaa, T. Inohara, N. Ohyamaa, and T. Sugiyama, Analysis of Soot Accumulation inside Diesel Engines, *JSAE Review*, Vol. 21, 303-308 (2000).
2. W. M. Needelman, and P. V. Madhavan, Review of Lubricant Contamination and Diesel Engine Wear, *SAE Technical Papers*, 881827 (1988).
3. P. Kamsrisuk, P. Karin, K. Sriprapha, and K. Hanamura. An Investigation on Particle Size Distribution in Used Lubricating, *JSAE Technical Paper*, 20165336 (2016).
4. M. Gautam, S. George, S. Balla, and V. Gautam, Effect of diesel soot on lubricant oil viscosity, *Tribology International*, Vol. 40. 809-818 (2007).
5. D. A. Green, and R. Lewis. The effects of soot-contaminated engine oil on wear and friction: A review. *Proc Inst Mech Eng Pt D: J Automobile Eng*, Vol. 222, 1669-89 (2008).
6. P.R. Ryason, I. Chan, and J.T. Gilmore, Polishing Wear by Soot, *Wear*, Vol.137, 15-24 (1990).
7. P. Karin, C. Supanamok and K. Hanamura. Impact of Soot on Metal Wear Characteristics Using Laser Diffraction Spectroscopy. *Journal of Research and Applications in Mechanical Engineering*, Vol. 4. No.2, 126-134 (2016).
8. E. Hu, X. Hu, T. Liu, L. Fang, K.D. Dearn, and H. Xu, The role of soot particles in the tribological behavior of engine lubricating oils, *Wear*, Vol. 304, 152-161 (2013).
9. P. Karin, J. Boonsakda, K. Siricholathum, E. Saenkhumvong, C. Charoenphonphanich, and K. Hanamura, Morphology And Oxidation Kinetics Of Ci Engine's Biodiesel Particulate Matters On Cordierite Diesel Particulate Filters Using TGA, *International Journal of Automotive Technology*, Vol. 18, 31-40 (2017).
10. Carbon Black. *IARC MONOGRAPHS*, Vol. 93, 43-191 (2010).
11. Standard test method for wear preventive characteristics of lubricating fluid (Fourball method). *ASTM D4172 -94* (2016).

ACKNOWLEDGMENTS

The authors gratefully acknowledge the support from Bangchak Corporation Pub. Co., Ltd., FOCUSLAB Ltd., Thailand Research Fund (TRF), KMITL and NSTDA.

ABBREVIATIONS

B100	Biodiesel
CB	Carbon Black (N220-N660)
EB	Fuel mixed with New Engine Oil
EC	Carbon Black mixed with New Engine Oil
EDX	Energy Dispersive X-Ray Analysis
LDS	Laser Diffraction Spectroscopy
NE	New Engine Oil
OM	Optical Microscopy
SEM	Scanning Electron Microscopy
TBN	Total Base Number
TEM	Transmission Electron Microscopy
WSD	Wear Scar Diameter

Asst.Prof.Dr.Preechar Karin

Position and Affiliation

Assistant Professor, Automotive Engineering Program
International College, King Mongkut's Institute of Technology Ladkrabang
1 Chalongkrung Road, Ladkrabang, Bangkok, 10520
Tel: +66-329-8260-1 Fax: +66-2-329-8262 Mobile: +66-85-128-5024
Email: kkpreech@staff.kmitl.ac.th, preechar.ka@kmitl.ac.th

Work Experience

- 2010-Present — Assistant Professor of Automotive Engineering Program, International College, King Mongkut's Institute of Technology Ladkrabang
- 2007-2010 — Research Assistant, Multidisciplinary Education and Research Center for Energy Science, Tokyo Institute of Technology, Japan
- 2007-2010 — Honors Scholarship for Privately Financed International Students (JASSO), Rotary Yoneyama Memmorial Foundation Inc., Japan
- 1997-2006 — Vehicle Design Engineer, Isuzu Technical Center of Asia Co.,Ltd., Isuzu Motor Ltd., Japan

Education

- D.Eng. (Mechanical Engineering), Tokyo Institute of Technology, Japan

Research Experience

- The Thailand Research Fund (TRF), Renewable Bio-oxygenated Fuel Particle Emission Trapping and Oxidation Behaviors inside Ceramic Micro-porous of Diesel Particulate Filters (2014-2016)
- The Thailand Research Fund (TRF), Renewable Bio-oxygenated Fuels Particulate Matter Trapping and Oxidation Behaviors (2012-2014)
- ASEA-UNINET Staff Exchange, One Month Scholarship, Engine After-treatment Technology for Particle Emissions Reduction (1-31 May 2013)
- International College, King Mongkut's Institute of Technology Ladkrabang, Physical and Chemical Characterization of Diesel Particulate Matter (March-September 2011)

Management Experience

- Committee and Secretary of Automotive Engineering Program, International College, King Mongkut's Institute of Technology Ladkrabang (2010-Present)
- Program Director of Automotive Engineering Program, TAIST-Tokyo Tech (King Mongkut's Institute of Technology Ladkrabang, King Mongkut's University of Technology Thonburi, National Science and Technology Development Agency and Tokyo Institute of Technology (2010-Present)
- Committee and Secretary of Thai Society of Mechanical Engineers (TSME) (2015-Present)
- Committee of Thai Society of Automotive Engineers (TSAE) (2014-2015)

International Journal Publications

- P. Karin, J. Boonsakda, K. Siricholathum, E. Saenkhumvong, C. Charoenphonphanich and K. Hanamura, "Morphology and Oxidation Kinetics of CI Engine's Biodiesel Particulate Matters on Cordierite Diesel Particulate Filters using TGA", International Journal of Automotive Technology, Vol. 18, No. 1, pp. 31–40, 2017.
- P. Karin, C. Supanamok and K. Hanamura, "Impact of Soot on Metal Wear Characteristics using Laser Diffraction Spectroscopy", Journal of Research and Applications in Mechanical Engineering, Transactions of the TSME Vol. 4, No. 2, pp.126-134, 2016.
- P. Karin, M. Borhanipour, Y. Songsaengchan, S. Laosuwan, C. Charoenphonphanich, N. Chollacop and K. Hanamura, "Oxidation Kinetics of Small CI Engine's Biodiesel Particulate Matter", International Journal of Automotive Technology, Vol. 16, No. 2, pp. 211–219, 2015.
- P. Karin, Y. Songsaengchan, S.Laosuwan, C. Charoenphonphanich, N.Chollacop and K.Hanamura, "Physical Characterization of Biodiesel Particle Emission by Electron Microscopy", SAE International; 2013-32-9150.
- P. Karin, Y. Songsaengchan, S.Laosuwan, C. Charoenphonphanich, N.Chollacop and K.Hanamura, (2013) "Nanostructure Investigation of Particle Emission by Using TEM Image Processing Method", Energy Procedia, Elsevier, Vol.34, pp.757-766, 2013.
- P. Karin, Y. Songsaengchan, S.Laosuwan, C. Charoenphonphanich, N.Chollacop and K.Hanamura, (March, 2013) "Nanostructure of Renewable Oxygenated Fuels Particulate Matter", ASEAN Engineering Journal, AUN/SEED-Net, Vol.3 No.1, pp. 72-83.
- P. Karin, H. Oki, K. Hanamura and C. Charoenphonphanich, (October, 2012) "Nanostructures and Oxidation Kinetics of Diesel Particulate Matters", The Journal of Research and Applications in Mechanical Engineering (JRAME), Vol.1 No.2, pp. 3-8.
- H. Oki, P. Karin and K. Hanamura, (2011) "Visualization of Oxidation of Soot Nanoparticles Trapped on a Diesel Particulate Membrane Filter", SAE International Journal of Engines, SAE International, Vol. 4 no. 1 pp.515-526.
- P. Karin and K. Hanamura, (2010) "Particulate Matter Trapping and Oxidation on Catalyst-Membrane", SAE International Journal of Fuels and Lubricants, SAE International, Vol.3 No.1 pp.368-379.
- P. Karin and K. Hanamura, (2010) "Microscopic Visualization of Particulate Matter Trapping and Oxidation Behaviors in a Diesel Particulate Catalyst-Membrane Filter", Transactions of Society of Automotive Engineers of Japan, Society of Automotive Engineers of Japan Inc, Vol.41, No.4, pp.853-858.
- P. Karin and K. Hanamura, (2010) "Microscopic Visualization of PM Trapping and Regeneration in a Diesel Particulate Catalyst-Membrane Filter (DPMF)", Transactions of Society of Automotive Engineers of Japan, Society of Automotive Engineers of Japan Inc, Vol. 41, No. 1, pp.103-108.
- P. Karin, L. Cui, P. Rubio, T. Tsuruta and K. Hanamura, (2009) "Microscopic Visualization of PM Trapping and Regeneration in Micro-Structural Pores of a DPF Wall", SAE International Journal of Fuels and Lubricants, SAE International, Vol.2 No.1, pp.661-669.
- K. Hanamura, P. Karin, L. Cui, P. Rubio, T. Tsuruta, T. Tanaka and T. Suzuki, (2009) "Micro- and macroscopic visualization of particulate matter trapping and regeneration processes in wall-flow diesel particulate filters", International Journal of Engine research, Professional Engineering Publishing, Vol.10, No.5/2009, pp.305-321.
- L. Cui, P. Rubio, P. Karin, T. Tsuruta and K. Hanamura, (2009) "Microscopic Visualization of Particulate Matter Trapping and Regeneration in Microstructural Pores on Diesel Particulate Filter Wall", Transactions of Society of Automotive Engineers of Japan, Society of Automotive Engineers of Japan Inc, Vol. 40, No. 1, pp.153-158.

The 34th Annual Conference of the Microscopy Society of Thailand (MST34)

Download Images Set 1 Download Images Set 2

All MST members are invited to attend the MST Annual General Meeting (Fortune I & II, 17.30-18.30).

The invited letter can be downloaded "HERE".

The Effect of Soot Nanoparticle Size on Metal Wear Using Electron Microscopy

Warawut Amornprapa [1*], Preechar Karin[1], Kobsak Sriprapha[2] and Katsunori Hanamura[3]
[1] International college, King Mongkut's Institute of Technology Ladkrabang, Bangkok, 10520, Thailand
[2] National Electronics and Computer Technology Center (NECTEC), Pathumthani, 12120, Thailand
[3] Departments of Mechanical Engineering, Tokyo institute of Technology, Japan
*Presenter e-mail address: Warawut_Amo@hotmail.co.th

Abstract

The impact of soot nanoparticles affecting metal wear was investigated. Several types of Commercial Carbon Black was used to simulate an engine soot. The wear tests were evaluated by using Four-ball wear tester. After the tests, the ball surfaces were examined by using High-Resolution Optical Microscope and Scanning Electron Microscope (SEM). The results showed that the ball wear scar diameter (WSD) increased when the primary particle size of carbon black was increased. In conclusion, it might be expected that the soot particle which was larger than the oil film thickness can increase the metal wear.

Keywords: Lubricant; Wear; Soot; Four-Ball wear tester; Electron microscopy; Laser diffraction spectroscopy

Background

Diesel engine is a compression ignition engine which converts chemical energy within the fuel into mechanical energy. Diesel fuel is injected under high pressure into the combustion chamber where the combustion process occurs. Soot is remain of incomplete combustion which consists mostly of carbon, hydrocarbon and metallic ash. The primary and agglomerated soot particles observed by Transmission Electron Microscopy (TEM) are in the range of 20 - 80 nm and 100 - 300 nm, respectively [1]. Soot can be entered into the engine oil through the piston ring clearance during the combustion process [2].

Khamsrisuk *et al.* [3] performed the used oil analysis by collecting the engine oil from the small diesel engine vehicles. The results showed that the percentage of wear metal, soot and fuel contamination increased as the engine mileage increase. The average of soot contamination was about 0.69 percent by weight. Guatam *et al.* [4] investigated the effect of soot contamination on engine oil viscosity by increasing the percentage of soot contamination. The results showed that the engine oil viscosity increased with the increase of soot contamination. The engine testing for evaluated soot tribological properties is challenging, because of the uncontrolled test parameter and the difficulty of wear measurement [5]. The specimen bench test which is easy to control test parameter and good repeatable results are used. Carbon black is a synthesis soot which has similar particle size and physical properties to engine soot. It can be used as soot representative. Ryason *et al.* [6] performed wear tests on a ball-on-flat-disk wear tester using carbon black, alumina and silica. The results showed that the balls were worn similarly in three different kinds of the samples. Karin *et al.* [7] performed wear tests on Four-Ball Wear Tester. He found that the Wear Scar Diameter (WSD) of the ball in the oil containing carbon black was higher than that of the oil alone. Hu *et al.* [8] also performed Four-Ball Wear Tester using base oil and formulated lubricant. The results showed that the WSD was high when carbon black levels increased. But, the WSD of the formulated lubricant was lower than that of the pure base oil. They suggested that the wear mechanism of soot-contaminated lubricant might be abrasion.

Biodiesel is an alternative fuel that plays an importance role in replacement using petroleum diesel. It is an oxygenated fuel that promotes more completely combustion. The soot diameter size and quantity from biodiesel engine emission is lower than that of diesel [9]. However, soot induced wear mechanisms are still not fully understood. This research aimed to investigate the effects of soot Nanoparticles on metal wear characteristics using Four-Ball Wear Tester, Laser Diffraction Spectroscopy, and Electron Microscopy.

Materials and Methods

A formulated engine oil which had the same grade as SAE0W30 was used in this research. The engine oil condition including viscosity, oxidation, nitration and total base number were measured according to ASTM standard test methods. Oil additives were measured by x-ray fluorescence.

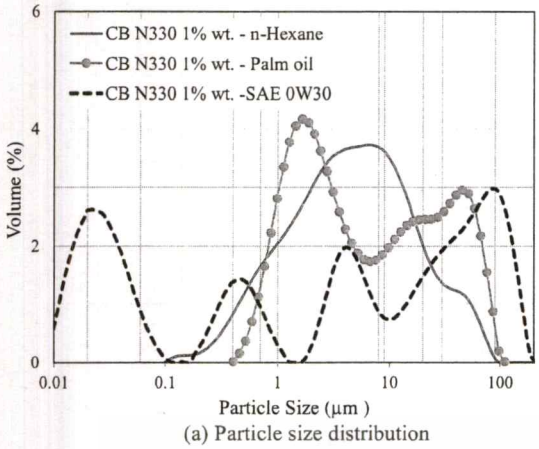

(a) Particle size distribution

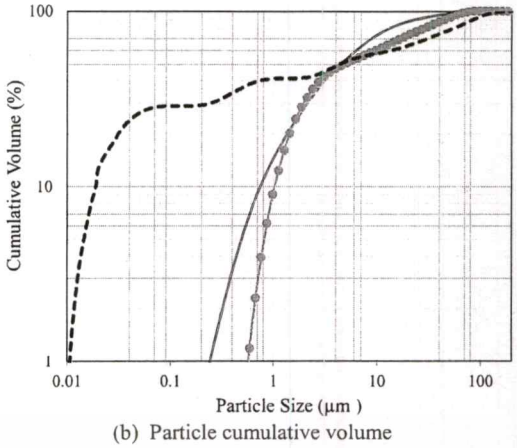

(b) Particle cumulative volume

Figure 1 Carbon black N330 (a) size distribution and (b) cumulative volume in different type of liquids by Laser Diffraction Spectroscopy.

Table 1 CB mixed with the engine oils.

Samples	Carbon Black	Average Primary Particle diameter (nm)*[10]	% CB (wt. / vol.)
NE	-	-	-
EC2	N220	21	1 %
EC3	N330	31	1 %
EC5	N550	53	1 %
EC6	N660	63	1 %

After that, the different types of carbon blacks (CB) were mixed with the engine oil at 1% by weight per volume for simulating soot contamination. They were Carbon black N220, N330, N550 and N660. The details of oil samples and CB average particle size [10] were shown in **Table 2.**

In order to investigate the effect of soot contamination on wear, the Four-Ball Wear Tester was chosen. The test methods and conditions followed the standard test ASTM D4172 [11]. The machine consists of four 12.7 mm. diameter steel balls, the three lower balls held in a steel cup with fixed position and the fourth ball was held in the upper chunk. The top ball was pressed with a force of 392 N and rotated at 1,200 rpm. The lubricant temperature and operating time were 75 °C and 60 min, respectively. After the tests, the three lower balls used to measure wear scar diameter (WSD) using a high-resolution optical microscope (OM). It was the average value of these balls. The surface roughness was also measured using 3D rendering system of that OM. The worn surface analysis was investigated by using Scanning Electron Microscopy (SEM). Moreover, the particle size distribution was measured using Laser Diffraction Spectroscopy.

Table 2 Properties of SAE0W30 engine oil

Oil conditions		Oil additives (ppm)	
Viscosity @ 40 °C	44.5 cSt	S	214.0
Viscosity @ 100 °C	9.6 cSt	Ca	166.0
Oxidation (Abs)	18.1	Zn	847.0
Nitration (Abs)	6.1	P	779.0
TBN (mgKOH/g)	5.6	Mo	454.0

Table 3 WSD and Roughness of each sample

Samples	Wear Scar Diameter (Micron)	Roughness (Micron)
NE	544	2.06
EC2	533	1.35
EC3	546	1.44
EC5	597	2.11
EC6	815	1.53

Results and Discussion

Soot particle size distribution

Table 2 shows oil properties of SAE 0W30 engine oil which is a diesel formulated lubricating oils. The several oil condition including viscosity, oxidation, nitration, and total base number were investigated. Oil additive elements were also analyzed by using X-ray fluorescence (XRF). **Figure 1** shows the size distribution of CB N330 mixing in n-Hexane, Palm oil and SAE 0W30 engine oil at 1% by weight. These tests were investigated by using laser diffraction technique. The results showed that soot dispersing in different liquids were significantly different. The results of carbon black dispersing in formulated lubricant seem better than those of n-hexane and palm oil that might be expected that the additives in an engine oil can help to disperse soot particle.

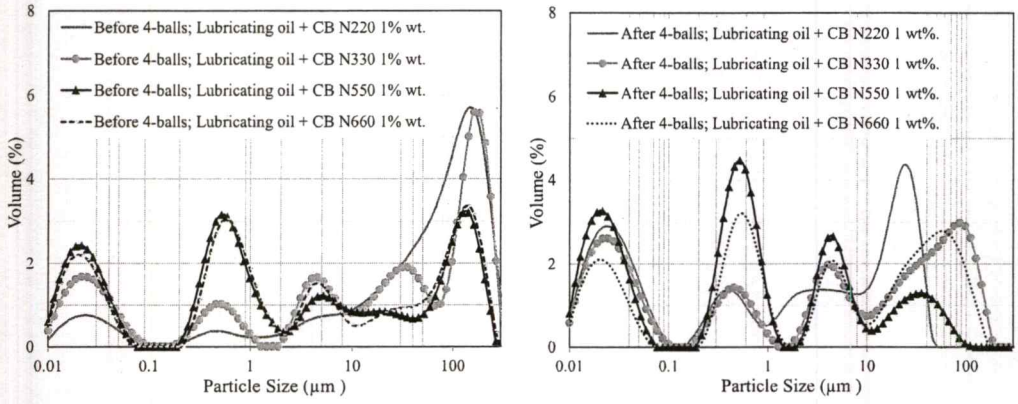

(a) Before Four-ball wear test (b) After Four- ball wear test

Figure 2 Particle size distribution of (a) Carbon black and (b) Carbon black with wear metal particles in lubricating oil before and after Four- ball wear test by Laser Diffraction Spectroscopy.

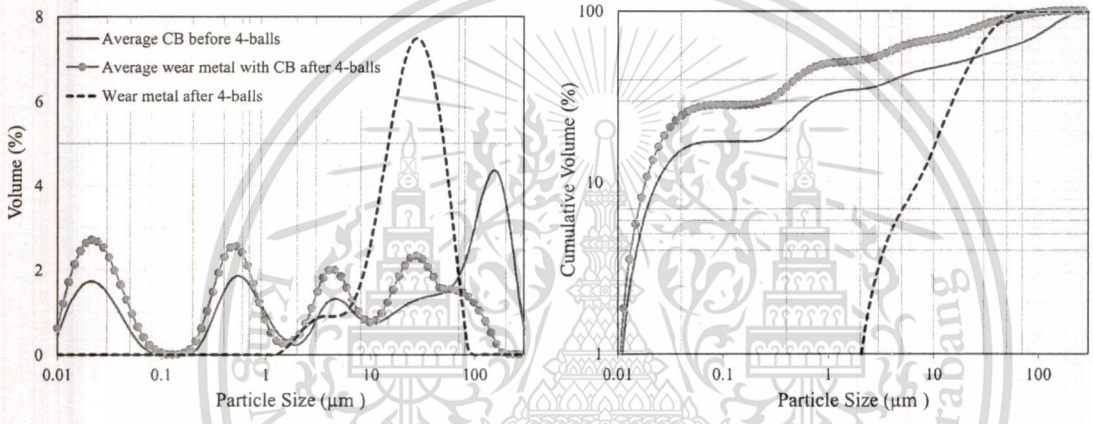

(a) Particle size distribution (b) Particle cumulative volume

Figure 3 Average Carbon black and wear metal particles (a) size distribution and (b) cumulative volume in lubricating oil before and after Four-ball wear test by Laser Particle Diffraction Spectroscopy.

Figure 2a shows size distribution of different types of carbon black mixing in the engine oil which were measured before Four-ball wear test. There were CB N220, N330, N550 and N660, respectively. The results showed that the different types of soot dispersing in the engine oil were not significantly different. They were in the range of 0.01 – 300 microns, which were small particle that have size of 10 - 100 nm. The first and second groups of agglomerate were in the range of 0.1 - 2 micron and 2 – 300 micron, respectively.

Impact of soot on metal wear

The wear scar diameters (WSD) and surface roughness were measured by using an optical microscope and 3D rendering analysis. They were the average value of the three lower balls. Additionally, the micro surface analyses were investigated by using Scanning Electron Microscopy (SEM). **Figure 4** shows microscopy image of wear scar found on the ball of (a) the engine oil without soot and engine oil containing 1% wt. of (b) N220, (c) N330, (d) N550 and (e) N660 Carbon Black. The average wear scar diameter and surface roughness were shown in **Table 3**. The results showed that the ball wear scar diameter (WSD) increased when the primary particle size of the carbon black was increased, but the surface roughness decreased. After Four-ball wear test, the tested oils were also measured size distribution. **Figure 2b** shows size distribution of particles inside the tested oils. They were in the range of 0.01 – 200 micron. **Figure 3** shows the comparison of particles size distribution before and after Four-ball wear test. After Four-ball test, the wear metal sizes were about of 1- 100 micron and the size of CB with wear metal seems smaller than those particles before the wear test.

The morphological and elemental composition of wear scar were studied. **Figure 5** shows SEM secondary and backscattered electron micrographs and energy dispersive X-ray (EDX) analysis.

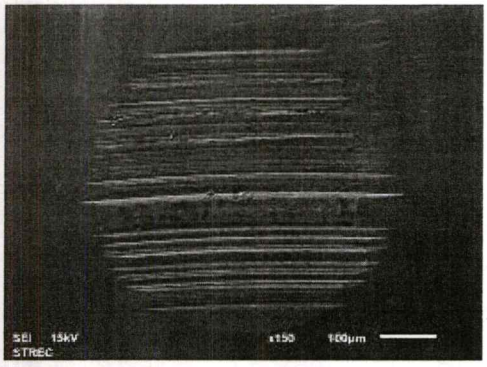

(a) The engine oil without soot

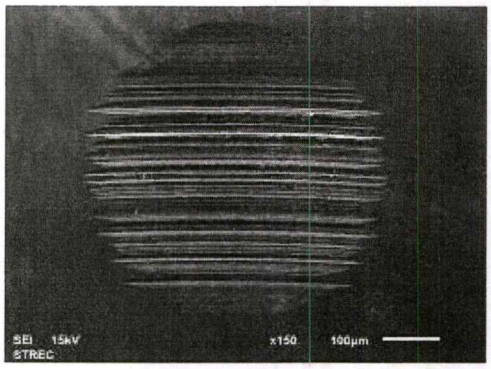

(b) The engine oil containing CB N220.

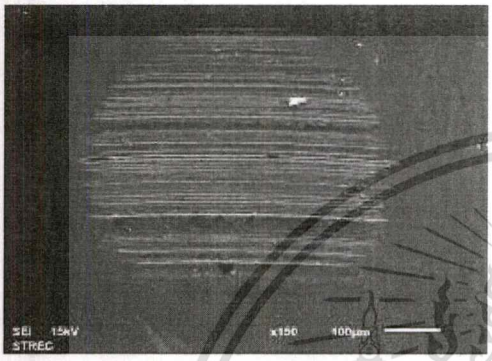

(c) The engine oil containing CB N330.

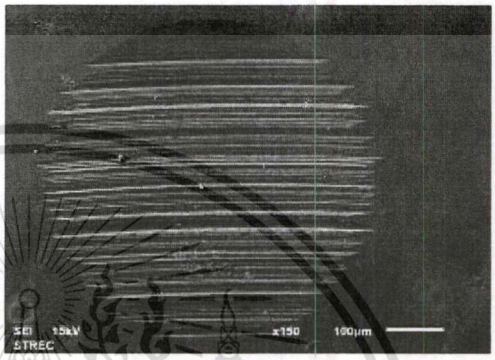

(d) The engine oil containing CB N550.

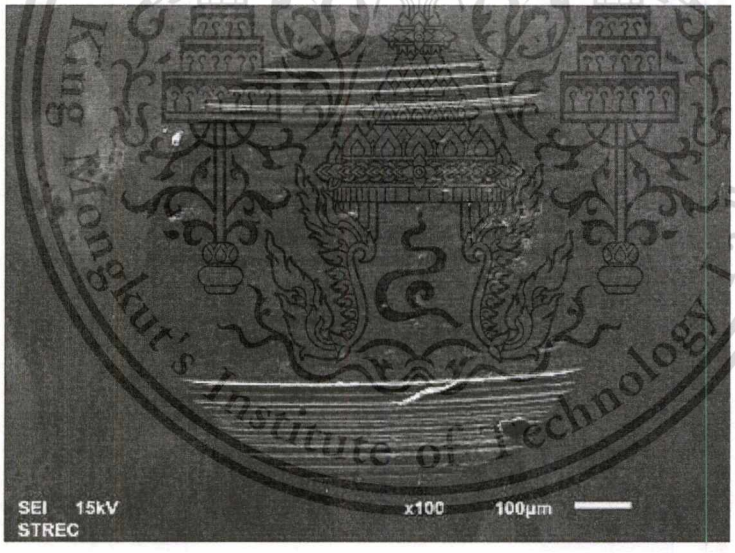

(e) The engine oil containing CB N660.

Figure 4 SEM micrographs taken using Secondary electron of the ball surface from (a) the engine oil without soot and the engine oil containing 1% wt. of (b) CB N 220, (c) CB N330, (d) CB N550 and (e) CB N660

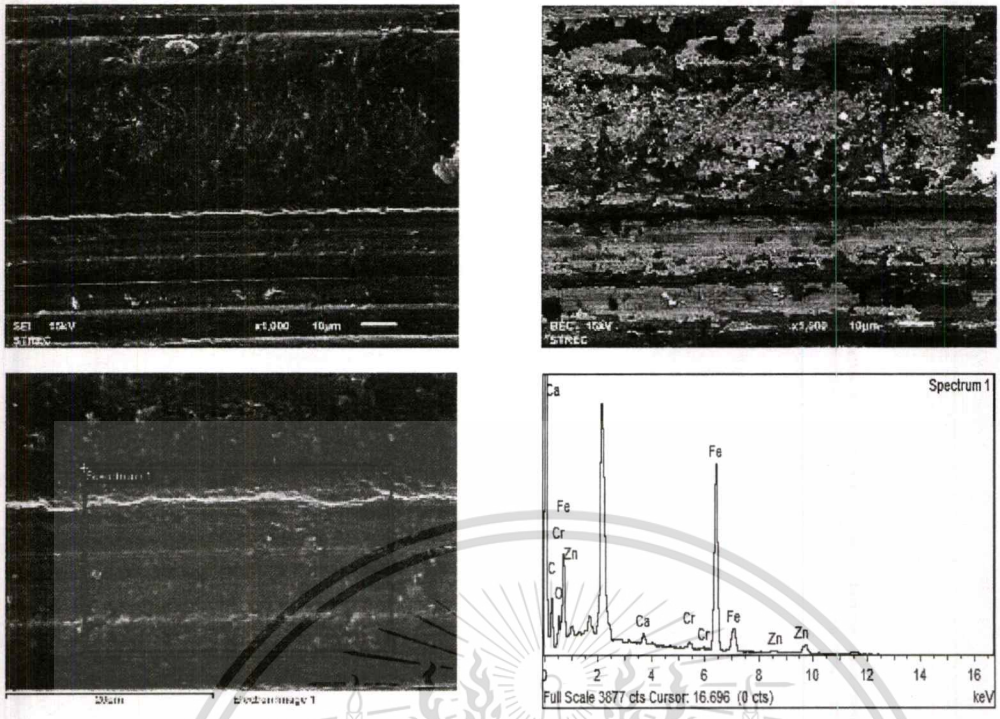

(a) The engine oil without soot.

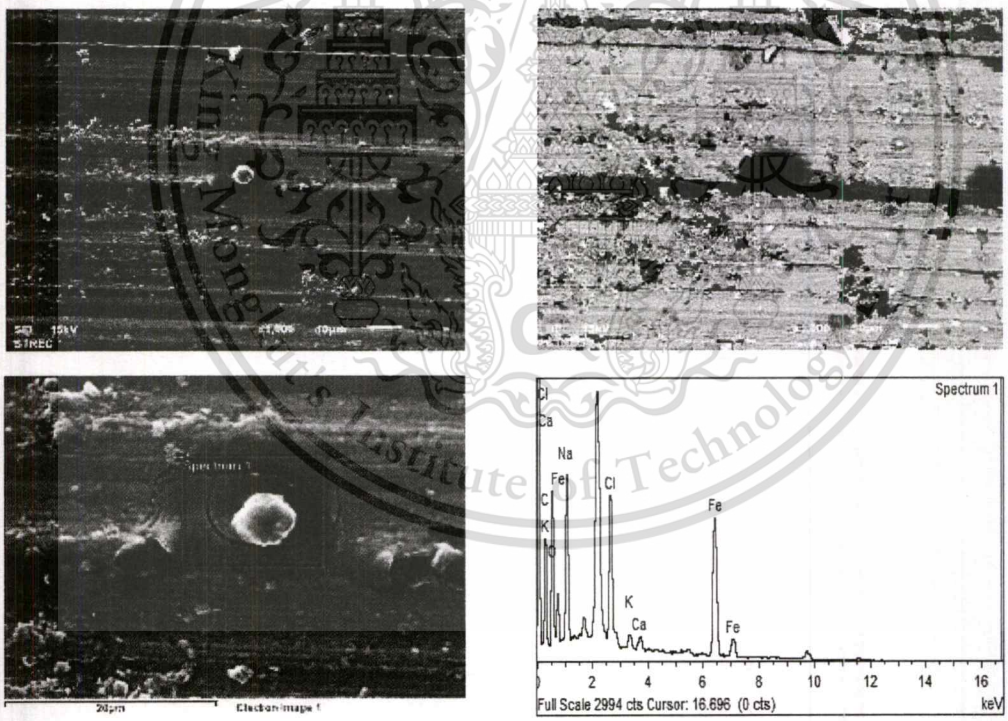

(b) The engine oil containing CB N550.

Figure 5 SEM micrographs taken using secondary and backscattered electron and EDX spectra of the ball surface from (a) the engine oil without soot and (b) the engine oil containing CB N550

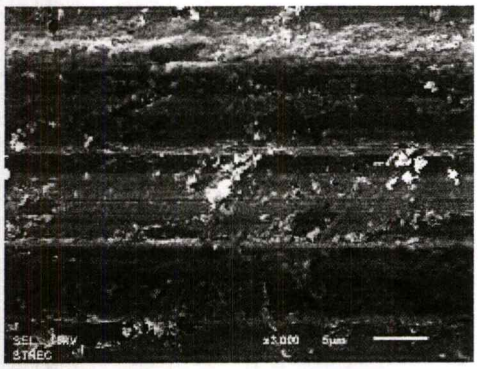

(a) The engine oil without soot.

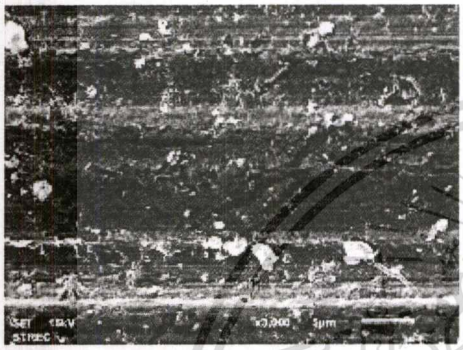

(b) The engine oil containing CB N330.

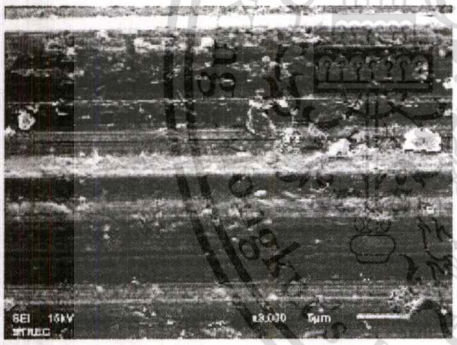

(c) The engine oil containing CB N550.

Figure 6 SEM micrographs taken using secondary electron at 3,000 magnification of the ball surface from (a) the engine oil without soot and (b) the engine oil containing CB N330 and (c) CB N550.

The EDX analysis indicated a composition of 41C-8O-1Ca-0.9Cr-47Fe-1Zn (in at. %) for the ball from the engine oil without soot and a composition of 50C-23O-8Na-5Cl-0.5K-0.5Ca-14Fe for the ball from the engine oil containing CB N550. **Figure** 6 shows the ball wear surface from (a) the engine oil without soot, (b) the engine oil containing CB N330 and CB 550. The ball surface of the engine oil containing CB N550 (**Figure 6c**) shows very clear wear trace that might be the result of soot abrasive wear.

Four-ball soot wear mechanisms

In this research, soot wear mechanisms might be expected as three-body abrasive wear. The role of lubricating oil is to generate an oil film between two surfaces and trap soot particles. If the soot particle size is smaller than the oil film, the surface can be separated, and no wear should occur. Further, if the soot particle size is larger the oil film thickness, then soot might occurr as three body abrasion. Therefore, viscosity improver additives would be a key to preventing soot abrasive wear

Conclusion

Soot particle distributions in liquids were observed by Laser Diffraction Spectroscopy. It was found that there were highly agglomerated in water, a smaller group of agglomeration in palm oil and well distribution in formulated lubricant. The impact of soot nanoparticle affecting on metal wear was investigated by Four-ball wear tester. It was found that the ball WSD increased proportionally to the soot primary particle size. It is expected that the soot particle which is larger than the oil film thickness can increase the metal wear.

Acknowledgements

The authors would like to acknowledge King Mongkut's Institute of Technology Ladkrabang, National Science and Technology Development Agency, Bangchak Corporation Pub Co., Ltd, and FOCUSLAB Ltd.

References

1. S. Daido, Y. K, T. I, N. O, and T. S, Analysis of Soot Accumulation inside Diesel Engines, *JSAE Review*, Vol. 21, 303-308 (2000).
2. W. M. Needelman, and P. V. Madhavan, Review of Lubricant Contamination and Diesel Engine Wear, *SAE papers*, 881827 (1988).
3. P. Kamsrisuk, P. Karin, K. Sriprapha, and H. KOSAKA. An Investigation on Physical and Chemical Properties in Used Lubricating Oil of Diesel Engine, Master Of Engineering Thesis *IC KMITL* (2016).
4. M. Gautam, S. George, S. Balla, and V. Gautam, Effect of diesel soot on lubricant oil viscosity, *Tribology International*, Vol. 40. 809–818 (2007).
5. D. A. Green, and R. Lewis. The effects of soot-contaminated engine oil on wear and friction: A review. *Proc Inst Mech Eng Pt D: J Automobile Eng*, Vol. 222, 1669-89 (2008).
6. P.R. Ryason, I. Chan, and J.T. Gilmore, Polishing Wear by Soot, *Wear*, Vol.137, 15-24 (1990).
7. P. Karin, C. SUPANAMOK and K. Hanamura. Impact of Soot on Metal Wear Characteristics Using Laser Diffraction Spectroscopy. *JRAME*, Vol. 4. No.2, 126-134 (2016).
8. E. Hu, X. Hu, T. Liu, L. Fang, K.D. Dearn, and H. Xu, The role of soot particles in the tribological behavior of engine lubricating oils, *Wear*, Vol. 304, 152-161 (2013).
9. P. Karin, J. Boonsakda, K. Siricholathum, E. Saenkhumvong, C. Charoenphonphanich, and K. Hanamura, Morphology And Oxidation Kinetics Of Ci Engine's Biodiesel Particulate Matters On Cordierite Diesel Particulate Filters Using TGA, *KSAE*, Vol. 18, 31-40 (2017).
10. Carbon Black. *IARC MONOGRAPHS*, Vol. 93, 43-191 (2010).
11. Standard test method for wear preventive characteristics of lubricating fluid (Fourball method). *ASTM D4172 -94* (2016).

SETC 2017 JAKARTA

The 23rd Small Engine Technology Conference

Call for Papers

Society of Automotive Engineers of Japan, Inc. | SAE INTERNATIONAL | IATO SAE-INDONESIA

Patronage of FISITA

VENUE : JAKARTA CONVENTION CENTER
PERIOD : November 15 to 17, 2017

DUE DATES
Abstracts due : January 31, 2017
Draft manuscripts due : April 14, 2017
Final manuscripts due : July 31, 2017

FOREWORD

JSAE, Society of Automotive Engineers of Japan, Inc., is pleased to announce that the 23rd Small Engine Technology Conference (SETC2017) will be held in Jakarta, Indonesia from November 15 to 17, 2017.

The conference is jointly organized by JSAE and SAE International with the support of Society of Automotive Engineers Indonesia (IATO) and Japan Land Engine Manufacturers Association (LEMA). We kindly ask prospective researchers and engineers in a diversified field of technologies and products with power source to submit electronic abstracts.

The conference offers up-to-date and new information in the development of technologies concerned in an exchange of participants from the globe. The events include technical visits, keynote speech, plenary session, exhibition and poster sessions besides ceremonial events of opening and awards & closing. Lunch & coffee-break for networking, welcome reception and banquet will be served as well.

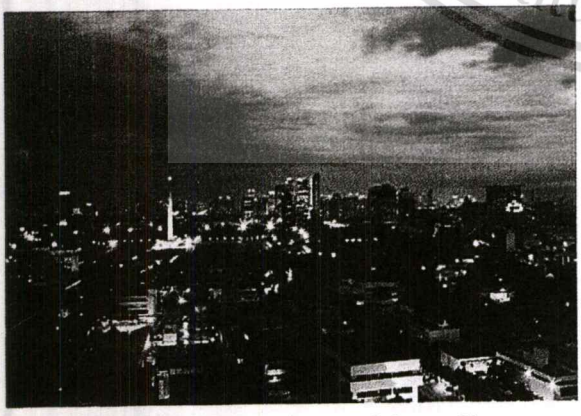

Central District of Greater Jakarta City

MAIN SUBJECT AREAS

- **Product Categories** focused in this conference are:

  Vehicles with power source such as ATV, Motorcycles, Scooters, Personal Mobility, Marine, Snowmobiles, Recreational Vehicles, Utility Vehicles, Power Assist Devices, Power Assist Bicycles and Unmanned Vehicles.
  *Automobiles, Large Vessels, Large Aircraft, Locomotives and Spaceships are inapplicable.

  Machines with power source such as Snow Removal Equipment, Portable Power Generators, Agricultural Equipment, Garden Equipment, Hand Tools and Powered Exoskeleton.
  Technologies applicable for the products above are to be presented in this conference.

- **Technological Areas** focused in this conference are:

  Combustion Engines such as 4 stroke Engines, 2 stroke Engines, SI Engines, Diesel Engines, HCCI Engines, Unconventional Engines and Competition Engines.

  New Energy Sources such as Hybrid Drives, Electric Drives, Fuel Cells and Solar Cells.

  Components such as Chassis, Suspensions, Brakes, Transmissions, Drivetrains, Electrical Systems, Electronic Systems, Fuel Supply Systems and Wheels & Tires.

  Development Technologies such as Numerical Simulations, Measurements and Production Technologies.

  Fuels, Lubricants, and Tribology such as Alternative Fuels, Fuel Reformations, Additives, Friction Loss and Wear.

  Vehicle Technologies such as Dynamics, Handling, Drivability, Safety Technology & Functional Safety and Human Factors & Ergonomics.

  Environmental Impacts such as Noise, Vibration, Emissions, Aftertreatment and Life Cycle & Recyclability.

  Materials such as Composites, Metal Alloys, Heat & Surface Treatment, New Material and Material Processing.

1. **Language**: English. No simultaneous translation will be provided

2. **Submission of Abstracts**
We kindly ask prospective researchers and engineers in a diversified field of technologies and products with power source to submit electronic abstracts of 300 to 500 words on-line via SETC website (URL: http://www.setc-jsae.com/) linked to JSAE Paper Entry System. You will receive an automatic reply upon the submission.
The abstract should include:
- Tentative paper title
- Author (and co-authors) with full name, affiliation, mailing address, e-mail address, telephone and fax numbers.

Each abstract should clearly state:
- The main issues and conclusions
- The process by which the conclusions were reached
- The significance of the work to progress of the relevant engineering area.

Abstract to be received on-line from December 2016.

3. **Papers/Presentations**
The papers should be written and presented at the conference, which should be applications oriented. No paper will be accepted without a presentation.
- The papers should be prepared in hard metric (SI) units.
- Material of a purely descriptive nature or containing commercialism should be omitted.
- Final manuscripts should make a contribution to the state-of-the-art technology or present a comprehensive review, be of high technical quality with conclusions supported by technical data.
- A presenting author when his/her final manuscript accepted, is asked to make on-line advanced registration via SETC website linked to the registration system and also to bring his/her own PC for presentation to the venue.
- Your technical paper could be selected for SAE Journal.

4. **Exhibition and Poster Session**
OEMs, suppliers and academia will be given an opportunity to exhibit products and technical information during the conference at the venue. Poster session in conjunction with technical session will be also provided to graduate & undergraduate university students, and their researchers.

5. **Advertisements and Sponsorship**
Advertisement banner and preliminary & final program will be offered.
Also, the conference sponsorship program will be planned. Information will be available at the SETC website late 2016.

REPUBLIC OF INDONESIA

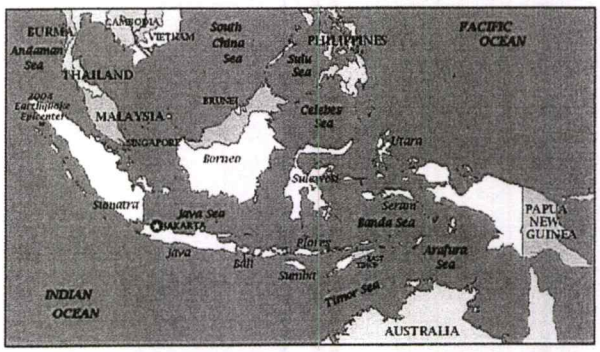

REPUBLIC OF INDONESIA AT GLANCE

Indonesia is a country in Southeast Asia. Located between the Indian and Pacific Ocean, it is the largest archipelagic state in the world, consisting of more than 18,000 islands. Moreover, Indonesia possesses the 2nd longest coastlines in the world, measuring of 54,716 km. The major islands are Java, Sumatra, Borneo (Kalimantan), Papua and Celebes (Sulawesi). With an estimated population of more than 256 million people, Indonesia is the world's fourth most populous country as well as the most populous Muslim majority country.

GREATER JAKARTA CITY

Jakarta is the capital city of the Republic of Indonesia which serves as the center of government, as well as the epicenter for finance, business and trade. As the biggest city in Indonesia, Jakarta acts as the main hub for international air connections in the archipelago. The city has many deluxe hotels that offer first class services in rooms, function halls and superb cuisine, whether for individuals or for large delegations. In addition, Jakarta is also famous for offering one of the best shopping venues in South East Asia with numerous modern shopping centers for your consumer needs.

ACCESS

If you fly to Jakarta using international airline, you will arrive in Terminal 2 or 3 of Jakarta Soekarno-Hatta International Airport. The airport is located on Cengkareng, a district northwest of the city. The distance from the airport to the venue at Jakarta Convention Center is about one to two hours depending on traffic condition. There are several ways that you can get from the airport to Jakarta. The easiest and most convenient is taking a taxi. You'll see plenty of taxi drivers as soon as you leave the arrival terminal.

INFORMATION ON THE WEB:

INDONESIAN TRAVEL GUIDE:
http://www.indonesia.travel/

JAKARTA TRAVEL GUIDE:
http://www.indonesia-tourism.com/jakarta/

VENUE – JAKARTA CONVENTION CENTER:
http://www.jcc.co.id

SETC2017 SECRETARIAT
Society of Automotive Engineers of Japan, Inc. E-mail: setc2017@jsae.or.jp
Website: http://www.setc-jsae.com/

JSAE 20179095 / SAE 2017-32-0095

Effect of Biofuel and Soot on Metal Wear Characteristic using Electron Microscopy and 3D Image Processing

Preechar Karin, Warawut Amornprapa, Phiranat Khamsrisuk, Pol-ake Budsayahem, Pattara Chammana
King Mongkut's Institute of Technology Ladkrabang

Kobsak Sriprapha
National Science and Technology Development Agency

Katsunori Hanamura
Tokyo Institute of Technology

ABSTRACT

The soot contamination in used engine oils of diesel engine vehicles was about 1% by weight. The soot and metal wear particle sizes might be in the range of 0-1 μm and 1-25 μm, respectively. The characteristics of soot affecting on metal wear was investigated. Soot particle contamination in diesel engine oil was simulated using carbon black. Micro-nanostructure of soot particles were studied by scanning electron microscopy (SEM), transmission electron microscopy (TEM) and laser diffraction spectroscopy (LDS). The metal wear behavior was studied by means of a Four-Ball tribology test with wear measured. Wear roughness in micro-scale was investigated by high resolution optical microscopy (OM) , 3D rendering optical technique and SEM image processing method. It was found that the ball wear scar diameter increased proportionally to the soot primary particle size. The effect of biodiesel contamination were also increasing in wear scar diameter.

INTRODUCTION

Diesel engine is a compression ignition engine which converts chemical energy within the fuel into mechanical energy. Diesel fuel is injected under high pressure into the combustion chamber where the combustion process occurs. Soot is remain of incomplete combustion which consists mostly of hydrocarbon, carbon and metallic ash. The primary and agglomerated soot particles observed by TEM are in the range of 20-80 nm and 100-300 nm, respectively [1]. Soot can be entered into the engine oil through the piston ring clearance during the combustion process [2].

Khamsrisuk *et al.* [3] performed the used oil analysis by collecting the engine oil from the small diesel engine vehicles. The results showed that the percentage of wear metal, soot and fuel contamination increased as the engine mileage increase. The average of soot contamination was about 0.69 percent by weight. Guatam *et al.* [4] investigated the effect of soot contamination on engine oil viscosity by increasing the percentage of soot contamination. The results showed that the engine oil viscosity increased with the increase of soot contamination. The engine testing for evaluated soot tribological properties is challenging, because of the uncontrolled test parameter and the difficulty of wear measurement [5]. The specimen bench test which is easy to control test parameter and good repeatable results are used. Carbon black is a synthesis soot which has similar particle size and physical properties to engine soot. It can be used as soot representative. Ryason *et al.* [6] performed wear tests on a ball-on-flat-disk wear tester using carbon black, alumina and silica. The results showed that the balls were worn similarly in three different kinds of the samples. Karin *et al.* [7] performed wear tests on Four-Ball Wear Tester. He found that the wear scar diameter (WSD) of the ball in the oil containing carbon black was higher than that of the pure oil without carbon black. Hu *et al.* [8] also performed Four-Ball wear tester using base oil and formulated lubricant. The results showed that the WSD was high when carbon black levels increased. But, the WSD of the formulated lubricant was lower than that of the pure base oil. They suggested that the wear mechanism of soot-contaminated lubricant might be abrasion.

Biodiesel is an alternative fuel that plays an importance role in replacement using petroleum diesel. It is an oxygenated fuel that promotes more completely combustion. The soot diameter size and quantity from biodiesel engine emission is lower than that of diesel [9]. However, soot induced wear mechanisms are still not fully understood. This research aimed to investigate the effects of soot Nanoparticles on metal wear characteristics using Four-Ball wear tester, laser diffraction spectroscopy, and electron microscopy.

EXPERIMENTAL SETUP

A formulated engine oil which had the same grade as SAE0W30 was used in this research. The engine oil condition including viscosity, oxidation, nitration and total base number (TBN) were measured according to ASTM standard test

methods. Oil additives were measured by x-ray fluorescence. The used engine oils were collected from the small diesel engine vehicles with different oil changed interval. The engine oil's mileage and oil aged were in the range 3,000-20,000 and 0-10,000 km, respectively. After that, the contaminants including fuel, soot and metal wear particles were measured. In order to investigate the effect of biodiesel contamination on metal wear, the different types of palm biodiesel blend were mixed with the engine oil at 2% by volume. The types of biodiesel were conventional diesel (B7), B20, B50 and B100. Moreover, the effect of soot contamination on metal wear were also investigated. The different types of commercial carbon blacks (CB) were mixed with the engine oil at 1% by weight per volume for simulating soot contamination. They were carbon black N220, N330, N550 and N660. The details of engine oil samples mixing with difference blend of biodiesel and carbon black are shown in Table 1.

In order to investigate the effect of soot contamination on wear, the Four-Ball wear tester was chosen. The test methods and conditions followed the standard test ASTM D4172 [11]. The machine consists of four 12.7 mm diameter steel balls, the three lower balls held in a steel cup with fixed position and the fourth ball was held in the upper chunk. The top ball was pressed with a force of 392 N and rotated at 1,200 rpm, as shown in Figure 1. The lubricant temperature and operating time were 75 °C and 60 min, respectively. After the tests, the three lower balls used to measure WSD using a high-resolution optical microscope (OM). It was the average value of these balls. The surface roughness was also measured using 3D rendering system of that OM. The worn surface analysis was investigated by using SEM. Moreover, the particle size distribution was measured using LDS.

Table 1. Fuel and carbon black mixed with the engine oils for four ball test.

Samples	% SAE0W30 (Volume)	Fuels or CB Types	% Fuel (vol.) %CB (wt.)
NE	100 %	-	-
EB7	98%	B7	2 %
EB20	98%	B20	2 %
EB50	98%	B50	2 %
EB100	98%	B100	2 %
EC2	100 %	N220	1 %
EC3	100 %	N330	1 %
EC5	100 %	N550	1 %
EC6	100 %	N660	1 %

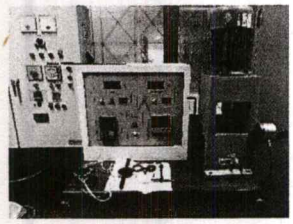

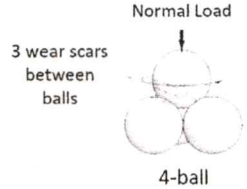

Figure 1. Four-Ball Wear Tester (ASTM D4172)

RESULTS AND DISCUSSION

Soot and Fuel in Diesel Engine Oil

A formulated engine oil which had the same grade as SAE0W30 was used in this research. The engine oil condition including viscosity, oxidation, nitration and TBN were measured according to ASTM standard test methods. Oil additives were measured by x-ray fluorescence. The oil conditions and additives are shown in Table 2. The used oil analysis showed that the fuel and soot contamination increased as the mileage and oil age increase. Fuel and soot are remain of the incomplete combustion process that can be transported to the engine oil during combustion process. The average fuel contamination in the small diesel engine vehicles was about 2 % by weight and the average soot was about 0.7 % by weight as shown in Table 3.

Figure 2 show TEM micrographs of commercial carbon black (CB) (a) N220, (b) N330, (c) N550 and (d) N660. Most of CB's primary nanoparticle diameter is smaller than 90 nm. The average primary nanoparticles of CB N660 was significant larger than that of N220. After that, primary nanoparticles of those CB were measured using image processing method. Figures 2 (e) shows carbon black's primary nanoparticle size distribution. The primary nanoparticle diameters are in the range of 5-90 nm. It was clearly observed much amount of particle diameters are in the range of 20-65 nm.

Table 2. Properties of SAE0W30 engine oil.

Oil conditions		Oil additives (ppm)	
Viscosity @ 40 °C	44.5 cSt	S	214.0
Viscosity @ 100 °C	9.6 cSt	Ca	166.0
Oxidation (Abs)	18.1	Zn	847.0
Nitration (Abs)	6.1	P	779.0
TBN (mgKOH/g)	5.6	Mo	454.0

Table 3. Fuel, soot and metal wear contaminations in conventional diesel vehicle's used oil.

Contaminations		
Fuel	% by weight	2.0
Soot	% by weight	0.7
Wear	Total metal (ppm)	111.0
	Iron (ppm)	74.38

Normal rubbing wear (%)	65
Fatigue bearing wear (%)	20
White metal (%)	5
Black oxide (%)	5
Dirt and dust (%)	5

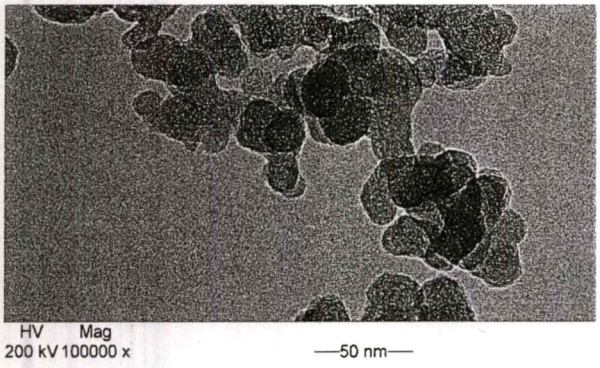

(a) CB N220

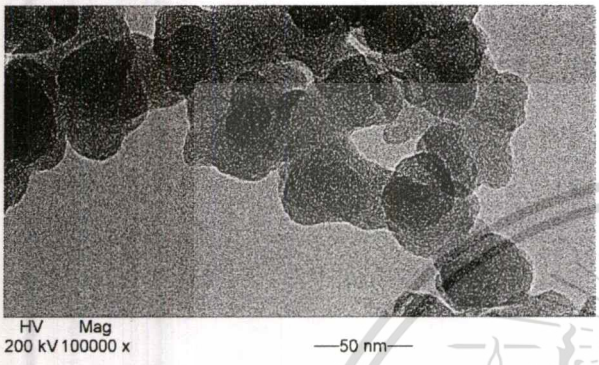

(b) CB N330

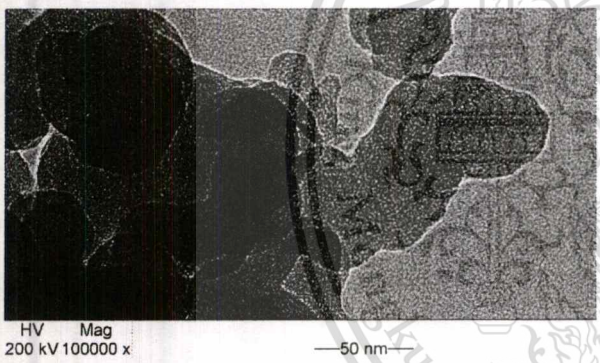

(c) CB N550

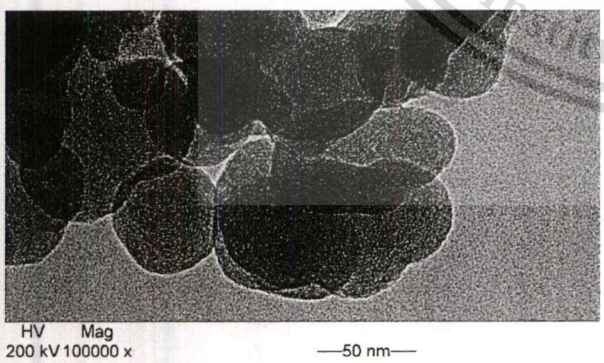

(d) CB N660

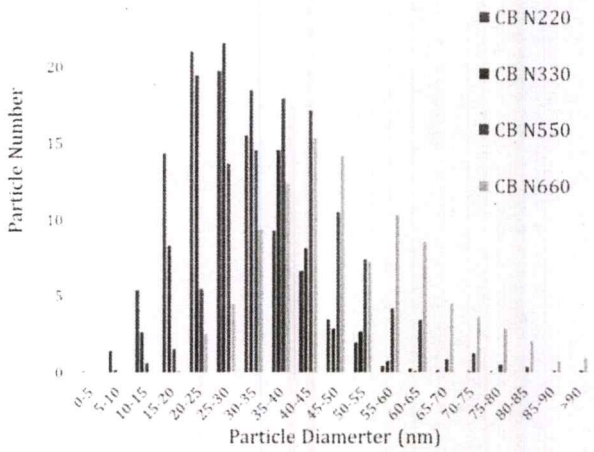

(e) Size distributions of CB's nanoparticle

Figure 2. TEM images of carbon black (a) N220, (b) N330, (c) N550 and (d) N660 and (e) size distributions of CB's nanoparticle using TEM image processing method.

(a) Metal wear particles

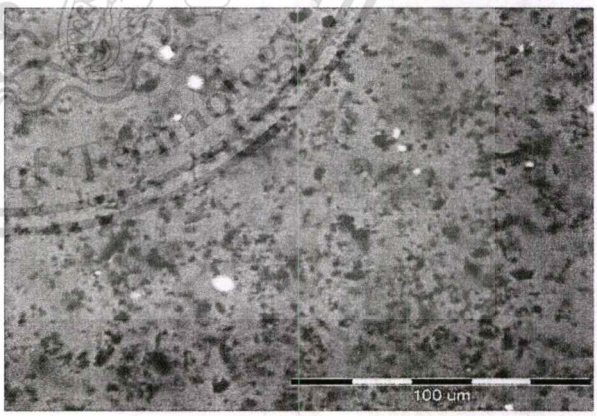

(b) Soot particles

Figure 3. Images of (a) metal wear and (b) soot particles contamination in the diesel engine's used lubricating oil using OM.

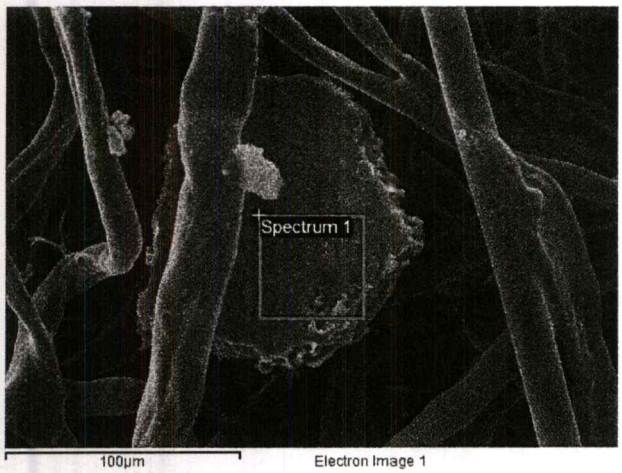

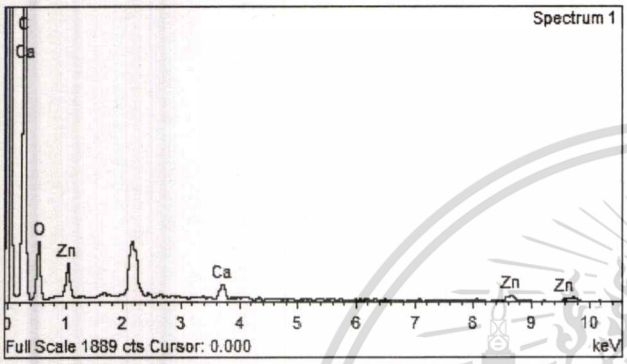

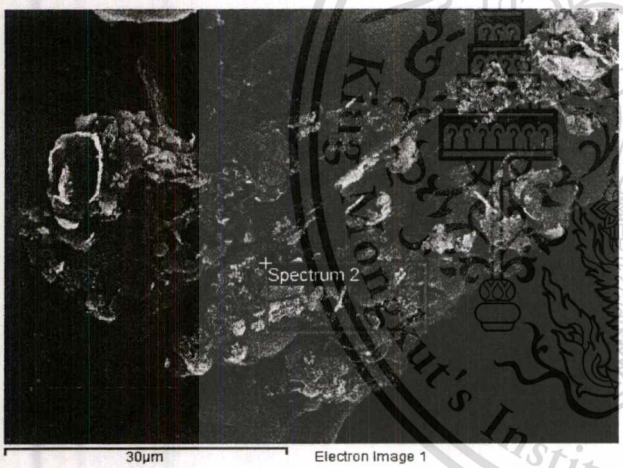

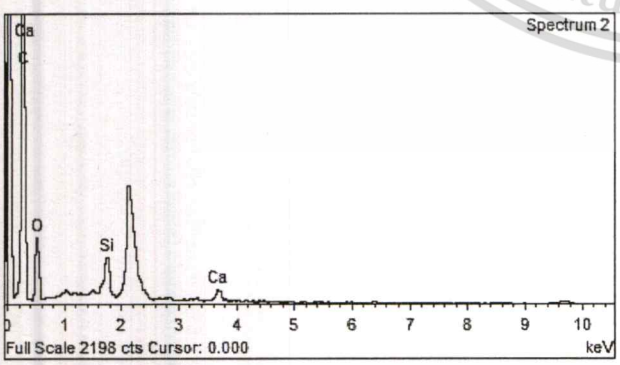

Figure 4. Metal wear and soot particles contamination in the diesel engine's used oil filter using SEM-EDX.

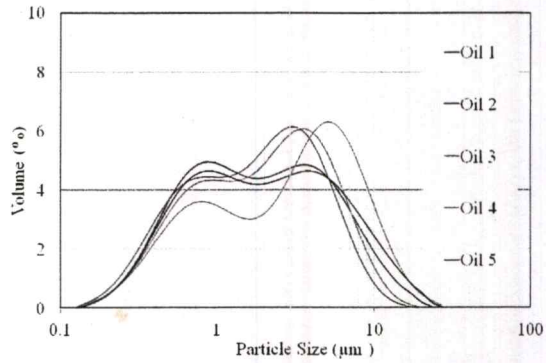

(a) Particle size distribution of the diesel engine's used lubricating oil

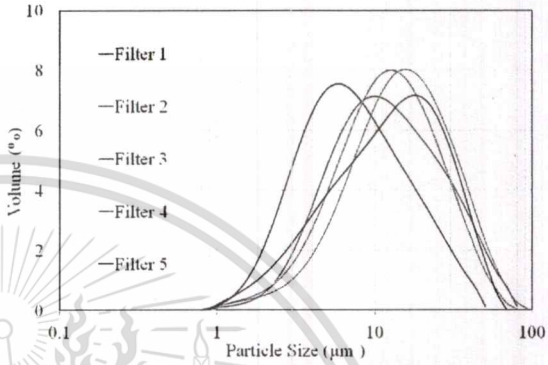

(b) Particle size distribution of the diesel engine's used oil filter

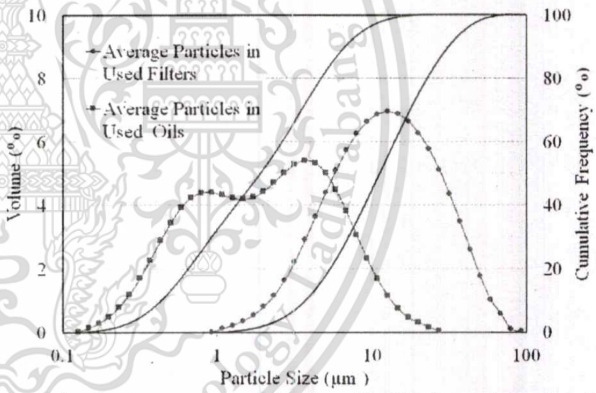

(c) The average particle size distribution of the diesel engine's used lubricating oil and used filter

Figure 5. Particle size distribution of the diesel engine's used (a) lubricating oil, (b) oil filter, and (c) the average particle size distribution inside used oil and used oil filter using LDS.

The main metal wear particles are normal rubbing wear and fatigue bearing wear of iron parts. Figures 3 and 4 show optical and SEM-EDX images of soot and wear particles. SEM-EDX analysis indicated a composition of 76C-22O-1Ca-1Zn (in at. %) for a big wear particle and a composition of 76C-21O-2Si-1Ca for a small wear particle. Figure 5 shows particle size distributions of used lubricating oils and used oil filters. They were both collected from the small diesel engine vehicles at the oil end interval. The used oil particles were in the range of 0.1-30 microns and the particles inside the filter were in the range of 1-100 microns.

(a) NE-A

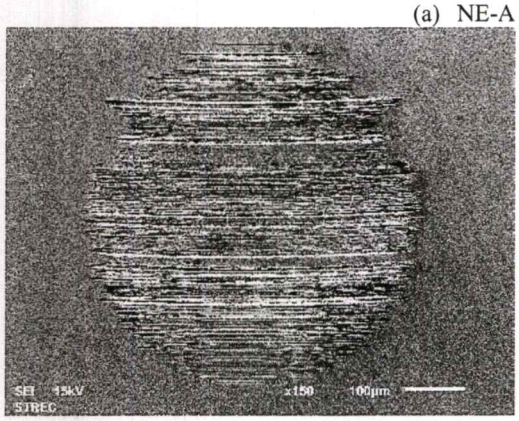

(b) EB7

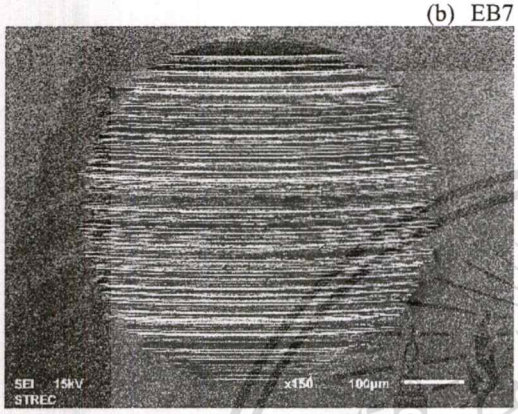

(c) EB20

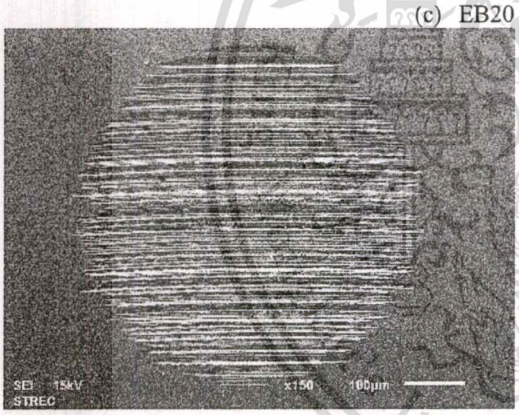

(d) EB50

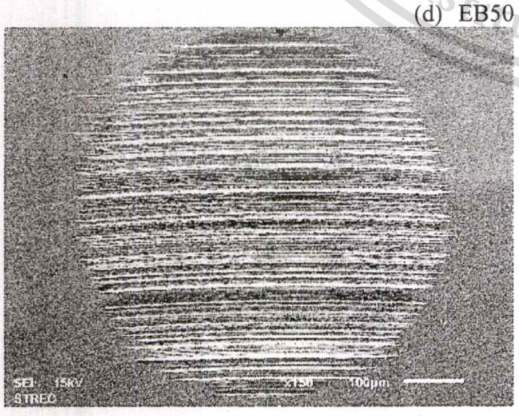

(e) EB100

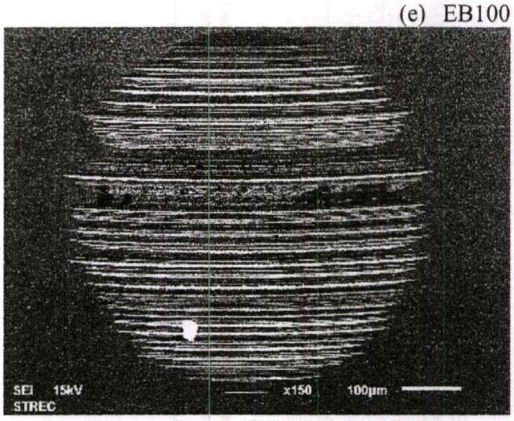

Figure 6. The wear surfaces of the diesel engine's oil contaminate with different fraction of biodiesel in diesel fuels using SEM.

Table 4. WSD and roughness of the diesel engine's oil contaminate with different fraction of biodiesel in diesel fuels.

Samples	WSD (micron)	Roughness (micron)
NE-A	533	1.32
EB7	588	1.18
EB20	569	1.17
EB50	604	1.21
EB100	625	1.68

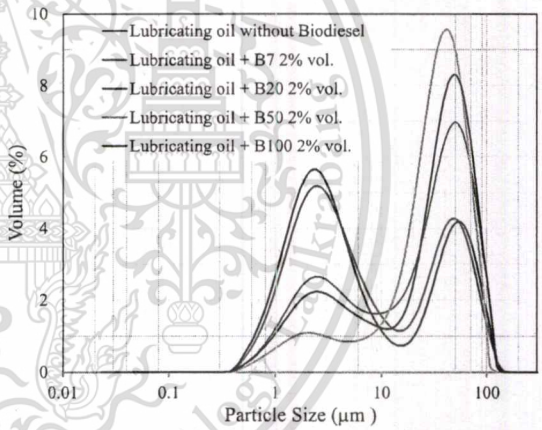

Figure 7. Wear particle size distribution of Four-Ball tested oils using LDS.

Impact of Biodiesel and Soot on Metal Wear

Figure 6 shows SEM micrographs of wear scar found on the ball of (a) the engine oil without fuel and engine oil containing 2% wt. of (b) B7, (c) B20, (d) B50 and (e) B100. The average wear scar diameter and surface roughness were shown in Table 4. The results showed that the ball WSD of the oil containing B100 was higher than that of the pure oil without fuel and it increased when the concentration of biodiesel was increased but the surface roughness is not significant different. Fuel contamination may decreases the viscosity of the engine oil that resulting in reducing oil film thickness. It might decreases the strength of anti-wear additives that make higher wear on metal surface. Figure 7 shows size distribution of particles inside the tested oils. They were in the range of 0.3-125 micron.

(a) NE-B

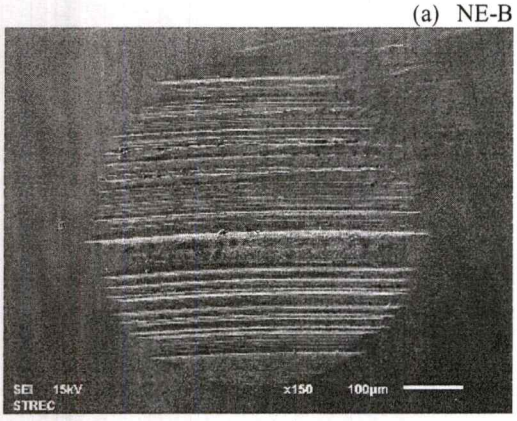

(b) EC2

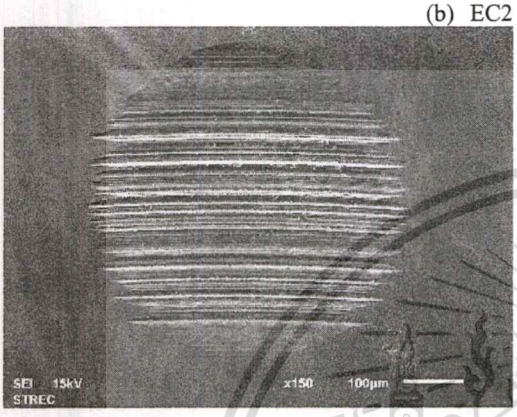

(c) EC3

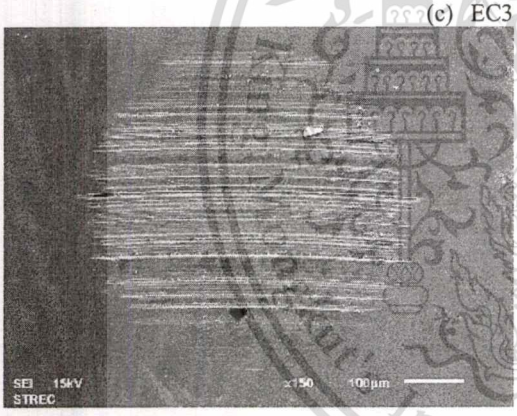

(d) EC5

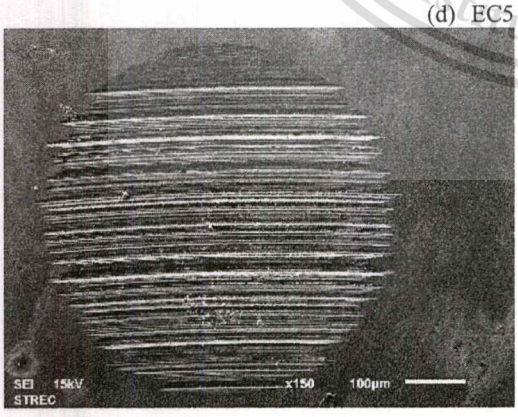

(e) EC6

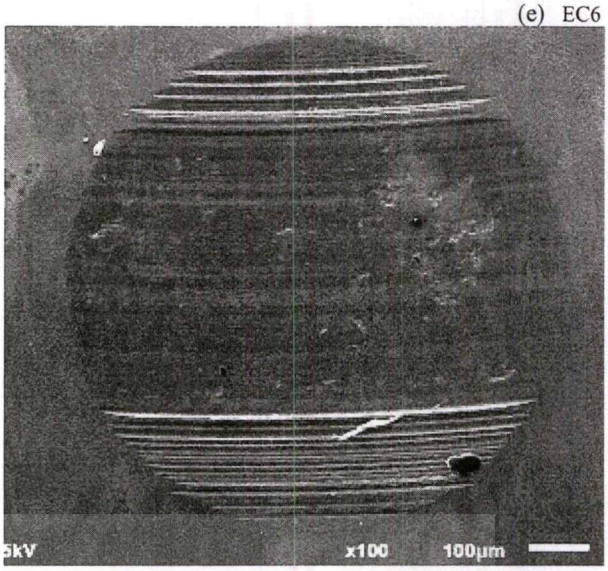

Figure 8. The wear surfaces of the diesel engine's oil contaminate with different size of primary particle size of carbon black.

Table 5. WSD and roughness of the diesel engine's oil contaminate with different size of primary particle size of carbon black.

Samples	WSD (micron)	Roughness (micron)
NE-B	544	2.06
EC2	533	1.35
EC3	546	1.44
EC5	597	2.11
EC6	815	1.53

Figure 8 shows microscopy image of wear scar found on the ball of (a) the engine oil without soot and engine oil containing 1% wt. of (b) N220, (c) N330, (d) N550 and (e) N660 carbon black. The average wear scar diameter and surface roughness were shown in Table 5. The results showed that the ball WSD of the oil containing CB N600 was higher than that of the pure oil without carbon black and it increased when the primary particle size of the carbon black was increased. However, the surface roughness is not significant different.

In this research, soot wear mechanisms might be expected as three-body abrasive wear. The role of lubricating oil is to generate an oil film between two surfaces and trap soot particles. If the soot particle size is smaller than the oil film, the surface can be separated, and no wear should occur. Further, if the soot particle size is larger the oil film thickness, then soot might occur as three body abrasion. Therefore, oil viscosity improver and soot agglomerate dispersant additives would be a key to preventing soot abrasive wear.

After Four-Ball wear test, the tested oils were also measured size distribution. Figure 9 shows size distribution of different types of carbon black and wear particles which were measured after Four-Ball wear test. They were in the range of 0.01-300 microns, which were small particle that have size of 10-100 nm. Figure 10 shows the average size distribution of particles inside the tested oils. They were in the range of 0.01-300 micron. It was clearly observed that metal wear particles size are larger than that of carbon black.

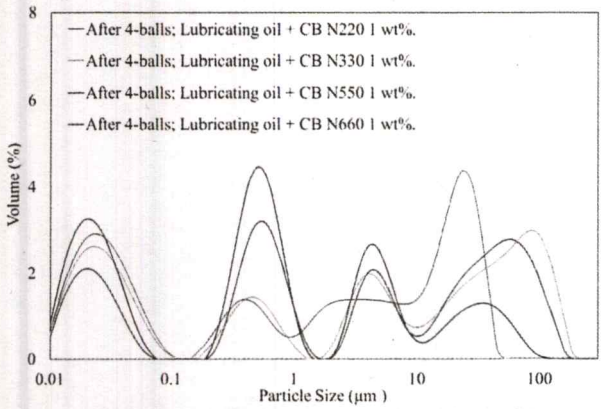

Figure 9. Particle size distribution of carbon black with wear particles in lubricating oil after Four-Ball tested by LDS.

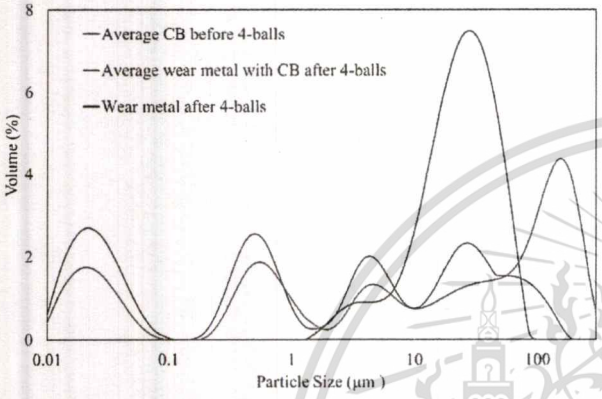

Figure 10. The average particle size distribution of carbon black with wear particles in lubricating oil before and after Four-Ball tested by LDS compared to wear particle without carbon black.

SUMMARY

The fuel and soot contamination in used engine oils of diesel engine vehicles was about 2% and 1% by weight, respectively. The particles size in the oil pan of the engine were in the range of 0.1-25 µm. The soot and metal wear particle sizes might be in the range of 0-1 µm and 1-25 µm, respectively.

It was clearly observed that the effect of biodiesel contamination were increasing in wear scar diameter. It might be expected that fuel contamination may decreases the viscosity of the engine oil and the strength of anti-wear additives that make higher wear on metal surface.

Moreover, the ball wear scar diameter increased proportionally to the soot primary particle size. It is expected that the soot particle which is larger than the oil film thickness can increase the metal wear.

The impact of biodiesel contamination and carbon black particle size could not observed in micro-scale of surface roughness. Submicron- and nano-scales of metal wear surface analysis is needed to characterize for more understanding of metal wear mechanisms.

REFERENCES

1. S. Daido, Y. Kodamaa, T. Inohara, N. Ohyamaa, and T. Sugiyama, Analysis of Soot Accumulation inside Diesel Engines, *JSAE Review*, Vol. 21, 303-308 (2000).
2. W. M. Needelman, and P. V. Madhavan, Review of Lubricant Contamination and Diesel Engine Wear, *SAE Technical Papers*, 881827 (1988).
3. P. Kamsrisuk, P. Karin, K. Sriprapha, and K. Hanamura. An Investigation on Particle Size Distribution in Used Lubricating, *JSAE Technical Paper*, 20165336 (2016).
4. M. Gautam, S. George, S. Balla, and V. Gautam, Effect of diesel soot on lubricant oil viscosity, *Tribology International*, Vol. 40. 809-818 (2007).
5. D. A. Green, and R. Lewis. The effects of soot-contaminated engine oil on wear and friction: A review. *Proc Inst Mech Eng Pt D: J Automobile Eng,* Vol. 222, 1669-89 (2008).
6. P.R. Ryason, I. Chan, and J.T. Gilmore, Polishing Wear by Soot, *Wear*, Vol.137, 15-24 (1990).
7. P. Karin, C. Supanamok and K. Hanamura. Impact of Soot on Metal Wear Characteristics Using Laser Diffraction Spectroscopy. *Journal of Research and Applications in Mechanical Engineering*, Vol. 4. No.2, 126-134 (2016).
8. E. Hu, X. Hu, T. Liu, L. Fang, K.D. Dearn, and H. Xu, The role of soot particles in the tribological behavior of engine lubricating oils, *Wear*, Vol. 304, 152-161 (2013).
9. P. Karin, J. Boonsakda, K. Siricholathum, E. Saenkhumvong, C. Charoenphonphanich, and K. Hanamura, Morphology And Oxidation Kinetics Of Ci Engine's Biodiesel Particulate Matters On Cordierite Diesel Particulate Filters Using TGA, *International Journal of Automotive Technology,* Vol. 18, 31-40 (2017).
10. Carbon Black. *IARC MONOGRAPHS*, Vol. 93, 43-191 (2010).
11. Standard test method for wear preventive characteristics of lubricating fluid (Fourball method). *ASTM D4172 -94* (2016).

ACKNOWLEDGMENTS

The authors gratefully acknowledge the support from Bangchak Corporation Pub. Co., Ltd., FOCUSLAB Ltd., Thailand Research Fund (TRF), KMITL and NSTDA.

ABBREVIATIONS

B100	Biodiesel
CB	Carbon Black (N220-N660)
EB	Fuel mixed with New Engine Oil
EC	Carbon Black mixed with New Engine Oil
EDX	Energy Dispersive X-Ray Analysis
LDS	Laser Diffraction Spectroscopy
NE	New Engine Oil
OM	Optical Microscopy
SEM	Scanning Electron Microscopy
TBN	Total Base Number
TEM	Transmission Electron Microscopy
WSD	Wear Scar Diameter